THESIS FOR THE DEGREE OF DOCTOR OF PHILOSOPHY (Ph.D.)

STUDYING THE TRANSPORT MECHANISM OF HUMAN P-GLYCOPROTEIN (ABCB1) AND BREAST CANCER RESISTANCE PROTEIN (ABCG2)

by
Szabolcs Tarapcsák
Supervisor: Katalin Goda, Ph.D.

University of Debrecen
Doctoral School of Molecular Cell and Immune Biology
Debrecen, Hungary
2021

Contents

1. List of abbreviations

(^{125}I)INA: Iodonaphthalene-1-azide
4-PBA: 4-Phenylbutyrate
ABC: ATP-binding cassette
ABCB11: Bile-salt export pump (BSEP)
ABCC1: Multidrug resistance protein (MRP1)
ABCG2: Breast Cancer Resistance Protein
ADME: Absorption, distribution, metabolism, elimination
ALL: Acute lymphoblastic leukemia
AM: Acetoxymethylester
AML: Acute myeloid leukemia
ANOVA: Analysis of variance
APL: Acute promyelocytic leukemia
apoA-I: Apolipoprotein A-1
ATRA: All-*trans*-retinoic acid
BeF_x: Beryllium-fluoride
BSA: Bovine serum albumin
BXP-21: Anti-ABCG2 antibody (western blot)
Calcein-AM: Calcein acetoxymethylester
CF: Cystic fibrosis
CFTR: Cystic fibrosis transmembrane conductance regulator (ABCC7)
CNS: Central nervous system
Cryo-EM: Cryo-electron microscopy
CsA: Cyclosporine A
DEER: Double electron-electron resonance
DMEM: Dulbecco's modified Eagle's medium
DPH: 1,6-Diphenyl-1,3,5-hexatriene
DTT: L-dithiothreitol
E1S: Estrone-3-sulfate
ECD: Extracellular domain
EGTA: Ethylene glycol-bis(β-aminoethyl ether)-*N*,*N*,*N*′,*N*′-tetra acetic acid
EM: Electron microscopy
EPR: Electron paramagnetic resonance
Fab: Antigen-binding fragment
FCS: Fetal calf serum
FRET: Förster resonance energy transfer
FSC: Forward scatter
G-1: Anti-Pgp antibody (western blot)
GAMIG: Goat anti-mouse immunoglobulin
GLOBOCAN: Global Cancer Statistics Database
HDL: High-density lipoprotein
IAAP: (^{125}I)-iodoarylazidoprazosine
IC_{50}: Half-inhibitory concentration
ICL: Intra-cytosolic loop
INFα-2a: Interferon alpha-2a

K_A: Apparent affinity for MgATP
$K_{D:}$ Binding affinity
$LogP_{ow}$: Octanol-water partition coefficient
LRET: Luminescence resonance energy transfer
mAb: Monoclonal antibody
MDR: Multidrug resistance
MDR1: Gene coding human P-glycoprotein
MFI_0: Mean fluorescence intensity in the absence of inhibitors
MFI_{inh}: Mean fluorescence intensity in the presence of inhibitors
MTX: Mitoxantrone
NBD: Nucleotide-binding domain
NBS: Nucleotide-binding site
NEM: N-ethylmaleimide
NSCLC: Non-small cell lung cancer
PBS: Phosphate-buffered saline
PC: Phosphatidylcholine
Pgp: P-glycoprotein
PI: Propidium iodide
Pi: Inorganic phosphate
PMSF: Phenylmethanesulfonylfluoride
PPAR: Peroxisome proliferator activated receptor
PP_i: Pyrophosphate
PXE: Pseudoxanthoma elasticum
RAR-RXR: Retinoic acid - retinoid X receptor
SB: Sleeping Beauty transposon vector
SCLC: Small cell lung cancer
SDS: Sodium dodecyl sulphate
Sf9: *Spodoptera frugiperda* insect ovary cells
SLO: Streptolysin-O toxin
SSC: Side scatter
TAF: Transport activity factor
TM: Transmembrane helix
TMA-DPH: (1-(4-Trimethylammoniumphenyl)-6-Phenyl-1,3,5-Hexatriene
TMD: Transmembrane domain
TMEP: Tris-Mannitol-EGTA-PMSF solution
VDR: Vitamin D receptor
Vi: Sodium-orthovanadate (Vanadate)

2. Introduction - The mysterious multidrug resistance phenomenon

Cancer is undoubtedly one of the leading causes of death worldwide. According to Global Cancer Statistics database (GLOBOCAN), in 2018 nearly 9.6 million patients died in cancer and the estimated number of new cases is more than 18 million per year (1). Numerous therapeutic modalities are available for the routine therapy of tumors including surgery, radiotherapy, immunotherapy, chemotherapy and the novel and promising chimeric antigen receptor (CAR) expressing T-cell therapy (2). Chemotherapy is primarily used in the treatment of patients with non-solid tumors (e.g., leukemia, lymphoma) or in cases when metastases appear. During chemotherapy, clinical oncologists often face the emergence of drug resistance. Following the promising results of the initial phase of chemotherapy, cancers gradually become resistant to several anti-neoplastic agents, including drugs they have never been exposed to. Numerous cellular processes can lead to chemotherapy resistance. Since anticancer drugs often target proteins involved in cell cycle regulation or apoptosis, alterations of these mechanisms may result in chemotherapy resistance (3). The success of chemotherapy also depends on the effective concentration of the drug(s) at the target site that is determined by many factors including their absorption, distribution and metabolism (4). In addition, at the level of the targeted tumor cells, the cellular uptake and the efflux of the drugs are of crucial importance in determining the efficiency of the treatment (5-9).

One of the major causes of cellular drug resistance is the over-expression of certain members of the ATP-binding cassette (ABC) transporter superfamily in tumor cells including P-glycoprotein (Pgp, ABCB1, MDR1), Multidrug Resistance Protein 1 (ABCC1, MRP1), and Breast Cancer Resistance Protein (ABCG2, BCRP) (10). These multidrug transporter proteins have exceptionally wide substrate specificity, as they can recognize and export the majority of anticancer drugs from the tumor cells. The phenomenon when tumor cells acquire cross-resistance against multiple agents is termed *multidrug resistance* (MDR). MDR is believed to be responsible for nearly 50% of ineffective tumor chemotherapies (11) and this ratio is even higher (up to 90%) in case of metastatic cancers (12).

In the 1970s, before the discovery of multidrug transporters, numerous hypotheses were formulated regarding the molecular basis of MDR. In a study from Keld Danø et al., daunorubicin resistant tumor cells were developed by stepwise selection in the presence of daunorubicin (13). They found that the daunorubicin uptake of intact resistant cells was significantly lower as compared to sensitive cells, while the isolated nuclei exhibited similar

daunorubicin uptake suggesting that the nuclear binding capacity did not change. This suggests that the expression of a membrane transporter or changes in the membrane structure might account for this phenomenon (14). Interestingly, addition of inhibitors of cellular metabolism (e.g., 2-deoxy-D-glucose and Na-azide) increased the daunorubicin accumulation of the resistant cells supporting the involvement of an active transport mechanism (15). Furthermore, co-administration of certain chemically unrelated drugs (e.g., vinblastine, vincristine) increased the intracellular accumulation of daunorubicin probably by competitive inhibition of its efflux, indicating that the underlying transport mechanism possesses wide substrate specificity (15).

Skovsgaard supposed that this highly pleiotropic nature of the MDR phenotype cannot be explained by a classical ATP-dependent efflux mechanism, rather it was the result of the decreased influx of drugs due to unspecific changes in the membrane of resistant cells (16). However, with cellular DNA transfer technology, it has been shown that transfection of DNA fragments from resistant mouse cells to sensitive cells results in MDR phenotype (17). This finding strongly supported the idea that a single gene product was responsible for MDR. With cell surface carbohydrate labeling and SDS-PAGE experiments carried out on several resistant and sensitive cell line pairs a 170 000 Da glycoprotein, exclusively expressed by the resistant cells was identified. This protein was named P-glycoprotein (Pgp, permeability glycoprotein), referring to the decreased membrane permeability of the expressing cells (18,19).

In further studies by Kartner et al., rabbit antisera and several monoclonal antibodies were generated against membrane components of resistant cell lines which specifically labeled Pgp (20,21). Western-blot experiments proved a strict correlation between the level of Pgp expression and the degree of drug resistance (21,22). The gene coding for the human Pgp was also identified and named *MDR1* gene in the 1980s (23). Finally, it has been shown that transfection of sensitive cells with the *MDR1* gene results in MDR phenotype (24).

Upon further investigation of multidrug resistant cell lines and chemotherapy resistant tumor samples, two other drug exporter proteins, ABCG2 and MRP1, were discovered (25). The substrate spectra of the above transporters include the majority of chemotherapeutic drugs used in cancer treatment (26) and it was also proved that they all belong to the ABC protein family.

3. Theoretical background

3.1. General structure of ABC proteins

ABC proteins form one of the largest and the most versatile protein families. Members of the ABC protein family are present in all domains of life, from bacteria to humans. A common structural feature of ABC proteins is their unique evolutionary conserved nucleotide-binding domain (NBD), the so-called "ATP-binding cassette" that consist of several conserved amino acid sequence motifs (27). These conserved NBD sequences, among others, include the Walker A and B sequences that are present in all ATP-binding proteins and the "signature" motif (C-loop) that can only be found in ABC proteins. Functionally active ABC proteins possess two NBDs that collectively form two composite nucleotide-binding sites (NBSs) in which ATP molecules are "sandwiched" between these conserved motifs (for more details see *Section 3.3.4*).

Members of the ABC protein family show enormous functional diversity. They are involved in several physiological processes including DNA repair, regulation of protein synthesis or even RNA processing. However, the majority of them are transmembrane proteins that function as channels, channel regulators or active transporters (28-30). Considering the direction of transport, ABC transporters can be either exporters or importers (31).

Importer type transporters are present only in archaea and bacteria and they are involved in the uptake of nutrients (e.g., carbohydrates) and micronutrients (e.g., vitamins) with high specificity (32-34). Prokaryotes also express a large number of exporter type ABC proteins. MsbA is a lipid A exporter protein of Gram-negative bacteria (35), the malfunction of which can lead to the accumulation of lipopolysaccharides and phospholipids in the cytoplasmic membrane of *E. coli* (36). MsbA displays a significant sequence similarity (30%) to LmrA, the multidrug transporter protein of *Lactococcus lactis* (37,38). Interestingly, the substrate specificities of LmrA and Pgp are strikingly similar (39). Expression of LmrA in mammalian cells can render the cells resistant to many Pgp substrates (37). This high level of sequence- and functional similarity suggests phylogenetic connection between bacterial transporters and Pgp (40). Of note, bacterial ABC exporters such as LmrA can also confer resistance against several antibiotics (41,42) hampering successful antimicrobial therapy.

As opposed to prokaryotic ABC transporters, according to our current knowledge, all eukaryotic ABC transporters function as exporters (43). Essentially each organism expresses multiple ABC transporters that can mediate various cellular transport processes (44,45).

The human genome encodes 48 ABC proteins that are classified into seven subfamilies from ABCA to ABCG based on their sequence similarity (**Fig. 1a**) (46). Interestingly, members of the ABCE and ABCF subfamilies are soluble proteins that do not contain TMDs (47) (**Fig. 1b**). The majority of them are membrane transporters that need at least four domains for transport activity: the two transmembrane domains (TMDs) build up the substrate-binding cavity and the substrate translocation pathway through which the transport of substrates is realized, while the two NBDs are responsible for the binding and hydrolysis of ATP (48). Half-transporters contain only one NBD and one TMD and form homodimers (e.g., ABCB7, ABCD1, ABCG2) or heterodimers (e.g., TAP1/TAP2, ABCG5/8) in the membrane (**Fig. 1b**) (49). In contrast, in full transporters all domains are encoded by a single gene and they may have been evolved from an ancestral half transporter, by a gene duplication event (50,51). Beside the two TMDs and two NBDs several human ABC transporters have additional domains, e.g., the extracellular domains (ECD1/2) of ABCA4 (52), the accessory TMD (TMD0) of MRP1 (ABCC1) (53) or the disordered, regulatory R domain of CFTR (ABCC7) (54) (**Fig. 1b**).

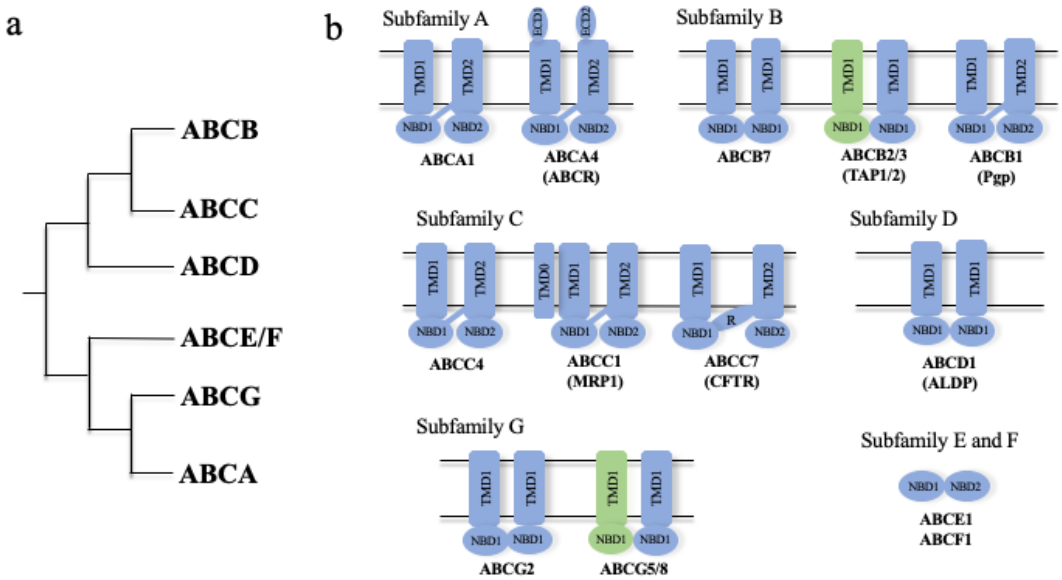

Figure 1: Simplified phylogenetic tree of human ABC transporters (a) and schematic representation of the structural diversity of human ABC proteins (b) (based on (55) and (56))

3.2. Examples of human ABC proteins and related diseases

ABC proteins are involved in many important physiological processes, consequently mutations leading to their complete deficiency or decreasing their activity or expression level often cause diseases or predispose to certain disorders (**Table 1** shows examples of diseases linked to mutations of human ABC proteins) (57,58).

Several ABC proteins, like ABCA1, ABCB4 or ABCD1, play a role in lipid transport processes. ABCA1 exports phospholipids and excess cholesterol from the cell membrane and loads them to lipid-free apolipoprotein A-1 (apoA-I) to form nascent HDL. Several mutations causing the lack of functional ABCA1 expression were identified and found to be associated with the rare autosomal disorder called Tangier-disease. Tangier-disease is characterized by a strongly reduced high-density lipoprotein (HDL) level in the blood and decreased reverse cholesterol transport (59). This leads to the accumulation of cholesterol-esters in peripheral reticuloendothelial tissues (e.g., tonsils, lymph nodes, thymus or spleen) leading to atherosclerosis and higher incidence of early onset cardiovascular diseases (60-62).

ABCD1 (ALD) is responsible for the transport of very-long chain fatty acids into the peroxisomes for degradation. Loss of function mutations of ABCD1 cause the fatal disorder adrenoleukodystrophy, which is identified by the accumulation of very-long chain fatty acids in various tissues. The central nervous system (CNS) is particularly affected by ABCD1-deficiency leading to demyelination and neurodegeneration (63).

Bile is a complex mixture that includes bile salts, phosphatidylcholine (PC), cholesterol and various endobiotic and xenobiotic toxins, each of which is secreted across the canalicular membrane of hepatocytes by different ABC transporters. Bile salts are synthesized from cholesterol in the hepatocytes and exported to the bile by ABCB11 (bile salt export pump, BSEP). Loss of function mutations of ABCB11 lead to the accumulation of toxic bile salts inside the hepatocytes resulting in the disease called familial intrahepatic cholestasis type II (64-66). ABCB4, similarly to ABCB11, is expressed in the canalicular membrane of hepatocytes and flops PC from the inner leaflet of the membrane to the outer leaflet where it is extracted by the bile salts to form a mixed micelle that reduces the detergent activity of bile salts. Reduced or missing activity of ABCB4 also causes cholestatic liver disease.

Pseudoxanthoma elasticum (PXE) is a metabolic disorder caused by the inactivating mutations of the ABCC6 transporter (67). PXE is characterized by a generalized late-onset ectopic calcification of several tissues including the skin, the blood vessels and the eye (68). The exact pathomechanism of the disease and the physiological substrate of ABCC6 remained unknown until recently. New studies proved that ABCC6 transports ATP through the

basolateral membrane of liver cells to liver sinusoids. Subsequently, ATP is converted to pyrophosphate (PP_i), a well-known inhibitor of calcification, by ectonucleotidase enzymes (69). The lack of ABCC6-mediated ATP transport significantly decreases the PP_i concentrations in the blood leading to the formation of hydroxyapatite precipitates in peripheral tissues. It has been shown that ectopic calcification can be prevented by pharmacological correction of the plasma membrane expression of misfolded or mislocalized ABCC6 mutants with preserved transport activity using the chemical chaperone 4-phenylbutyrate (4-PBA) (70). In addition, several studies proved that oral PP_i administration can also inhibit ectopic calcification (70-72).

Table 1: Examples of diseases linked to the mutation of human ABC proteins

Name	Physiological/endogenous substrates	Related disease
ABCA1 (ABC1)	Cholesterol, phospholipids	Tangier disease *
ABCA4 (ABCR)	Vitamin A derivatives	Stargardt disease *
ABCB1 (MDR1)	Non identified	Multidrug resistance **
ABCB2/3 (TAP1/2)	8-15 amino acid peptides from ER	Immunodeficiency *
ABCB4 (MDR3)	Phosphatidylcholine	Familiar intrahepatic cholestasis*
ABCB7	Iron	X-linked sideroblastic anemia*
ABCB11 (BSEP)	Bile acids	Familial intrahepatic cholestasis type II*
ABCC1 (MRP1)	Leukotriene C_4, estrogens, prostaglandins, glutathione	Multidrug resistance **
ABCC2 (MRP2)	Bilirubin	Dubin-Johnson syndrome *
ABCC6	ATP	Pseudoxanthoma elasticum*
ABCC7 (CFTR)	Cl^-	Cystic fibrosis *
ABCC8 (SUR1)	K^+	Familial hyperinsulinemic hypoglycemia *
ABCD1 (ALD)	Very long chain fatty acids (22 or more carbon atoms)	Adrenoleukodystrophy *
ABCG2 (BCRP)	Uric acid	Multidrug resistance **, Gout*
ABCG5/8	Cholesterol	Sitosterolemia*

** - due to loss-of-function mutation, ** - due to gain-of-function mutation)* (based on (57,58)

Cystic fibrosis (CF) is a multi-organ disease that is linked to the loss-of-function mutations of the cystic fibrosis transmembrane conductance regulator protein (CFTR, ABCC7). CF is one of the most prevalent ABC-protein related diseases. CFTR is a channel protein conducting Cl^- ions across epithelial cell membranes. The decreased function or expression of CFTR protein may lead to dysregulation of the epithelial fluid transport in many organs including the lungs, the pancreas and the intestinal epithelium. One of the major symptoms of CF include the serious recurrent respiratory infections caused by the abnormal

composition of airway surface liquid and consequential decreased mucociliary clearance. (73). In almost 85% of CF cases the deletion of one phenylalanine amino acid at the position of 508 is observed that leads to abnormal folding of the protein and its subsequent degradation in proteasomes resulting in the lack of functional CFTR chloride channels in the apical membrane of epithelial cells (74).

Beside many anticancer drugs, uric acid is also a substrate of ABCG2 (BCRP) and accordingly ABCG2 is involved in intestinal uric acid excretion (75). Certain ABCG2 mutations, e.g., 141K mutation, decrease the cell surface expression of ABCG2 (76), resulting in elevated uric acid blood concentrations (hyperuricemia) and an increased risk of gout, a painful inflammatory arthritis characterized by monosodium urate crystal deposition in the synovial fluid (77).

Taken together, the majority of the above discussed diseases are caused by aberrant folding of an ABC protein that can lead to proteasomal degradation and strongly reduced cell surface expression of the protein (78). Progress in chemical correction of trafficking- or folding mutant variants of CFTR and other ABC proteins showed that chemical chaperons, (e.g., 4-PBA) can be used generally to improve the function of multiple defective ABC proteins (79). Most recently, cryo-electron microscopy (cryo-EM) studies of different trafficking-deficient ABC proteins made it possible to obtain structural insights into the action of chemical chaperones (78,80). These studies provide foundation for structure-based development of novel chemical correctors.

3.3. P-glycoprotein and ABCG2

3.3.1. Physiological tissue expression of Pgp and ABCG2

As it was highlighted in *Section 2,* human multidrug transporters, including Pgp and ABCG2, are frequently expressed in various tumor cells and might be responsible for the chemotherapy resistance of tumors. However, Pgp and ABCG2 are also expressed in various normal tissues. Several studies have been performed to precisely map their physiological expression pattern. Of note, mRNAs of both transporters were detected at low levels in numerous tissues, however, only a few tissues showed constitutively high transporter expression in the plasma membrane of cells (81,82). It has been shown in Pgp knock-out mice that disruption of Pgp expression under physiological circumstances results in no major phenotypical effect in mice (83). However, serious neurotoxicity was observed when knock-out mice were treated with certain Pgp substrate cytotoxic drugs, suggesting that Pgp can

protect the central nervous system (CNS) from toxic compounds (84). In accordance with their protective role both Pgp and ABCG2 were detected in the luminal membrane of endothelial cells, in the blood-brain and blood-testis barriers as well as in the syncytiotrophoblasts of placenta (85,86). Both Pgp and ABCG2 show high expression levels in the apical membrane of intestinal epithelial cells, hepatocytes and kidney proximal tubule cells (87,88). In addition, high ABCG2 and Pgp expression levels were found in different stem cell populations, e.g., in hematopoietic stem cells or in stem cell-like cancer cells present in different tumor types, and therefore ABCG2 is deemed a ubiquitous stem cell marker (89-92).

The tissue expression patterns of Pgp and ABCG2, along with *in vitro* and *in vivo* functional studies suggest that restricting the transmembrane passage of numerous drugs these transporters can contribute to the formation of effective pharmacological barriers and thus they are important determinants of drug absorption, distribution, excretion and toxicity (93).

3.3.2. Structure of Pgp and ABCG2

Pgp is a 1280 amino acid long single polypeptide chain consisting of two TMDs, each containing 6 transmembrane helices, and two NBDs (18). As opposed to Pgp, ABCG2 is a 655 amino acid long half-transporter consisting of only one TMD with 6 transmembrane helices and one NBD with a reversed NBD-TMD orientation compared to Pgp (**Fig. 2a, b**).

Eukaryotic ABC transporters seem to share common major conformational states as it was shown in several crystal structures of ABC transporters and indicated by biochemical and biophysical experiments (94-97), including the "inward-facing" and "outward-facing" conformations. In the inward-facing conformation, Pgp and ABCG2 form an inverted "V"-shape, with a large cavity in the center that is accessible from the intracellular space (**Fig. 2b**). The inward-facing conformation allows substrates to enter and bind to the drug-binding cavity lined by TMD helices. The "outward-facing" conformer is characterized by the close contact of the NBDs and opening of the central cavity to the extracellular space (**Fig. 2b**). The proposed role of the outward-facing conformation is the release of substrates to the extracellular space (98).

Membrane topology and structure of Pgp was first studied by electron microscopy (EM): an 8Å resolution structure was published that confirmed the predicted membrane topology of the transporter possessing two TMDs, each formed by 6 membrane spanning alpha helices and two intracellular NBDs (**Fig. 2a, b**) (99). The first mammalian Pgp X-ray crystal structure was reported by Aller et al. in 2009. They described the structure of mouse Pgp in ATP-free (apo) inward-facing state, in the presence or absence of bound inhibitors, at

3.8-4.4 Å resolution (96,100). The transmembrane alpha helices form two bundles (TMs 1-3,6,10,11 and TMs 4,5,7-9,12) that surround a large internal cavity open to both the cytoplasm and the inner leaflet of the plasma membrane for substrate entry (**Fig. 2b**).

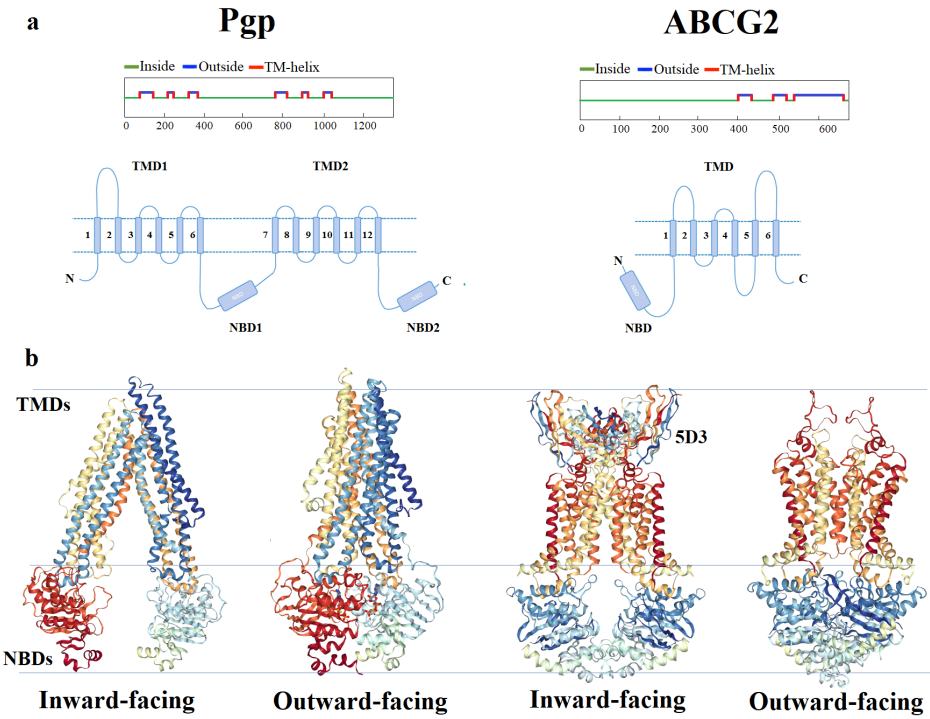

Figure 2: Structure of Pgp and ABCG2. Predicted membrane topology of Pgp and ABCG2 based on their amino acid sequences using the OCTOPUS membrane topology predicting tool (**a**). Cryo-EM structures of Pgp and ABCG2 in the nucleotide-free (apo) inward-facing and in the outward-facing ATP-bound conformations (**b**) The inward-facing conformation of ABCG2 was visualized in complex with two antigen-binding fragments (Fabs) of the monoclonal human-specific, inhibitory antibody 5D3 (101,102)

The first low-resolution ABCG2 structural data came from EM analysis of purified proteins in the presence or absence of the substrate mitoxantrone (103,104). Due to the lack of ABCG2 crystals, further studies aimed to model the structure of ABCG2 using available high-resolution inward-facing crystal structures of various ABC transporters. First studies used the structures of bacterial multidrug transporters, such as MsbA and Sav1866 (105,106), despite their low sequence similarity and known differences in their domain organization, while a recent study used the crystal structure of human ABCG5/G8, a close homologue of ABCG2, as a template (107). These structural studies showed a compact, inward-facing homodimer fold with an apparent large cavity lined by TMD helices, shorter intracellular loops and NBDs in close proximity of TMDs. Moreover, distinct structural elements of ABCG fold were observed, e.g., the elbow helix parallel with the inner membrane leaflet (**Fig. 2b**) (107).

Until recently, one major caveat of crystallographic studies was that they were only able to capture the apo, inward-facing conformation of Pgp and ABCG2. The first outward-facing Pgp structure (CmABCB1 from *Cyanidioschyzon merolae*) was published in 2019 (108). Recently, a large number of new transporter structures were reported that were obtained using cryo-EM to provide crucial structural information. Inward- (apo) and outward-facing (ATP-bound) conformations of Pgp and ABCG2 have been published serving insights into nucleotide, substrate- and modulator binding (**Table 2**, **Fig. 2b**). Analysis of human Pgp and ABCG2 using available high-resolution cryo-EM structures confirmed the anticipated conformational changes similar to those observed in other ABC transporters (94,95,109,110).

Table 2: List of currently available Pgp and ABCG2 cryo-EM structures (based on (111)**)**

Protein	Ligand	Orientation	Source	Resolution	PDB ID	Ref.
Pgp	UIC2-Fab	Inward-facing	Mouse/Human	4.14	6FN4	(112)
Pgp	UIC2-Fab, zosuquidar	Inward-facing	Mouse/Human	3.58	6FN1	(112)
Pgp	UIC2-Fab, taxol	Inward-facing	Human	3.6	6QEX	(101)
Pgp	UIC2-Fab, zosuquidar	Inward-facing	Mouse/Human	3.9	6QEE	(101)
Pgp	ATP	Outward-facing	Human	3.4	6C0V	(113)
ABCG2	5D3-Fab, cholesterol	Inward-facing	Human	3.8	5NJ3	(114)
ABCG2	5D3-Fab, E1S	Inward-facing	Human	3.58	6HCO	(102)
ABCG2	5D3-Fab, MZ29	Inward-facing	Human	3.1	6ETI	(115)
ABCG2	MZ29	Inward-facing	Human	3.56	6FFC	(115)
ABCG2	ATP	Outward-facing	Human	3.09	6HBU	(102)

Nonetheless, the major conformers represent only snapshots of the whole catalytic cycle with multiple different transition states. Importantly, cryo-EM technique can be used for structural studies even under active turnover conditions. Cryo-EM allowed for capturing multiple different transition states of various ABC transporters and provided unprecedented insights into their transport mechanism (116,117).

3.3.3. Transmembrane domains and substrate binding

Pgp is a full transporter consisting of two TMDs (TMD1 and TMD2), while ABCG2 is a half transporter that forms a homodimer, as it was already discussed in *Section 3.3.2*. Pgp is thought to have arisen from an ancient half-transporter by a gene duplication event, followed by randomly occurring point mutations upon its evolution resulting in a pseudo-symmetric protein (118). Surprisingly, there is only 59.4% sequence similarity between the

two "halves" of mouse Pgp. More specifically, there is 77.3% similarity between the NBDs, while the TMDs diverged more, exhibiting only 43.5% sequence similarity (119). The TM helices collectively form a large substrate-binding cavity that spans almost the entire width of the lipid membrane (**Fig. 3a**) (101,120). As it is shown in (**Fig. 3)**, both halves of Pgp contribute in a pseudo-symmetric fashion to substrate binding, as the contacting amino acid residues belong to TM1, TM4, TM5, and TM6 of TMD1 and to TM7, TM10, TM11 and TM12 of TMD2. In addition to the aromatic and hydrophobic residues, there are also polar or charged side chains on the surface of the substrate-binding cavity. On the other hand, the homodimer ABCG2 shows complete axial rotational symmetry, implying that every structural element in the protein is found twice. As opposed to Pgp, the substrate-binding cavity of ABCG2 is narrower (see **Fig. 2b**), more hydrophobic and because of the symmetric structure of ABCG2 it is delimited by TM helices 1, 2 and 5 from both monomers (**Fig. 3b**) (114). Moreover, a second smaller drug-binding cavity (cavity 2), close to the extracellular gate of the translocation apparatus, can be observed in cryo-EM structures of ABCG2 (see **Fig. 2b**) (114). The surface area of cavity 2 is less hydrophobic as compared to cavity 1, probably resulting in a lower substrate-binding affinity, and thus it might have a role in the release of substrates to the extracellular space (115). Taken together, the structural differences between the substrate-binding cavities of Pgp and ABCG2 probably imply different substrate translocation mechanisms (121).

Earlier studies aiming to describe how polyspecific substrate binding is accomplished by Pgp and ABCG2 applied photoactive substrate analogs. Photolabeling of Pgp and ABCG2 with a substrate analog (125I)-iodoarylazidoprazosine (IAAP) or Pgp with propafenone derivatives suggested that these ligands were recognized by at least two distinct regions of the proteins (122-126). Based on studying the kinetics of Pgp-mediated drug transport, Shapiro et al. supposed the presence of three drug-binding sites that were specific to particular substrates, namely the H-site (for Hoechst 33342), R-site (for rhodamine 123) and the P-site (for prazosin and progesterone) (127,128). On the other hand, radio-ligand saturation studies identified four pharmacologically distinct substrate-binding sites in Pgp with complex allosteric interactions between them (129).

Similar to Pgp, studying the kinetics of anthracycline (daunorubicin and doxorubicin) transport by ABCG2, the presence of two symmetric binding sites with extensive allosteric interactions with other substrates was demonstrated (130). Taken together, these findings strongly support the existence of multiple substrate-binding sites in the substrate-binding

cavity of Pgp and ABCG2. However, these kinetic studies could not answer the question whether these sites are spatially separated, or they overlap with each other.

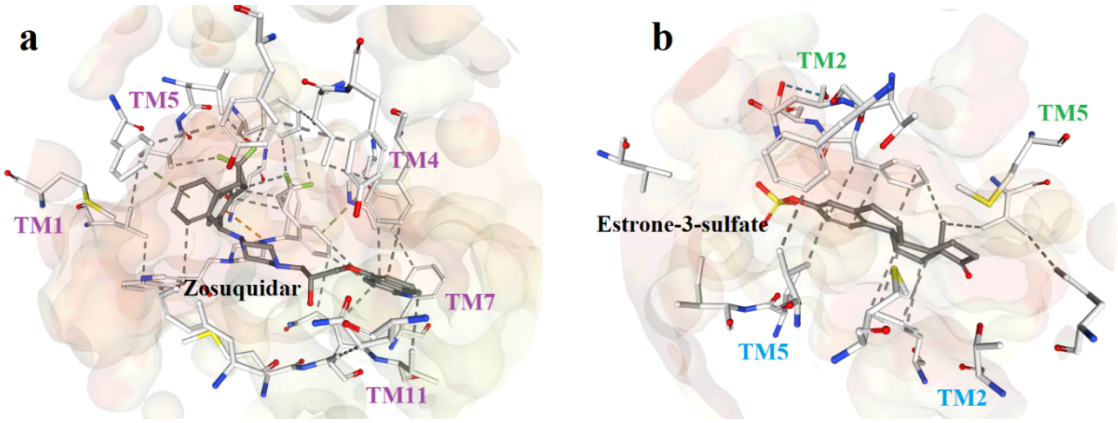

Figure 3: Interactions of the TMD residues with zosuquidar in Pgp (a) and estrone-3-sulfate (E1S) in ABCG2 (b). In panel (**a**) TM6, TM10, TM12 and the second bound zosuquidar molecule are not shown because of steric reasons. Blue dashed lines represent hydrogen bonds, while grey dashed lines show hydrophobic interactions. (102,112)

X-ray crystallography and cryo-EM studies of Pgp showed that different drugs bind to distinct, but sometimes overlapping sites in a larger binding cavity formed by TM helices (112,131,132). In addition to structural data, cysteine mutagenesis experiments were used to identify residues involved in substrate binding (133,134). These studies proved that the binding sites of several drugs including cyclosporine A, tariquidar or valinomycin spatially overlapped in Pgp (132). Furthermore, it has been shown in transport and ATPase activity measurements, that drugs can interact with an auxiliary binding site and can be transported, when amino acids forming the primary binding site are mutated (122,135-137). These findings support the complex and flexible nature of the substrate-binding pocket. According to the "substrate-induced fit" mechanism, the complex substrate-binding pocket can accommodate structurally different substrate molecules by exposing different amino acid residues on the surface of the pocket as a result of substrate-specific rotational and lateral movements of the TM segments (138).

3.3.4. Nucleotide-binding domains and ATP binding

NBDs of ABC transporters are the functional units responsible for ATP binding and hydrolysis. Both NBDs of ABC proteins contain a RecA-like domain and a α-helical domain (139). The RecA-like subdomain was first identified in RecA, an *E. coli* protein involved in DNA recombination (140). The RecA-like subdomain is formed by the evolutionary conserved Walker A and Walker B sequences and it is present in many ATPases and molecular motors (141). On the other hand, the α-helical domain, which contains the

signature sequence (LSGGQ motif) is characteristic for the NBDs of ABC transporters (139). In all ABC transporters, the two NBDs collectively form two nucleotide-binding sites (NBS1 and NBS2). Upon ATP binding, the ATP molecules are sandwiched between the Walker A and Walker B motifs of one NBD and the signature motif of the contralateral NBD (142). Beside the Walker A, Walker B and signature motifs, NBSs of Pgp and ABCG2 are characterized by a series of additional evolutionary conserved sequence elements (**Table 3 and Fig. 4**). In accordance with their crucial role in ATP binding and hydrolysis, mutations of highly conserved residues within these sequence motifs significantly reduce or completely abolish ATPase and transport activity, as it was highlighted in many mutagenesis studies (143,144).

The Walker A motif of NBDs is primarily involved in hydrogen-bond formation with the beta and gamma phosphates of ATP. Mutation of a conserved Walker A lysine to methionine or arginine (in human Pgp: K433M/R, K1076M/R) in one or both NBDs is thought to prevent ATP hydrolysis, while it does not circumvent nucleotide binding (145-147).

The Walker B motif is believed to play a role in the coordination of Mg^{2+} needed for ATP hydrolysis, however, its exact function in the hydrolysis reaction remains disputed (148). Neutralization of the acidic Walker B glutamate – frequently termed as the "catalytic glutamate" - in one or both NBSs (E556 and/or E1201 in human Pgp) leads to high-affinity binding (trapping) of a single ATP in Pgp (149,150). Similarly to human Pgp, high affinity ATP binding was observed in mouse Pgp (Mdr3) with mutant catalytic glutamates at the homologous positions (E552Q and E1197Q in NBD1 and NBD2, respectively) (151,152). Single amino acid changes at the adjacent positions (D555N or D1200N in human Pgp) also resulted in a catalytically dead protein in accordance with the role of these residues in Mg^{2+} binding (153). In ABCG2, homodimers of E211Q Walker B mutant proteins showed no transport and ATPase activity (154).

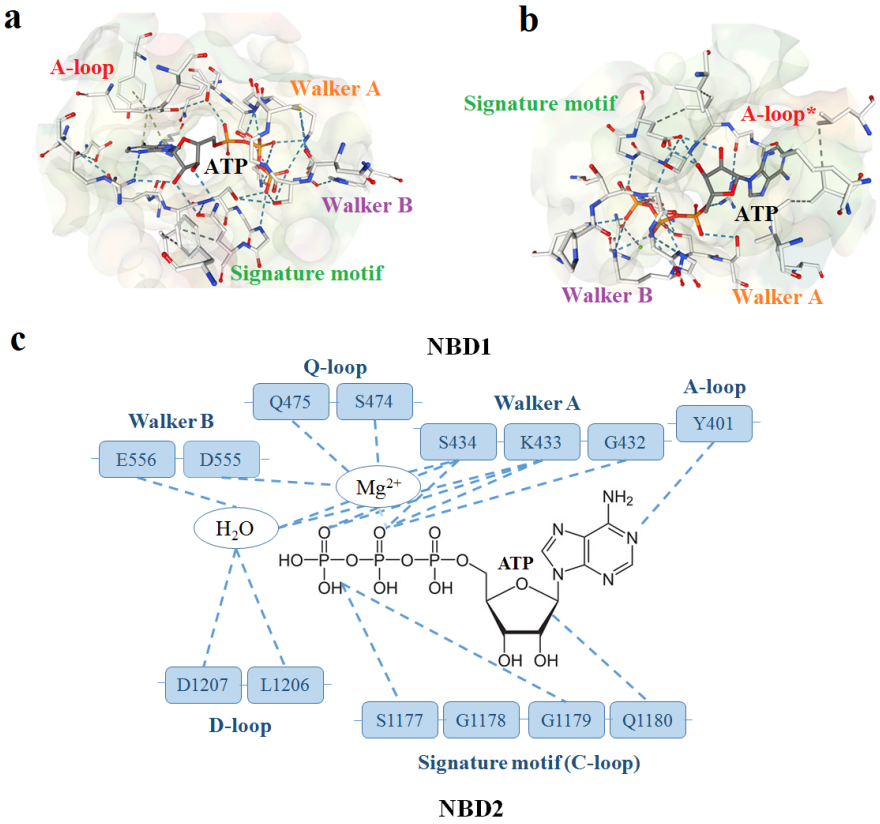

Figure 4: Interactions of conserved NBS motifs with ATP in human P-glycoprotein (a) and ABCG2 (b) represented in available cryo-EM structures. (102,113) (*blue dashed line = hydrogen bonds, grey dashed line = hydrophobic interactions*, * = putative A-loop replacement site in ABCG2). Schematic representation of ATP binding by NBS1 in Pgp (**c**)

The ABC-signature motif or C-loop is unique to ABC transporters and is essential to proper ATP binding and NBD-dimer formation. Mutagenesis studies in Pgp showed that C-loop mutations in one or both NBDs reduce cell surface expression and the mutant variants are functionally inactive (155,156).

In Pgp – along with many other ABC proteins – an aromatic residue (A-loop), usually a tyrosine, interacts with the adenosine ring of the nucleotide. According to numerous site-directed mutagenesis studies, A-loop is identified as a motif needed for proper ATP binding (157,158). Mutation of the conserved A-loop tyrosine (Y401 or Y1044 in human Pgp) either at one or both NBDs abolishes nucleotide binding and ATPase activity (157,159). According to new structural data, the A-loop is missing from ABCG2 and residues in the putative replacement site form van der Waals interactions with the nucleobase of ATP (102).

Table 3: Conserved NBS motifs/residues and their main functions in human Pgp and ABCG2

Motif name	Amino acid position		Proposed function
	Pgp NBS1	ABCG2	
A-loop	401	185*	Adenosine binding
Walker A	427-434	80-87	ATP-binding pocket formation
Q-loop	473-477	126	Inter-domain communication
Signature	531-536	186-200	Cross-dimer ATP-binding pocket formation
Walker B	551-556	206-211	ATP-binding pocket formation
D-loop	559-562	217	Cross-dimer interaction
His-loop	583-587	243	ATP-dependent switch region

* = putative A-loop replacement site (based on (160,161)

The interaction between TMDs and NBDs is mediated by intra-cytosolic loop (ICL) domains that specifically connect the TMDs to the Q-loops of NBDs (162). Structural data showed that the evolutionary conserved Q-loop is positioned in the upper surface of the NBDs, strongly interacting with TMD helices (102,163). Moreover, it has been demonstrated that Q-loops - similarly to the Walker B motifs - play important roles in the coordination of Mg^{2+} and they are also in contact with the γ-phosphate of ATP (162,164). As a corroborating finding, cryo-EM structure of the outward-facing Pgp demonstrated that Q475 and Q1118 residues reach into the ATP-binding sites and contribute to the closed NBD-dimer interface formation (113).

Pgp and ABCG2 – as primary active transporters – use energy derived from ATP-hydrolysis to fuel the transport cycle (163). Interestingly, Pgp, ABCG2 and several other ABC transporters show weak ATP hydrolysis activity, often termed as “basal” ATPase activity even in the absence of substrates, which can be increased several folds by the addition of substrates and referred as “substrate-stimulated” ATPase activity. Certain studies linked “basal” ATPase activity to the transport of endogenous substrate molecules present in the plasma membrane (e.g., cholesterol, phospholipids) (119,165,166). Other explanations emphasized that “basal” ATPase activity is necessary for resetting the inward-facing substrate binding conformation of the transporter and thus it is an inherent mechanistic property of certain ABC transporters (167).

3.4. Catalytic cycle and drug transport mechanism of Pgp and ABCG2

3.4.1. Catalytic cycle models

Despite decades of intense research on Pgp and ABCG2 there are still questions unanswered regarding the fine details of their catalytic cycles. Partly it is due to experimental and instrumental limitations of membrane protein research, e.g., difficulties related to the purification and crystallization of large membrane proteins (168). On the other hand, computational limitations of molecular dynamics simulations (nanosecond range) make *in silico* analysis restricted to only certain events of the catalytic cycle (169,170). However, recent developments in structural biology and spectroscopic techniques (e.g., double electron-electron resonance (DEER) spectroscopy) helped to better understand the mechanism of these enigmatic transporters (101,102,113,171).

Based on the controversial findings of several biochemical experiments and computational simulations, many different models were formulated to describe the catalytic cycle of Pgp. These models can be classified in many different ways based on their specific features. One way of classification is based on the interactions between the NBDs during the catalytic cycle. Certain models predict that NBDs dissociate in the absence of nucleotides (e.g., **ATP-switch model** (172) or the **processive clamp model** (173)), while other models anticipate that the two NBDs remain associated at all steps of the catalytic cycle (e.g., **alternating catalytic sites model** (174), **nucleotide occlusion model** (175) or the **constant contact model** (176)) (for details see **Table 4**). Despite their important differences, the models describing the molecular details of the catalytic cycle of Pgp share similar steps including: (1) binding of two ATP molecules to the inward-facing high-affinity conformer, (2) NBD-NBD sandwich dimer formation, (3) conformational remodeling of TMDs leading to the low substrate-binding affinity outward-facing conformation, (4) nucleotide hydrolysis at the NBDs, (5) release of ADP and inorganic phosphate (Pi) and (6) resulting conformational changes in the TMDs and resetting the cycle (102,113,177) (**Table 4**).

One of the first catalytic models, the **alternating sites model** is hinged on the strictly alternating nature of ATP hydrolysis by the two NBDs of Pgp (174). The model makes the assumption that both NBSs bind ATP with similar affinity and NBSs strongly interact with each other and they cannot hydrolyze ATP independently. Following ATP-binding and hydrolysis at NBS1, a high-energy conformational state is formed with the bound hydrolysis products ADP and Pi. Due to the dissociation of Pi from NBS1 another ATP molecule can bind to NBS2, the high energy state relaxes and the drug-binding affinity decreases allowing for the efflux of the bound substrate. ATP hydrolysis at NBS2 catalyzes the transport of a

second substrate molecule. Of note, in a single cycle two substrate molecules are transported and two ATP molecules are hydrolyzed. Proposed functional inter-dependency and strict alternation of ATP hydrolysis by NBSs was established relying on experiments using cys-less Pgp molecules with a single cysteine residue re-introduced to one of the NBDs and covalently labeled with N-ethylmaleimide (NEM) (178). Covalent modification of either NBSs led to complete inactivation of the ATPase activity of Pgp molecules.

Table 4: Brief overview of the major molecular steps of the different catalytic cycle models (based on (179)

	NBD-dissociation		**NBD-association**		
Steps	**ATP-Switch** (172)	**Processive clamp** (173)	**Alternating sites** (174)	**Constant contact** (176)	**Nucleotide occlusion** (163)
1	NBDs: Empty, completely separated TMDs: Inward open, substrate binding	NBDs: Two ATPs bound; sandwich dimer formed	NBDs: semi-open dimer *NBS1:* ATP binding *NBS2:* Empty TMDs: Inward open, substrate bound	NBDs: Semi-open dimer *NBS1:* Occluded ATP-bound *NBS2:* Empty	NBDs: Semi-open dimer *NBS1:* Occluded ATP *NBS2:* Loosely bound ATP TMDs: Inward open
2	NBDs: ATP binding, dimer formation TMDs: Outward open, substrate release	*NBS1:* ATP hydrolysis	*NBS2:* ATP binding *NBS1:* Hydrolysis, formation of transition state	*NBS1:*Occluded, hydrolysis *NBS2:* Open	TMDs: Substrate binding
3	NBDs: Hydrolysis	*NBS2:* ATP hydrolysis, P_i release	*NBS1:* P_i release TMDs: Outward open	*NBS1:* P_i release, open *NBS2:* ATP binding	*NBS1:* Hydrolysis *NBS2:* Occluded TMDs: Outward open
4	NBDs: ADP, P_i release, separated NBDs TMDs: Inward open	NBDs: Separated, ADP release	*NBS1:* ADP release TMDs: Inward open, substrate release	*NBS1:* ADP release, empty, occluded *NBS2:* ATP occluded	*NBS1:* ADP, P_i release TMDs: Inward open

Similarly, **nucleotide occlusion model** also assumes an intimate interaction between the NBDs (163). In the beginning of the catalytic cycle, the TMDs are open to the cytoplasmic side, while the NBDs are in a semi-open state characterized by a loose binding of an ATP molecule at one site and a tight binding of an ATP molecule at the other site. Such strong interaction between the ATP molecule and the NBS is termed “nucleotide occlusion”

(180). Following substrate binding, the "occluded" ATP is hydrolyzed switching the TMDs from an inward-facing state to the outward-facing, low substrate-binding affinity conformation. Subsequently, the previously loosely bound ATP gets occluded and dissociation of the hydrolysis products from the other site reopens the TMDs to the intracellular side.

The **constant contact model** proposes that the NBDs stay in close contact throughout the whole cycle without dissociation (176). The proximity of NBDs is supported by a series of experimental evidences, such as the chemical cross-linking of the signature- and Walker A motifs at conditions excluding ATP-hydrolysis (4^{o}C and absence of nucleotides) (156). In the constant contact model, no double ATP-bound intermediate can be observed, ATP-hydrolysis occurs alternately at each NBSs. ATP-hydrolysis at one site opens up the other site for ATP binding and hydrolysis due to specific rotational movements of the RecA-like and α-helical domains (176).

In contrast to the previously described models, X-ray crystallographic and cryo-EM structures of Pgp in the inward-facing state demonstrated complete separation of the NBDs (96,101,112). In accordance with the above structural data, the **ATP-switch** model suggests that in the initial state of the catalytic cycle NBDs are completely separated without any bound nucleotide and the transporter is in an inward-facing conformation (172). Substrate binding to the TMDs triggers a low-to-high switch in the nucleotide-binding affinity of NBDs resulting in the binding of two ATP molecules. Moreover, as opposed to the previously described models, in the ATP-switch model the binding of ATP and not the hydrolysis of it is responsible for the reorganization of TMDs to form an outward-facing conformer. Following the transport of the bound substrate molecule, both ATP molecules are hydrolyzed. Finally, the release of Pi and ADP resets the inward-facing conformation of Pgp. Similar to the ATP-switch model, the **processive clamp model** also suggests that hydrolysis of two ATP molecules is needed for the transport of a single bound substrate. In the beginning of the cycle, two ATP molecules are bound to the transporter leading to the NBD-NBD dimer formation and the opening of TMDs to the extracellular space. Sequential hydrolysis of both ATP molecules and the dissociation of Pi and ADP leads to the dissociation of the NBD dimer and switching of the TMDs back to the inward-facing state (173).

Interestingly, prevalent catalytic cycle models agreed that the functional activity of both catalytic centers is needed for the conformational changes and the transport activity of Pgp. As a corroborating evidence, phosphate analogues (e.g., vanadate (Vi), beryllium-fluoride (BeF_x)), which can replace the cleaved gamma phosphate forming a stable Pgp-ADP-

Vi/BeF_x complex at a single NBS, were shown to inactivate Pgp (181). Similarly, covalent modification of a single NBS by NEM prevents nucleotide binding and abolishes the ATPase activity of Pgp (178). In addition, several studies demonstrated that point mutations in the highly conserved key residues (see *Section 3.3.4*) of a single NBS also completely inactivate Pgp (143,146,149,154,155). However, in contrast to these findings, our group demonstrated that single Walker A mutant Pgp molecules show significant residual transport and ATPase activity when they are studied in their natural plasma membrane environment (177). Since the majority of studies reporting the inactivating effect of single catalytic site mutations have been performed using heterologous expression systems such as Sf9 (146,182), *Saccharomyces cerevisiae* (183) or purified and reconstituted proteins, it may be that the weak ATPase activity of the single Walker A mutants was missed due to the different plasma membrane composition of the heterologous expression systems, or artefacts related to the solubilization, purification and reconstitution of the proteins (162). On the other hand, the above-mentioned chemical modifications not only prevent ATP binding and hydrolysis at one of the NBSs but also, they may have more overall effects on the communication between the NBSs of Pgp.

Taken together, new approaches and experimental systems are required to clarify the fine details of the communication between the NBSs upon the catalytic cycle of Pgp (163,184).

3.4.2. Asymmetry in the nucleotide-binding sites

In about half of the human ABC transporters both NBDs are fully functional and either identical such as in ABCG2 or highly similar, such as in Pgp. Interestingly, in the other half of the human ABC transporters, the sequence of NBS1 has diverged from the consensus sequence (185).

In several ABC proteins including SUR1, MRP1, CFTR and the main bile acid transporter ABCB11, the glutamate residue in the Walker B sequence, often termed as "catalytic glutamate", is replaced with other "non-canonical" amino acids, such as aspartate in SUR1 and MRP1, or methionine and serine in ABCB11 and CFTR, respectively (186-188). In addition to the lack of "catalytic glutamate", other non-consensus substitutions occur simultaneously in particular conserved residues of the NBS1. For instance, ABCB11 has three additional substitutions, one in the Q-loop (E502) and the other two in the signature sequence (R1221 and E1223), as it is shown in (**Fig. 5)**. Interestingly, ABCB11 shows a remarkable sequence similarity to Pgp and the NBD-NBD interfaces of the two proteins differ only in the above mentioned four amino acids (**Fig. 5**). Interestingly enough, when the amino acid M584 was substituted with the canonical glutamate, ABCB11 showed transport and ATPase activity

comparable to wild-type protein. However, substitution of the other three non-canonical amino acids with the canonical ones reduced the transport activity of ABCB11 to about 35% of the wild-type protein supporting the crucial role of these amino acids in the catalytic mechanism (189).

Photo-labeling experiments using 8-azido-ATP suggested that ATP remains stably bound to the NBS1 for up to several minutes without hydrolysis in CFTR and MRP1 suggesting that the non-canonical type NBSs are unable to hydrolyze ATP at a rate comparable to canonical NBSs (190,191). As opposed to the listed transporters with a degenerate site, mutation of the "catalytic glutamate" in human Pgp in one or both NBSs (E556 and/or E1201) leads to trapping of ATP at the mutant site(s) and results in the inhibition of Pgp activity (149,152).

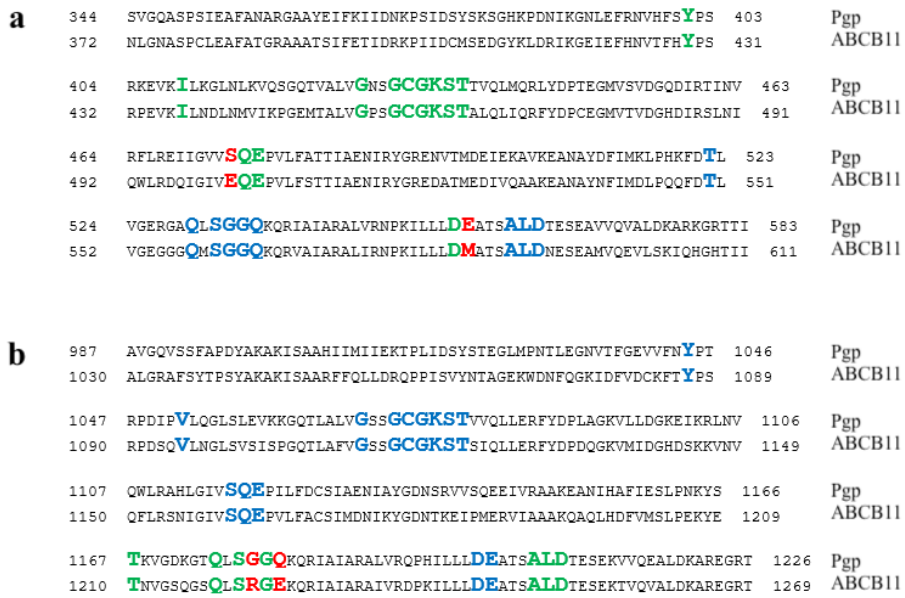

Figure 5: Alignment of Pgp and ABCB11 amino acid sequences using pBLAST. NBD1 (**a**) and NBD2 (**b**) sequences of human Pgp and ABCB11 were aligned, and residues involved in the formation of the ATP-binding sites are highlighted: NBS1 (green) and NBS2 (blue). The NBD-NBD interface of Pgp and ABCB11 differs only in four amino acids all located to NBS1: M584, E502, R1221 and E1223 in ABCB11 (highlighted in red).

Interestingly, even symmetrical ABC proteins, like Pgp or ABCG2, may exhibit transient functional asymmetry between NBS1 and NBS2. The binding affinity (K_D) of different nucleotides to Pgp was determined by tryptophan fluorescence quenching experiments using purified hamster Pgp molecules. Interestingly enough, the two NBSs of hamster Pgp exhibited significantly different K_D values (6 μM and 0.74 mM) for ATPγS, a non-hydrolysable ATP analogue (175). The high affinity binding of ATPγS at one NBS is probably indicative of nucleotide-occlusion. Similarly, such high-affinity ATP binding was

observed in catalytically dead Walker B mutant Pgp variants (152). Most recently, Verhalen et al. also observed structural asymmetry between the NBSs of mouse Pgp in the vanadate-trapped transition state applying DEER spectroscopy (192). Using spin labeled Pgp molecules, they monitored the conformational changes in the NBSs by measuring the distances between specific spin label-pairs. In the vanadate-trapped transition state, a short-distance component was observed for the spin label pairs monitoring the A-loop of NBS2, whereas minor changes in the distance distributions were observed for the equivalent pair at NBS1. The emergence of this short distance component was considered indicative of nucleotide occlusion, because in case of the double "catalytic glutamate" mutant variant (E552Q/E1197Q) this short distance component could be observed in both NBSs (192). This structural asymmetry at the A-loop region appeared only in the presence of substrates in accordance with the substrate stimulation of the ATPase activity, while it was not observable in the absence of substrates or in the presence of inhibitors (193). Molecular dynamic simulations also showed a more occluded NBS2 as a result of drug-binding (194).

Taken together, in the catalytic intermediates of human ABC proteins, the NBDs are not strictly symmetrical rather they can be either structurally asymmetric or they possess transient functional asymmetry in the absence of structural in-equivalence.

3.4.3. Tracking conformational changes of Pgp using conformation sensitive antibodies

Over the last few decades, several antibodies have been developed against human Pgp. Most of the antibodies recognize the extracellular loops connecting the TMDs. Some of these antibodies bind to linear epitopes (e.g., MM4.17) (195), while a series of antibodies have complex discontinuous epitopes (e.g., MRK16, MRK17, HYB-241, 4E3, 15D3, UIC2) (196-198). Some members of the latter group (e.g., MRK16, HYB-241 and UIC2) have been reported to inhibit the transport activity of Pgp (199-201).

UIC2 is an IgG2a isotype mouse monoclonal antibody that was developed against human Pgp. One of the most remarkable features of the UIC2 antibody is that it can bind to Pgp in a conformation-sensitive manner, recognizing the inward-facing, high substrate-binding affinity conformer (177,202). The conformation-specific binding of UIC2 is supported by a series of experimental findings. In intact cells, only a minor fraction of cell surface Pgp molecules are UIC2-reactive, while in the presence of certain Pgp substrates or modulators (e.g., vincristine, taxol, actinomycin D or cyclosporine A), a 2- to 4-fold increase in UIC2-reactivity can be observed that is often referred as "UIC2-shift" (94). Of note, ATP depletion switches Pgps into a UIC2-reactive conformation (94), while addition of MgATP to permeabilized cells decreases UIC2-reactivity in a concentration-dependent manner (177).

Xia et al. crystallized the Fab fragment of UIC2 and determined its crystal structure at a 1.65Å resolution (**Fig. 6b, c**) (203). Their study showed that UIC2-Fab has a positively charged surface, similarly to MRK-16 mAb (204), suggesting that the negatively charged extracellular loops of Pgp are important in its recognition by these monoclonal antibodies (203). Recently, the molecular structure of a chimeric Pgp variant in complex with UIC2-Fab was resolved by cryo-EM. It was demonstrated that UIC2-Fab binds to human Pgp with 1:1 stoichiometry and recognizes the inward-facing conformation of the transporter (**Fig. 6a**) (112). The discontinuous epitope of UIC2 mAb is formed by short peptide sequences in the 1st, 4th and 6th extracellular loops of the human Pgp (205-207).

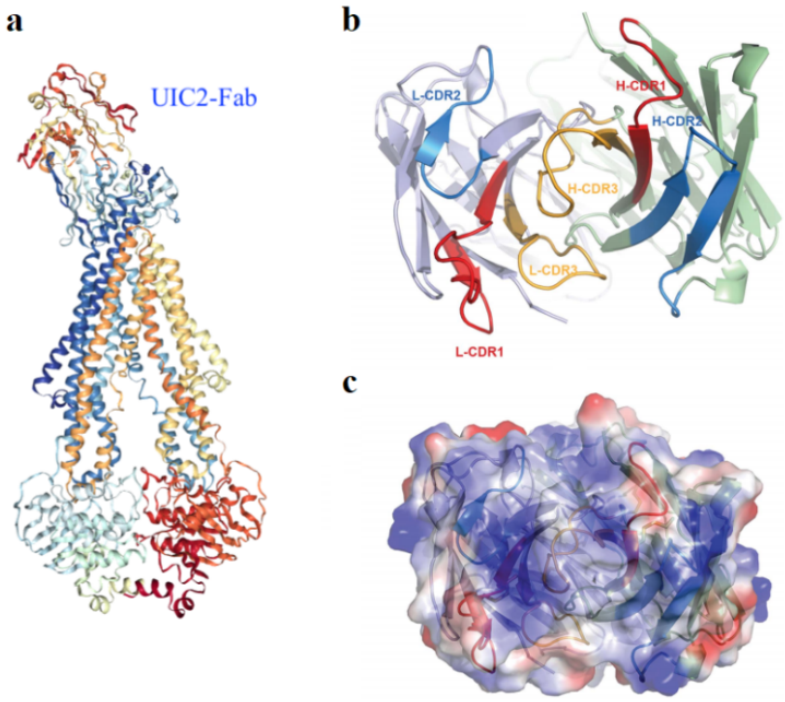

Figure 6: UIC2 binding to Pgp. Structure of a human-mouse chimeric Pgp variant in complex with UIC2-Fab (**a**). Ribbon representation of UIC2-Fab from the antigen side displaying the antigen-binding regions of the light- and heavy chains (**b**) and the electrostatic potential surface of UIC2-Fab showing the positively charged regions (**c**) (*blue color*) (203).

3.4.4. Drug transport mechanism by Pgp and ABCG2

The molecular details of the substrate translocation process by Pgp and ABCG2 were studied using several biochemical and biophysical techniques and have led to the development of different transport models.

Early studies suggested that similarly to ion transporting pumps, Pgp recognizes and transports its substrates from the cytoplasm (termed as the "pump" model) (208). However, most of the Pgp and ABCG2 substrates are hydrophobic or amphiphilic compounds characterized by high $logP_{ow}$ values and therefore they can reach significantly higher

concentrations within the membrane as compared to the cytoplasm (209). In accordance with this, fluorescent Pgp substrates doxorubicin and rhodamine 123 were shown to induce specific labelling of Pgp with iodonaphthalene-1-azide ((^{125}I)INA), a photosensitive membrane probe, in live cells. Since photoactivation of the probe is triggered by energy transfer from doxorubicin or rhodamine 123, this experiment proved that Pgp substrates accumulate in the membrane bilayer in the close proximity of the transporter (210). Moreover, several studies demonstrated that acetoxymethylester (AM) derivatives of various fluorescent calcium and pH indicators (e.g., Fura-2, Indo-1, Fluo-3, BCECF) and fluorescent dyes (calcein) can be expelled directly from the plasma membrane by Pgp before they could enter the cytosol and undergo hydrolysis by non-specific esterases (211).

Based on a detailed kinetic analysis, it has been shown that similarly to Pgp, ABCG2 can expel its substrates (e.g., mitoxantrone) directly from the plasma membrane (212). In accordance with this, crystal structure of Pgp and cryo-EM structures of Pgp and ABCG2 demonstrated the presence of portals through which substrates can reach the substrate-binding pocket directly from the inner-leaflet of the membrane thus ensuring a thermodynamically favorable access for hydrophobic substrates (101,132,213).

Two models were formulated to describe the transport of hydrophobic substrates by Pgp and ABCG2. The hydrophobic “vacuum cleaner” model supposes that substrates are transported from the plasma membrane directly to the extracellular space (214) (**Fig. 7**), while the “flippase” model assumes that substrates are moved from the inner membrane leaflet to the outer leaflet from where they can diffuse into the extracellular space or get back to the inner leaflet by a spontaneous flip-flop (**Fig. 7**) (215). Therefore the “flippase” mechanism supposes that substrate molecules have a specific localization within each bilayer leaflet, rather than being randomly distributed in the hydrophobic core of the membrane (216).

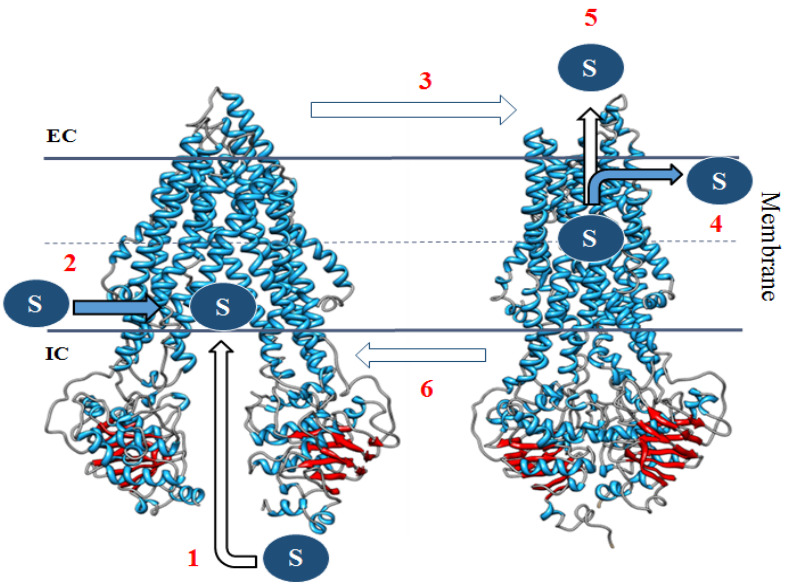

Figure 7: Mechanistic models of Pgp-mediated substrate efflux, the "flippase" and the "vacuum cleaner" model. Substrate is recognized either from the cytoplasm (1) or from the inner leaflet of the membrane (2). Due to the conformational changes mediated by ATP binding and NBD dimer formation (3) the binding affinity of the substrate-binding pocket decreases leading to the flipping of the substrate, to the outer membrane leaflet (4) or to the export of the substrate to the extracellular milieu. Following ATP-hydrolysis, the transporter switches back to the inward-open conformation (6).

Currently it is hard to distinguish between the two models experimentally and none of them can be ruled out (209). Based on our recent understanding, the hydrophobicity of a substrate determines if it is flipped to the outer membrane leaflet or it is directly transported to the extracellular space (215).

3.4.5. Importance of the membrane environment in modulating drug transport

Transmembrane proteins, Pgp and ABCG2 are in an intimate relationship with the surrounding membrane environment. Cryo-EM structures of Pgp and ABCG2 demonstrated that some lipid molecules directly interact with the TM helices of both Pgp and ABCG2 (101,114), forming a lipid belt, and removal of these strongly associated annular lipid molecules by detergents leads to the inactivation of the transporters (217-220).

Cholesterol is one of the major components of mammalian plasma membranes. Certain membrane microdomains, such as lipid rafts and caveolae, are selectively enriched in cholesterol. Both Pgp and ABCG2 have been reported to reside in cholesterol-rich lipid rafts in several cell types (221,222). Of note, cholesterol depletion of mammalian cells significantly decreases the drug transport activity of both transporters (223). High membrane cholesterol levels were found to potentiate the ATPase and transport activity of ABCG2 (220). It has been shown that certain Pgp inhibitors (e.g., zosuquidar or tariquidar) did not affect the ATPase activity of Pgp when studied in detergent micelles. Moreover, a 30- to 150-

fold decrease was observed in the apparent affinity of Pgp to its substrate verapamil in detergent micelles (224). These findings strongly suggest that membrane-lipid interactions with cholesterol and phospholipids are crucial for the functional activity of Pgp and ABCG2 and changes in these interactions can alter the conformational changes of transporters and their substrate or inhibitor binding (225).

Besides the specific lipid composition of the membrane, its physicochemical properties can also affect the function of membrane proteins. As it was mentioned in *Section 3.4.4*, Pgp and ABCG2 substrates are mostly hydrophobic molecules with high $logP_{ow}$ value. Passive diffusion of such molecules through the cell membrane decreases with increasing lateral packing-density, which is highly dependent on the lipid composition of the membrane (226). It has been demonstrated using chemically unrelated Pgp substrates in different model membranes that their membrane partitioning is greatly affected by the acyl chain lengths of phospholipids and the lipid phase state (227). Consequently, such changes in the membrane can significantly alter drug binding by Pgp and ABCG2. Furthermore, changes in membrane fluidity can also affect drug-binding and transport by membrane transporters (228). Several surfactant molecules, including Pluronic 85, Tween 20 and 80, Brij-97 and Brij-98 have been shown to inhibit Pgp function by altering the membrane fluidity (229). Well-known membrane fluidizers, such as benzyl alcohol, inhibited the Pgp-dependent accumulation of ^{3}H-labeled daunorubicin and vinblastine in bile canalicular membrane vesicles (230). Furthermore, membrane fluidization by anesthetics (e.g., diethyl ether, chloroform) or by neutral mild detergents inhibited the ATPase activity of Pgp (231).

Function of Pgp has been studied in various experimental systems: lipid-detergent micelles (192), artificial lipid-bilayers (193) or membrane vesicles derived from Pgp-overexpressing cells (232). These experimental systems might not reflect the physiological membrane environment and because of the differences in their physicochemical properties (e.g., lateral pressure, curvature, lipid composition) they might lead to conflicting results. Of note, in a recent study on mouse Pgp reconstituted in lipid nanodiscs ATP-hydrolysis has been described to be responsible for switching Pgp from the outward-facing to the inward-facing conformation. This observation is further supported by cryo-EM structures of Pgp (109,113). However, a recent DEER study on purified mouse Pgp molecules showed that ATP-hydrolysis powers the transition from the inward-facing to outward-facing conformation (192).

Taken together, the function of Pgp and ABCG2 is greatly affected by their membrane environment, therefore, model systems where the transporters can be studied in their natural membrane environment are of crucial importance (177,233).

3.5. Substrate spectra and inhibitors of Pgp and ABCG2

Pgp and ABCG2 possess extremely wide and partially overlapping substrate spectra involving structurally diverse hydrophobic or amphiphilic compounds in the molecular weight range of 300 to 2000 Da. There are many clinically important compounds among their substrates such as anticancer drugs, HIV-protease inhibitors, immunosuppressive agents, calcium-channel blockers, antibiotics and steroids (examples are shown in **Table 5**). Pgp and ABCG2 can also transport various fluorescent compounds that are frequently used in drug accumulation or efflux experiments to assess their transport activity *in vitro* (**Table 5**).

Table 5: List of representative substrates of Pgp and ABCG2 (based on (178,227,234-236))

Pgp substrates		**ABCG2 substrates**	
Anticancer drugs	Vinca alkaloids (vinblastine, vincristine and vinorelbine) Anthracyclines (doxorubicin, daunorubicin and epirubicin) Taxanes (paclitaxel, docetaxel) Epipodophyllotoxins (etoposide, teniposide) Camptothecins (topotecan, irinotecan, SN-38, cisplatin	**Anticancer drugs**	Mitoxantrone Anthracyclines (doxorubicin, daunorubicin) (Only R482T mutant) Epipodophyllotoxins (etoposide, teniposide) Camptothecins (topotecan, irinotecan) Anthracenes (bisantrene) (Only R482T mutant)
HIV protease inhibitors	Ritonavir, saquinavir, nelfinavir	**Carcinogens**	Aflatoxin B, PhiP
Antihistamines	Terfenadine, fexofenadine	**Antiviral drugs**	Zidovudine, lamivudine
Immunosuppressive agents	Cyclosporine A, tacrolimus (FK506)	**Fungal toxins**	Fumitremorgin C, Ko143
Antiarrhythmics	Quinidine, amiodarone, propafenone	**Antihypertensives**	Reserpine
Fluorescent compounds	Calcein-AM, Hoechst 33342, rhodamine 123	**Fluorescent compounds**	Hoechst 33342, BODIPY-prazosin, mitoxantrone
Tyrosine kinase inhibitors	Imatinib, gefitinib, dasanitib, nilotinib, erlotinib	**Tyrosine kinase inhibitors**	Imatinib mesylate, gefitinib, dasanitib
Calcium-channel inhibitors	Verapamil, nifedipine, azidopine, diltiazem	**HMG CoA reductase inhibitors**	Rosuvastatin, pravastatin, cerivastatin
Antibiotics	Erythromycin, gramicidin A	**Antibiotics**	Ciprofloxacin, norfloxacin
Steroids	Corticosterone, dexamethasone, aldosterone, cortisol	**Drug conjugates**	Estron-3-sulfate, Acetaminophen-sulfate, Dehydroepiandrosterone sulfate, Dinitrophenyl-S-glutathione
Natural products	Curcuminoids, colchicine, flavonoids	**Natural products**	Curcuminoids, quercetin

Interestingly, despite the extremely wide substrate spectrum of Pgp and ABCG2, only a few physiologically relevant substrates were identified so far. Of note, ABCG2 can transport urate promoting urate excretion in the human kidney and intestine (see *Section 3.2*) (237). Only a few biomolecules are potential endogenous substrates of Pgp, including certain phospholipids (e.g., phosphatidylcholine or sphingomyelin) (238,239), hormones, such as aldosterone (240) or β-estradiol-17β-D-glucuronide (241) and interleukins (242).

Due to the strong contribution of Pgp and ABCG2 to the clinical drug resistance, numerous studies aimed to identify molecules having potent inhibitory effects on Pgp and/or ABCG2 (243). The most important characteristic of the transporter inhibitors is their ability to reverse resistance to commonly applied anticancer drugs without severe adverse effects *in vivo*. Eventually, only few drug candidates turned out to be suitable in this respect (**Table 6,** for further details see *Section 3.7*).

Table 6: List of clinically relevant inhibitors of Pgp and ABCG2 (based on (234,243))

Clinically relevant Pgp inhibitors	**First generation:** - Verapamil - Cyclosporine A - Tamoxifen	**Second generation:** - PSC833 (valspodar) - VX-710 (biricodar)	**Third generation:** - LY335979 (zosuquidar) - XR9576 (tariquidar) - GF120918 (elacridar) - OC144-093 (ontogeny)
Clinically relevant ABCG2 inhibitors	- GF120918 (elacridar) - Ko143 - Pantoprazole - XR9576 (tariquidar) - VX-710 (biricodar)		

Nevertheless, the classification of compounds interacting with Pgp and/or ABCG2 is far more complex and there is no clear distinction between inhibitors and substrates. Several molecules that are transported, e.g., cyclosporine A (CsA) for Pgp, also can act as competitive inhibitors for other substrates recognizing the same binding-site on the transporter (244). Furthermore, extremely high substrate concentrations can similarly lead to the inhibition of the transporter (245,246). In addition to competitive inhibitors, a number of Pgp and ABCG2 inhibitors interact with the transporters at allosteric binding sites (247). Although it is still not entirely clear how Pgp and ABCG2 can differentiate between substrates and inhibitors, cryo-EM structures of Pgp and ABCG2 with bound substrates and inhibitors (**Table 2, Fig. 3**) provided a better understanding of these interactions (101,115,248). According to these structures, inhibitor molecules fill up the substrate-binding cavity and form larger number of interactions with the drug-binding pocket, as compared to substrates. These high-affinity interactions can prevent NBD-dimerization and the subsequent steps of the catalytic cycle in a

competitive manner (101,115). Therefore, binding affinity is a key determinant of substrate-inhibitor discrimination (101).

3.6. Retinoids and ABC transporters

Retinoids are a large group of biomolecules derived from vitamin A. A series of major cellular processes including cell survival, proliferation or differentiation is regulated by retinoids. Since retinoids are hydrophobic compounds with an average molecular mass of 300 Da, they are potential Pgp and/or ABCG2 substrates.

Retinol (vitamin A) is present in the human plasma at 1-2 μM concentration under physiological circumstances (249), while its natural metabolites e.g., retinyl-esters, all-*trans*-retinoic acid (ATRA), 13-*cis*-retinoic acid or 9-*cis*-retinoic acid are present at significantly lower (pM to nM) concentrations (250,251) (**Fig. 8**). Transcriptionally active retinoids regulate the activation of nuclear receptors including RAR-RXR (retinoic acid - retinoid X receptor) heterodimer nuclear receptors, PPARs (peroxisome proliferator activated receptors) and VDRs (vitamin D receptor, calcitriol receptor) (252-254) (**Fig. 8**). Because of their major role in the regulation of cell proliferation and differentiation, retinoids are routinely applied in chemotherapy at supra-physiological concentrations (app. 10-20 μM final plasma concentrations) (255-257). ATRA and 13-*cis*-retinoic acid are primarily used in the chemotherapy of neuroblastoma and squamous cell carcinoma. Moreover, they are also applied in the therapy of acute promyelocytic leukemia (APL), acute lymphoblastic leukemia (ALL), T-cell lymphoma, basal cell carcinoma and prostate cancer (256,258,259). In dermatology practice, 13-*cis*-retinoic acid and ATRA are used for the treatment of acne and for metastatic melanoma in combination with INFα-2a (255). Retinyl-esters, like retinyl-acetate and retinyl-palmitate, are frequently used food additives and they are also applied as components of anti-aging cosmetics (260). Furthermore, retinyl-acetate showed promising results in the treatment of certain degenerative diseases of the retina (261).

Despite their well-known physiological role and their importance in anti-cancer therapy, little is known about the interaction of retinoids with ABC transporters. Yang et al. have proved that stem cells (expressing ABCG2) derived from the umbilical cord can be differentiated into neurons and glial cells upon ATRA treatment (262). Hessel and Lampen have studied the effect of ATRA on the ABCG2 expression of Caco-2 cells and found that ATRA supplementation increased the ABCG2 expression in a time- and concentration-dependent manner through the activation of RAR/RXR heterodimer nuclear receptors (263). Sulová et al. demonstrated that combined treatment of Pgp expressing vincristine resistant

L1210/VCR mouse leukemia cells with verapamil and ATRA induces a significant downregulation of Pgp expression (264). In another study, human colorectal carcinoma cell lines were treated with sub-lethal doses of retinol that led to a 40% decrease in the Pgp mRNA levels and increased etoposide sensitivity supporting the role of retinol as an adjuvant compound in the combined treatment of Pgp expressing tumors (265).

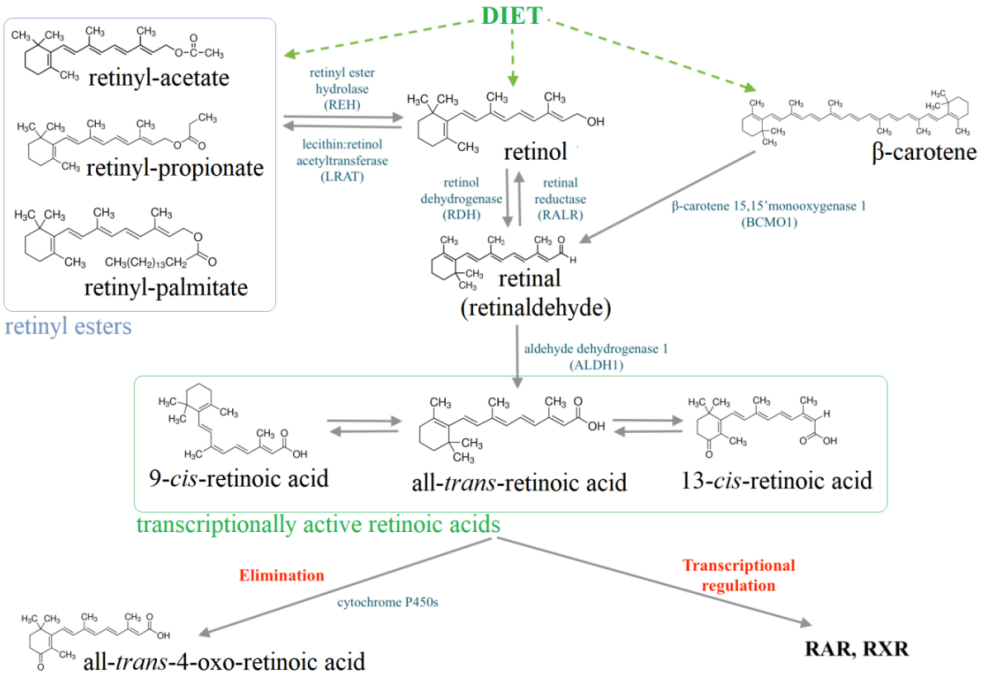

Figure 8: Simplified pathway map of retinoid metabolism in humans. (RAR – Retinoic acid receptor, RXR – retinoid X receptor, based on (266))

Nonetheless, direct interactions of retinoids with Pgp or ABCG2 have not been studied so far. According to literature data, several retinoid derivatives exhibit uneven distribution between the placenta and the developing embryo, raising the possibility that active transporters might be involved in the transport of these compounds (267). Since both Pgp and ABCG2 are expressed in the placental syncytiotrophoblasts, together with several other ABC transporters, they might have roles in the transport of retinoids and consequently in the protection of the fetus from their teratogenic effects by maintaining significantly lower retinoid concentrations in the embryonic tissues (268).

3.7. Clinical aspects of Pgp and ABCG2

As it was noted previously in *Section 3.3.1*, Pgp and ABCG2 are expressed in several physiological tissue barriers including the blood-brain-, blood-placenta- and blood-testis barriers, intestinal epithelium and liver where they have substantial effect on the absorption, distribution, metabolism and elimination (ADME) of numerous chemotherapeutic drugs and

drug candidates (269). Moreover, both Pgp and ABCG2 are frequently expressed in tumor cells decreasing the efficacy of anti-cancer chemotherapy.

Certain cancer types are intrinsically chemotherapy resistant, because they originate from Pgp and/or ABCG2 expressing tissues, e.g., colon- or hepatocellular cancers (270). In some tumors, the resistant sub-populations of tumor cells are selected out by the drug treatment itself. Another scenario of acquired drug resistance when Pgp/ABCG2 expression is induced in non-expressing tumor cells by mutations or changes in the tumor microenvironment (271).

In order to generally understand how the expression of Pgp and ABCG2 is linked to the phenomenon of clinical drug resistance, the expression levels of the transporters were studied in various tumor samples (120). Pgp expression was first detected in human leukemic cells from acute myeloid leukemia (AML) patients, and it was found to be an adverse prognostic factor for complete remission and survival in adults. Similarly, the expression of ABCG2 correlated with poor prognosis in AML as well as in ALL patients (272). Of note, solid tumors generally display heterogeneous ABC transporter expression patterns. Nonetheless, simultaneous expression of Pgp and ABCG2 was demonstrated in ovarian cancer (273), small cell lung cancer (SCLC) (274) and non-small cell lung cancer (NSCLC) (275), tumors of the CNS, breast cancer and many other solid tumor types (276,277).

Several studies found remarkable increase in the expression of Pgp and ABCG2 in patient samples after chemotherapy. As it was demonstrated in a breast cancer meta-analysis, more than 40% of breast cancers showed increased plasma membrane Pgp expression post-therapy (278). Another study carried out on AML patients demonstrated a significant increase of Pgp positivity from 24% in treatment-naïve patients to 67% in relapsed patients (279). Similarly, in plasma cell myeloma patients, the fraction of Pgp-positive patient samples increased from 6% to 43%, following chemotherapy (280). Significant increase of ABCG2 expression at both mRNA and protein levels has been found in myeloma and colon cancer patients following topotecan or irinotecan therapy (281,282).

The widespread expression of Pgp and/or ABCG2 in tumor cells and the frequent increase of their expression level following chemotherapy suggested that supplementation of chemotherapy with Pgp and/or ABCG2 inhibitors may enhance the accumulation of anticancer drugs in tumor cells and thus can increase treatment efficacy. Numerous clinical trials were designed and performed to test the effects of Pgp and/or ABCG2 modulators (e.g., valspodar, tariquidar, zosuquidar, fumitremorgin C) in combination with cytotoxic drugs to treat multidrug resistant tumors (see *Section 3*.5 and **Table 6**). Unfortunately, first generation

Pgp inhibitors (such as verapamil and CsA) exhibited high levels of toxicity and low efficiency in reversal of drug resistance. Second generation modulators (such as PSC833 (valspodar), a non-immunosuppressive derivative of CsA) were generated to increase specificity and avoid unwanted toxicity. However, severe adverse effects have emerged upon their clinical application because of the overlapping substrate specificity of Pgp and CYP3A4 P450 cytochrome enzymes (283). Third generation Pgp inhibitors (e.g., LY335979 or XR9576) had increased selectivity, compared to previous generations (284), but they also failed in clinical trials due to the large number of "off-target" interactions and inhibition of Pgp molecules at their physiological expression sites (285). Taken together, the above disappointing results led to the conclusion that inhibition of Pgp is probably not a plausible strategy to overcome drug resistance *in vivo* (286,287).

As an alternative strategy novel classes of anticancer agents can be designed which do not interact with Pgp or ABCG2, and thus can evade transporter-mediated efflux (276). Another promising therapeutic approach can be the targeted down-regulation of MDR-related genes applying repressor peptides or siRNAs (288,289). Detailed understanding of the MDR phenomenon may also help us to better target the Achilles heel of therapy resistant tumors. Although, overexpression of Pgp generally provides a fitness advantage for tumor cells upon chemotherapy, it also makes the cells hypersensitive to certain compounds (290). This phenomenon is often referred as "collateral sensitivity" of Pgp-positive tumor cells, and it may be exploited for the selective killing of Pgp expressing tumor cells in the future (291,292).

Taken together, despite recent developments in anticancer drug discovery, MDR still poses a serious impediment to successful anti-tumor treatment. Understanding the fine details of the function and catalytic mechanism of Pgp and ABCG2 is essential for the development of new chemotherapeutic protocols to combat MDR.

4. Aims of the study

Despite the large number of substrates that are recognized by Pgp and ABCG2 (*Section 3.5*) only a few endogenous Pgp or ABCG2 substrates were identified so far. Retinoids are potential Pgp and/or ABCG2 substrates/modulators because of their highly hydrophobic character and molecular weight of app. 300 Da. In view of their physiological and clinical significance, we have studied their interaction with Pgp and ABCG2 and aimed to answer the following questions:

- Whether retinoids can interact with Pgp and ABCG2 as substrates or inhibitors?
- Whether stereo-chemical differences between retinoid derivatives can affect their interaction with Pgp and ABCG2?
- Do retinoids affect the function of Pgp and ABCG2 directly or they act indirectly by changing the membrane environment?

In the second part of our work, we investigated various aspects of the functional collaboration of the NBSs upon the catalytic cycle of Pgp by studying mutant Pgp variants with one intact NBS. We tried to answer the following questions:

- Whether human Pgp molecules with one intact and one ABCB11-like degenerate NBS are functional?
- Whether mutant Pgp variants that possess a single point mutation in the A-loop (Y401A or Y1044A) or in the Walker B sequence (D555N or D1200N) are transport competent?
- Whether the transport deficient mutants have any partial activity including capability for nucleotide binding, nucleotide hydrolysis and concomitant conformation changes?

5. Materials and methods

5.1. Chemicals

All chemicals, cell culture media and supplements were purchased from Sigma-Aldrich (Budapest, Hungary). Fluorescent dyes including calcein acetoxymethylester (calcein-AM), mitoxantrone, Hoechst 33342 and Alexa 647 succinimidyl ester (A647) were purchased from Life Technologies Inc. (Carlsbad, CA, USA). All-*trans*-4-oxo-retinoic acid was kindly provided by DSM Nutritional products (Basel, Switzerland). UIC2, 5D3 and 15D3 mAbs were prepared from hybridoma supernatants using affinity chromatography and were >97% pure by SDS/PAGE. The UIC2 and 15D3 producing hybridoma cell lines were obtained from the American Type Culture Collections (Manassas, VA, USA), while the 5D3 hybridoma was a kind gift of Brain P. Sorrentino (Division of Experimental Hematology, Department of Hematology/Oncology, St. Jude Children's Research Hospital, Memphis, Tennessee, USA). Antibodies were labeled with A647 and were separated from the unconjugated dye by gel filtration on a Sephadex G-50 column. The dye-to-protein labeling ratio (F/P) was around 2 for each antibody preparation. Stock solutions of transporter substrates, modulators including calcein-AM, CsA, mitoxantrone, quercetin, tariquidar and retinoid derivatives were prepared in dimethyl-sulfoxide (DMSO). The final DMSO concentration in the samples was always less than 1% (v/v) and it did not have any effect on the activity of the transporters.

5.2. Cell lines

The NIH 3T3 mouse fibroblast cell line and its wild-type human Pgp expressing counterpart (NIH 3T3 MDR1 G185) was a kind gift from Michael Gottesman (National Institutes of Health, Bethesda, MD). The MDCK II (Madin-Darby canine kidney) cell line and its ABCG2 transfected counterpart were kindly provided by Balázs Sarkadi (Institute of Enzymology, Research Center for Natural Sciences, Eötvös Loránd Research Network, Budapest). All cell lines were grown as monolayer cultures in Dulbecco's modified Eagle's medium (DMEM). Cell culture media were supplemented with 10% heat-inactivated fetal calf serum, 2 mM L-glutamine and 0.1 mg/ml penicillin-streptomycin cocktail. Cells were checked regularly for mycoplasma infection by the MycoAlert® mycoplasma detection kit (Lonza Rockland Inc., Rockland, ME, USA) and were found to be negative.

5.3. Vector constructs

Sleeping Beauty (SB) transposon vectors containing wild-type human ABCB1 cDNA and its different mutant forms were constructed. Site-directed mutagenesis was performed

using the QuikChange II Site-Directed Mutagenesis Kit (Agilent Technologies, Santa Clara, CA, USA) on the pAcUW-LMDR1 vector carrying the wild-type human ABCB1 cDNA. Mutations were generated according to the manufacturer's instructions. Full-length ABCB1 cDNAs were sequenced and mutations were confirmed in all SB constructs.

5.4. Establishment of transgenic cell lines

NIH 3T3 cells stably expressing the wild-type or the mutant Pgp variants were established by the SB transposon-based gene delivery system, using the 100-fold hyperactive SB transposase. Cells were co-transfected with the SB transposase and SB transposon vector constructs using Lipofectamine2000 reagent (Life Technologies, Carlsbad, CA, USA) in accordance with the manufacturer's instructions. Briefly, 3×10^5 cells were seeded in 6-well-plates, 24 hours later cells were transfected with 2 μg vector DNA per well in a 10:1 ratio, for the SB transposon and transposase constructs. 48 hours after the transfection, transgene positive cells were sorted by flow cytometry (Becton Dickinson FACSAria III Cell Sorter (Becton Dickinson, Mountain View, CA, USA)) based on the cell surface expression of wild-type and mutant Pgp variants using the MRK16 (Abnova GmbH Heidelberg, Germany) or 15D3 anti-Pgp mAbs. The vector constructs and the transgenic cell lines were generated by Dóra Türk and Gergely Szakács (Institute of Enzymology, Research Center for Natural Sciences, Eötvös Loránd Research Network, Budapest). The sorting procedure was repeated 2 weeks after transfection in our lab to obtain homogeneously expressing cell populations.

To generate Sf9 (*Spodoptera frugiperda* insect ovary) cells overexpressing human Pgp or ABCG2, cDNAs of the transporters were cloned into recombinant baculovirus transfer vectors. Sf9 insect ovarian cells were cultured in spinner flasks and surface attached cells were infected with the baculoviruses (293). Virus infected Sf9 cells were harvested 72 h after infection. Pgp and ABCG2 expressing Sf9 cells were established by Ágnes Telbisz (Institute of Enzymology, Research Center for Natural Sciences, Eötvös Loránd Research Network, Budapest).

5.5. Substrate accumulation tests

Calcein-AM was applied to measure the effects of retinoids on the transport activity of Pgp, while ABCG2-mediated transport was measured in mitoxantrone accumulation tests. Cells were harvested and washed three times in PBS containing 7 mM glucose (gl-PBS). Cells (5×10^5 cells/ml in gl-PBS) were pre-incubated in the presence or absence of the tested retinoids at different concentrations or specific inhibitors of Pgp (10 μM cyclosporine A) and ABCG2 (2 μM Ko143) for 20 min at 37 °C and then stained with 5 μM mitoxantrone for

40 min or 0.5 μM calcein-AM for 20 min. Cells were washed and then stored on ice until flow cytometric measurement.

For the measurement of transport activity of mutant Pgp variants, we performed calcein-AM as well as Hoechst 33342 accumulation tests. Hoechst 33342 accumulation experiments were carried out in HEPES buffer (20 mM HEPES, 123 mM NaCl, 5 mM KCl, 1.5 mM $MgCl_2$, 1 mM $CaCl_2$) containing 7 mM glucose (gl-HEPES). Cells (5×10^5 cells/ml in gl-HEPES) were pre-incubated in the presence or absence of 1 μM tariquidar, a specific Pgp inhibitor, for 20 min at 37 °C and then stained with different concentrations of Hoechst 33342 for 30 min. Samples were washed once with ice-cold HEPES buffer containing 0.5% FBS. Calcein-AM, mitoxantrone or Hoechst 33342 stained cells were kept on ice until flow cytometric measurement. Dead cells were excluded from the analysis on the basis of propidium iodide (PI) staining.

The calcein-AM and Hoechst 33342 transport activity of the wild-type and mutant Pgp variants were described by the Transport Activity Factor (TAF) calculated according to the following formula:

$$TAF = \frac{(MFI_{inh} - MFI_0)}{MFI_{inh}}$$

where MFI_{inh} and MFI_0 are the mean fluorescence intensity values measured in the presence and absence of Pgp inhibitors, respectively.

5.6. Membrane preparations

For ATPase activity measurements we used membrane samples derived from Sf9 (*Spodoptera frugiperda*) insect ovarian cells expressing human Pgp or ABCG2 and membrane preparations from NIH 3T3 cells expressing wild-type or mutant Pgp variants. Sf9 or NIH 3T3 cells were harvested and cell membranes were isolated by differential centrifugation. Cell debris and nuclei were sedimented at 500 × g for 10 min at 4 °C. Membrane fractions were isolated with centrifugation at 12000 × g for 60 min at 4 °C. Membrane pellets were re-suspended in TMEP solution (50 mM Tris, pH=7.0 with HCl), supplemented with 50 mM mannitol, 2 mM EGTA, 0.5 mM phenylmethylsulphonyl fluoride (PMSF) and protease inhibitor cocktail (Sigma-Aldrich, Budapest). The protein concentration of the membrane samples was determined by the Lowry method (294). The ABCG2 expressing Sf9 membrane samples were loaded with cholesterol by cholesterol-methyl-beta-cyclodextrin complex (Chol-RAMEB) in order to obtain high specific ATPase activity of the transporter (295,296). Membrane samples were stored at −80 °C until use. The transporter

expression of membrane samples (5 µg membrane protein/slot) was routinely checked by immunoblot as described in *Section 5.7*.

5.7. Western blot analysis

Sf9 or NIH 3T3 cell membrane samples (2.5 or 5 µg/slot) were subjected to SDS-polyacrylamide gel electrophoresis on 8% polyacrylamide gel and were electro-blotted to 0.45 µm pore size nitrocellulose membrane (GE Healthcare Life Sciences, Little Chalfont, Buckinghamshire, UK). Pgp expression was detected using the G-1 monoclonal anti-Pgp mAb (Santa Cruz Biotechnology Inc., Santa Cruz, CA, USA), while ABCG2 was detected by the BXP-21 monoclonal anti-ABCG2 mAb (Santa Cruz Biotechnology Inc., Santa Cruz, CA, USA), at 1:5,000 dilution. As a secondary antibody, a goat anti-mouse HRP-conjugated IgG mAb (Santa Cruz Biotechnology Inc., Santa Cruz, CA, USA) was applied, at 1:5,000 dilution.

5.8. ATPase activity measurements

The vanadate-sensitive ATPase activity of wild-type and mutant Pgps and ABCG2 was determined by a colorimetric assay. Specific ATPase activity of the transporters was calculated from the amount of released Pi. The ATPase reaction was started with the addition of 3.2 mM MgATP. After 25 min incubation at 37 °C, the reaction was stopped by 40 µl 5% SDS, then the samples were incubated with 105 µl color reagent at room temperature for 30 min as described in (297). The absorbance of the samples was measured at 700 nm using a BioTek Synergy HT plate reader (BioTek Instruments, Winooski, VT, USA).

The half-inhibitory doses (IC_{50}) of retinoids were determined by fitting the dose-response relationships with a four-parameter sigmoidal curve, where A_{max} and A_{min} are the ATPase activities measured at zero and at infinitely high inhibitor concentrations, respectively, n is the Hill coefficient and x is the concentration of the inhibitor:

$$y = A_{min} + \frac{A_{max}+A_{min}}{1+10^{(lgx-lgIC_{50})n}}$$

Upon studying the kinetics of inhibition of the substrate-stimulated ATPase activity by retinoids data points were fitted with a modified form of the Michaelis-Menten equation, which includes the Hill coefficient, n:

$$v = \frac{v_0+(v_{max}-v_0)xS^n}{S^n+K_M}$$

where v_0 is the basal ATPase activity measured in the absence of the stimulatory substrate, while v_{max} is the maximal extent of ATPase stimulation and K_M is the Michaelis constant (i.e., the substrate concentration at which the reaction rate is half of v_{max}).

5.9. Cellular uptake of retinoids and transporter inhibitors

NIH 3T3 cells (1×10^6 cells/ml) in gl-PBS containing 1% bovine serum albumin (BSA) were incubated with retinoids or transporter ligands (quercetin, cyclosporine A, Ko143) applied at different concentrations (1, 10 and 100 µM) for 30 min at 37 °C. After incubation, the cells were pelleted by centrifugation at 400 × g and supernatants were collected. The cellular uptake of the examined compounds was determined by calculating the ratio of the absorbances measured in the supernatants at their absorption maximum before and after incubation with cells. Absorbances were determined using a NanoDrop 1000 UV/VIS Spectrophotometer (Thermo Fisher Scientific, Wilmington, DE, USA).

5.10. Fluorescence anisotropy measurements

Transporter expressing and non-expressing NIH 3T3 and MDCK cells (1×10^6 cells/ml in Hank's buffer (0.137 M NaCl, 5.4 mM KCl, 0.25 mM Na_2HPO_4, 0.44 mM KH_2PO_4, 1.3 mM $CaCl_2$, 1.0 mM $MgSO_4$, 4.2 mM $NaHCO_3$, 7 mM glucose)) were pre-treated with 100 µM of various retinoid derivatives for 10 min at 37 °C and then further incubated with 2 µM diphenylhexatriene (DPH) or 2 µM 1-[4-(trimethylammonium)phenyl]-6-phenyl-1,3,5-hexatriene (TMA-DPH) at room temperature, in dark for 20 min. Steady-state fluorescence anisotropy measurements were carried out at 37 °C using a Horiba Jobin Yvon Fluorolog-3 (Yvon Horiba, Edison, NJ, USA) spectrofluorometer equipped with a thermostated cell holder.

The fluorescence of DPH and TMA-DPH was excited at 358 nm and their emission was measured at 427 nm. The steady-state fluorescence anisotropy of the dyes was calculated using the formula:

$$r = \frac{I_{VV} - G I_{VH}}{I_{VV} + 2G I_{VH}}$$

where I_{VV} and I_{VH} are the vertically and horizontally polarized components of the fluorescence intensities, respectively, excited by vertically polarized light and G is a correction factor compensating for the unequal sensitivity of the detection system for vertically and horizontally polarized light. There is an inverse correlation between membrane fluidity and fluorescence anisotropy: the lower the anisotropy value, the higher the membrane fluidity; hence, the increase of fluorescence anisotropy is indicative of lower fluidity and higher structural order within the membrane (298).

5.11. Cytotoxicity assays using Alamar Blue

Pgp-negative, wild-type or mutant Pgp expressing NIH 3T3 cells were seeded in 96-well plates at a cell density of 5×10^3 cells/well. 24 hours later, the tested compound (e.g., retinyl-acetate or vinblastine) was added to the wells at different concentrations and the plates were further incubated for 72 h at 37ºC. The cell viability was determined using the Alamar Blue assay (Serotec, UK) measuring the 530/590 nm fluorescence intensity of the dye in an automated BioTek Synergy HT plate reader (BioTek Instruments, Winooski, VT, USA). The fluorescence intensities of the samples were normalized to the fluorescence of the untreated control samples and were plotted as a function of retinyl-acetate or vinblastine concentrations.

5.12. Cell permeabilization with streptolysin-O

Streptolysin-O (SLO) (Sigma-Aldrich, Budapest, Hungary) is an exotoxin of *Streptococcus pyogenes.* It binds to the plasma membrane of cells and forms ring-structured toxin hexamers making the plasma membrane permeable for small water-soluble molecules including nucleotides (299). Cell suspensions (1×10^7 cells/ml) were treated with 20 µg/ml (app. 300 U/ml) SLO in PBS in the presence of 1% BSA, 10 mM DTT, 100 µg/ml PMSF and protease inhibitor cocktail (Sigma-Aldrich, Budapest) at 37 °C for 30 min in PBS (allowing permeabilization of 50–70% of cells). The reaction was stopped with 10 ml of 37 °C PBS and the cells were centrifuged for 5 min at 525 × g at 4ºC. Unbound toxin was removed by washing the cells 3 times with PBS and the cell pellet was re-suspended in PBS.

5.13. Measurements of the apparent ATP-binding affinity of Pgp

SLO permeabilized NIH 3T3 cells (1×10^6 cells/ml) expressing wild-type or mutant Pgp variants were pre-incubated with nucleotides added in a broad concentration range for 20 min, in the presence or absence of 0.5 mM vanadate, and then further incubated with 10 µg/ml A647-conjugated UIC2 monoclonal antibody for another 30 min (all treatments were carried out at 37 °C). UIC2 mAb binding to Pgp is a reversible reaction in the presence of MgATP, thus, UIC2 was applied at quazi saturating concentrations. The UIC2-A647 fluorescence intensity of the cells was measured by flow cytometry and plotted as a function of the nucleotide concentration. To determine the apparent affinity of Pgp to nucleotides (K_A), data points were fitted with the four-parameter Hill function, where F_{min} and F_{max} values were the minimum and maximum fluorescence intensities:

$$F = \frac{F_{min} x K_A^n + F_{max} x X^n}{K_A^n + X^n}$$

5.14. UIC2-reactivity assay

Intact wild-type, E556M, quadruple mutant, different Walker B and A-loop mutant Pgp expressing NIH 3T3 cells (5×10^5 cells/ml) were treated with 10 µM CsA in gl-PBS for 30 min at 37°C. Alternatively, cells were ATP depleted by Na-azide (10 mM) and 2-deoxy-D-glucose (8 mM) treatment for 30 min at 37°C in glucose-free PBS. UIC2-A647 (10 µg/ml) or the conformation insensitive 15D3-A647 (30 µg/ml) antibodies were added directly without washing step and samples were further incubated for another 30 min at 37°C. Cells were washed twice with ice-cold gl-PBS and then re-suspended in ice-cold gl-PBS (for ATP-depleted cells glucose-free PBS was used) before flow cytometric analysis. UIC2-reactivity (i.e., the percentage of cell surface Pgp molecules in a UIC2-reactive conformation) was calculated as a ratio of the F/P-corrected UIC2 and 15D3 signals.

5.15. Measurement of the kinetics of UIC2 dissociation

Wild-type and mutant Pgp expressing NIH 3T3 cells were harvested and washed three times in gl-PBS. Subsequently, cells were permeabilized with SLO toxin for 30 min at 37 °C as described in *Section 5.12* and were washed three times with ice-cold PBS to remove the nucleotides from the cells. Permeabilized cells were labeled with 10 µg/ml UIC2-A647 Fab fragments for 20 min at 37 °C and after washing twice with excess volume of gl-PBS they were kept on ice until flow cytometric analysis. Before measurement, cells (2×10^5 cells/ml) were mixed with 10 ml of pre-warmed 37 °C PBS containing different concentrations of MgATP and/or 40 µM verapamil. Fluorescence intensities were measured continuously at 37°C for 15 min with a Becton Dickinson FACSAria III Cell Sorter (Becton Dickinson, Mountain View, CA, USA). Mean values of UIC2-Fab fluorescence intensities were averaged for 20 s intervals.

5.16. Flow cytometry

Calcein-AM, mitoxantrone and Hoechst 33342 accumulation measurements were carried out on a Becton Dickinson FACSAria III Cell Sorter (Becton Dickinson, Mountain View, CA, USA). Calcein was excited by the 488 nm line of a solid-state laser and the emitted light was detected using a 502 nm dichroic mirror and a 530/30 nm band-pass filter. Mitoxantrone was excited with a 631 nm solid state laser end emitted fluorescence intensity was detected using a 685/15 band-pass filter. Hoechst 33342 was excited with a 365 nm UV laser and the blue intensity of the dye was recorded using a 445/40 band pass filter. PI was

excited by the 562 nm line of a solid-state laser and the emitted light was detected applying a 590 nm dichroic mirror and a 595/50 nm band-pass filter.

UIC2-A647 labeling of permeabilized cells was measured by using a Becton Dickinson FACSArray flow cytometer (Becton Dickinson, Mountain View, CA, USA). A 635 nm laser was used for the excitation of A647 dye and fluorescence values were detected in the red channel (661/16 nm) while the 532 nm laser was used for the excitation of PI (detected at 585/42 nm).

UIC2-dissociation was measured with the Becton Dickinson FACSAria III Cell Sorter. Alexa647 conjugated UIC2 was excited with a 631 nm solid state laser and fluorescence intensities were detected using a 660/20 band pass filter while PI was excited with a 562 laser and emitted light was detected applying a 590 nm dichroic mirror and a 595/50 nm band-pass filter. For the continuous monitoring of UIC2 dissociation, the sample injection chamber was kept at 37 °C.

In all flow-cytometric measurements cell debris was excluded from the analysis on the basis of FSC and SSC signals. Cytofluorimetric data were analyzed by using FCS Express 4 Research Edition (De Novo Software, Glendale, CA, USA).

5.17. Statistical analysis

Data were analyzed using SigmaStat (version 3.1, SPSS Inc., Chicago, IL, USA) and are presented as means ± SD. Comparison of two groups was carried out by unpaired *t*-test, while in the case of three or more groups, statistical significance was assessed using analysis of variance (ANOVA). For *post hoc* pair-wise comparison of the treatment groups with identical variances, the Holm-Sidak multiple comparison test was applied, while groups with unequal variances were analyzed by Dunnett T3 *post hoc* test. Differences were considered significant at $P < 0.05$. Dose-response curves were fitted using SigmaPlot 12.0 (SPSS Inc., Chicago, IL, USA).

6. Results

6.1. Interactions of retinoids with Pgp and ABCG2

6.1.1. Retinoid derivatives inhibit Pgp- and ABCG2-mediated substrate transport

We have studied the effects of various retinoid derivatives (see **Table 7** for the complete list of applied retinoids) on the drug transport activity of Pgp and ABCG2 using the NIH 3T3/NIH 3T3 MDR1 and MDCK/MDCK ABCG2 cell line pairs. The Pgp-positive NIH 3T3 MDR1 and the ABCG2-positive MDCK ABCG2 cell lines showed high transporter expression levels as it was demonstrated by direct immunofluorescence staining applying the 15D3-A647 anti-Pgp and 5D3-A647 anti-ABCG2 monoclonal antibodies (**Fig. 9a**).

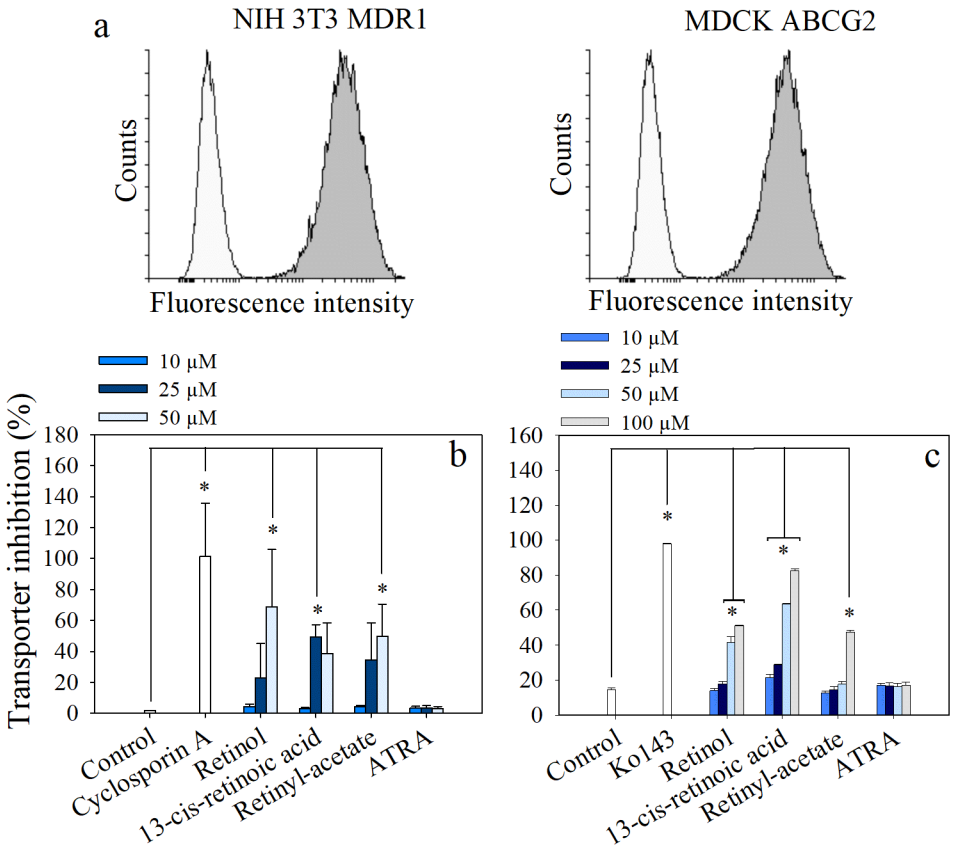

Figure 9: Effect of retinoid derivatives on the transport activity of Pgp (b) expressed in NIH 3T3 cells and ABCG2 (c) expressed in MDCK cells. The expression levels of the transporters were determined by direct immunofluorescence using the 15D3-A647 (for Pgp) and 5D3-A647 (for ABCG2) monoclonal antibodies (white histograms – Pgp/ABCG2 negative cells, grey histograms – Pgp/ABCG2 positive cells) (**a**). Cells were pre-treated with retinoids or transporter inhibitors CsA and Ko143 for 20 min at 37 ºC and then the NIH 3T3/NIH 3T3 MDR1 cell line pair was stained with 0.5 µM calcein-AM for 20 min at 37 ºC, while the MDCK/MDCK ABCG2 cell line pair was stained with 5 µM mitoxantrone for 40 min at 37˚C. The calcein and mitoxantrone accumulation of the transporter expressing cells is shown as a percentage of the transporter negative cells. Mean ± SD values of three independent experiments are shown **(b, c)** (* — significant difference compared to the control, $P < 0.05$ by ANOVA, Holm-Sidak *post-hoc* analysis).

Calcein-AM and mitoxantrone accumulation assays were used to study the transport function of Pgp and ABCG2, respectively. Our results showed that retinol, 13-*cis*-retinoic acid and retinyl-acetate increased the cellular accumulation of the fluorescent transporter substrates in a concentration dependent manner in both transporter-expressing cell lines (**Fig. 9b and c**). Applied at supra-physiological concentrations (25-100 µM, **Fig. 9b, c**), the effect of retinoid derivatives retinol, 13-*cis*-retinoic acid and retinyl-acetate was comparable to that of the Pgp- or ABCG2-specific inhibitors (**Fig. 9b and c**).

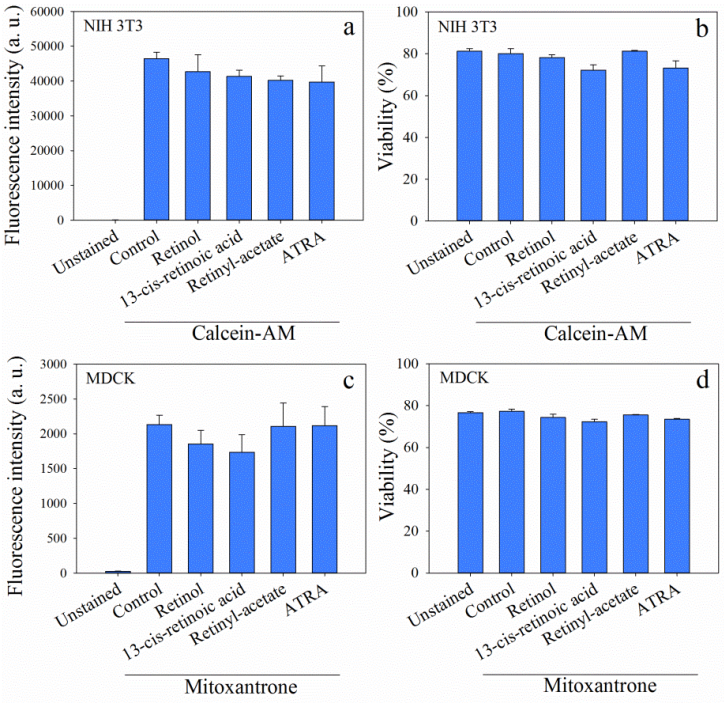

Figure 10: Effects of retinoid derivatives on the calcein (a) and mitoxantrone (c) accumulation and viability (b, d) of Pgp- and ABCG2-negative NIH 3T3 and MDCK cells. Cells were pre-treated with retinoids added at 50 µM for 20 min at 37°C. Subsequently, NIH 3T3 cells were stained with 0.5 µM calcein-AM, for 20 min, while MDCK cells were stained with 5 µM mitoxantrone, for 40 min at 37°C. Cell viability was determined on the basis of propidium iodide (PI) exclusion.

The increased accumulation of the fluorescent dyes cannot be attributed to the cytotoxic effect of retinoid derivatives, as treatment of transporter non-expressing NIH 3T3 and MDCK cells with different retinoid derivatives, added at 50 µM concentration, did not decrease the viability of cells significantly (**Fig. 10b and d**). In addition, retinoids did not have significant effect on the intracellular accumulation of calcein or mitoxantrone by the transporter non-expressing control cells supporting that the above observed effects are explained by the inhibition of the transporters (**Fig. 10a and c**).

6.1.2. Retinoids inhibit Pgp- and ABCG2-mediated basal- and substrate-stimulated ATPase activity

In further experiments, instead of intact cells, we used membrane preparations to avoid or reduce isomerization of retinoids to other derivatives by cellular metabolism (300). We studied the effects of retinoids on the ATPase activity of Pgp and ABCG2 using Sf9 membrane samples. Sf9 cells are ideal for these studies, because they express endogenous ATPase proteins at relatively low levels, while we can achieve high expression of the transgenes using the baculovirus expression system (297). Due to the high expression of human Pgp or ABCG2 demonstrated in Western blot experiments (**Fig. 11**), our Sf9 cell membrane preparations showed high specific ATPase activities (**Fig. 12**).

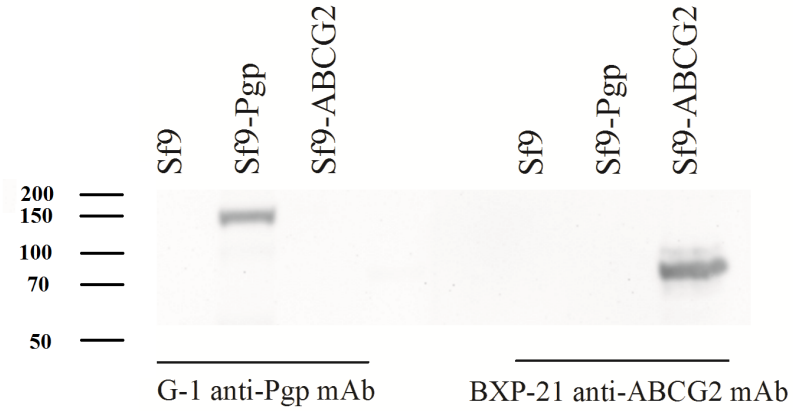

Figure 11: Western blot of membrane samples prepared from Sf9 cells expressing wild-type human Pgp and ABCG2. Non-transfected Sf9 membrane sample is shown as a control. Preparation of membrane samples was carried out as described in (*Section 5.6*). 5 µg protein was used per slot. The immunoblot was developed by the human Pgp-specific mouse monoclonal antibody (G-1) and ABCG2-specific monoclonal antibody BXP-21.

We measured the effects of the retinoids on the basal and the substrate-stimulated ATPase activity of the transporters, using a method developed by Sarkadi et al., based on the colorimetric measurement of Pi released in the ATPase reaction (see *Section 5.6* and *5.8*) (297). Previously, using Pgp and ABCG2 expressing Sf9 cell membrane preparations, we determined the substrate concentrations required to reach maximum ATPase stimulation (**Fig. 12a and b**). According to these experiments, we treated the cells with 40 µM verapamil that stimulated the ATPase activity of Pgp by 3-4-fold (approximately to 20-30 nmol Pi/mg protein/min) (**Fig. 12c, d, e**), while 10 µM quercetin induced about a 2-3-fold stimulation of ABCG2 activity up to 60-70 nmol Pi/mg protein/min (**Fig. 12f, g, h**).

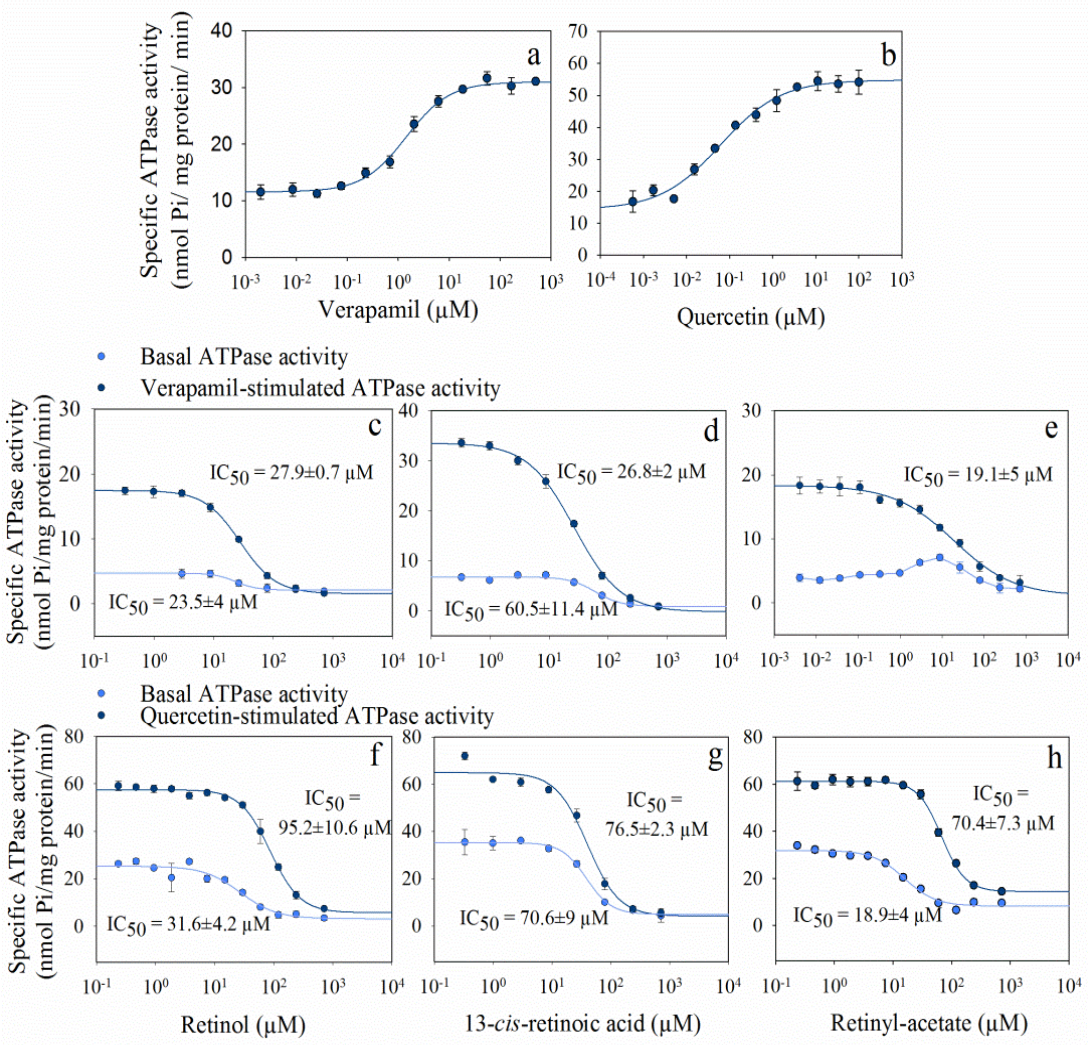

Figure 12: Dose-response curves demonstrating the effects of retinoids on the ATPase activity of Pgp (c, d, e) and ABCG2 (f, g, h). Pgp and ABCG2 expressing Sf9 cell membrane preparations were pre-treated with retinoids for 10 min at 37 ºC and then further incubated in the presence of 3 mM MgATP for 25 min. The substrate-dependent ATPase activity of Pgp was measured in the presence of 40 µM verapamil (**a**) while substrate-stimulated ATPase activity of ABCG2 was measured in the presence of 10 µM quercetin (**b**). Representative graphs are shown out of three independent experiments performed in triplicates (mean ± SD). The dose-response curves were fitted with a four-parameter sigmoidal dose-response curve (see *Section 5.8*). The mean IC_{50} values are shown in **Table 7** ($R^2 \geq 0.98$, where R^2 is the coefficient of determination).

Retinyl-acetate slightly increased the basal ATPase activity of Pgp (showing maximal stimulation at 10 µM conc.) indicating that it is probably transported by Pgp (**Fig. 12e**). However, we did not see significant difference in the cytotoxic effect of retinyl-acetate between Pgp-positive and Pgp-negative NIH 3T3 cells (**Fig. 13**) suggesting that it is not transported by Pgp or alternatively the rate of its Pgp-mediated transport is below the sensitivity of the cytotoxicity assay.

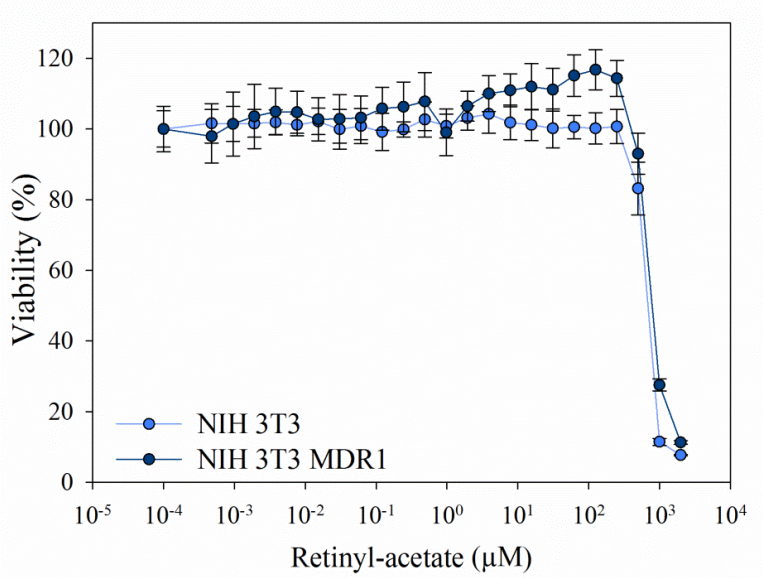

Figure 13: Cytotoxic effect of retinyl-acetate on Pgp-positive and Pgp-negative NIH 3T3 cells. Alamar Blue based *in vitro* cytotoxicity assay was performed as previously described (301) (see *Section 5.11*). Cells were seeded in 96-well plates at a cell density of 5×10^3 cells/well. 24 hours later retinyl-acetate was added at different concentrations and the plates were further incubated for 72 h at 37 °C. The cell viability was determined by measuring the 530/590 nm fluorescence intensity of the dye in an automated microplate reader. The Alamar Blue fluorescence intensity of the samples was normalized to the fluorescence of the retinyl-acetate untreated sample and plotted as a function of retinyl-acetate concentration. Data points are means of eight parallel samples (mean ± SD).

In good agreement with the results of calcein-AM and mitoxantrone accumulation studies (see **Fig. 9**), retinyl-acetate decreased the substrate-stimulated ATPase activity of both Pgp and ABCG2 (**Fig. 12e and h**). Additionally, retinol and 13-*cis*-retinoic acid exhibited a pronounced concentration-dependent inhibitory effect on both the basal- and the verapamil-stimulated ATPase activity of the transporters (**Fig. 12c, d and f, g**). Based on the dose-response curves obtained, we calculated the IC_{50} values of the particular retinoids for the basal and the substrate-stimulated ATPase activities of both transporters (**Table 7**). Other physiologically relevant retinoid derivatives (e.g., retinyl-propionate, retinyl-palmitate or all-*trans*-4-oxo-retinoic acid) did not have any effect on the transport and ATPase activity of Pgp and ABCG2 (**Table 7**).

We have found that 9-*cis*-retinoic acid and ATRA did not show any inhibitory effect on Pgp and ABCG2. Interestingly, their stereoisomer, 13-*cis*-retinoic acid inhibited the basal- and the substrate-stimulated ATPase activities of both transporters in a concentration-dependent manner (**Fig. 12d, g**). Since inhibitors and substrates supposed to reach the drug binding pocket of the transporters directly from the plasma membrane, low membrane partitioning of the compounds could explain the lack of effects.

Table 7: Effects of retinoid derivatives on the ATPase activity of Pgp and ABCG2.

	IC_{50} values (µM)			
Drug	**Pgp**		**ABCG2**	
	Basal activity	Stimulated activity	Basal activity	Stimulated activity
Retinol	23.5±4	27.9±0.7	31.6±4.2	95.2±10.6
All-*trans*-retinoic acid	No effect	No effect	No effect	No effect
9-*cis*-retinoic acid	No effect	No effect	No effect	No effect
13-*cis*-retinoic acid	60.5±11.4	26.8±2	70.6±9	76.5±2.3
All-*trans*-4-oxo-retinoic acid	No effect	Weak inhibition at high conc.	No effect	No effect
Retinyl-acetate	36.8±4	19.1±5	18.9±4	70.4±7.3
Retinyl-propionate	No effect	No effect	No effect	No effect
Retinyl-palmitate	No effect	No effect	No effect	No effect

The IC_{50} values were calculated by fitting the dose-response curves with a four-parameter logistic function ($R^2 \geq 0.98$)

However, the octanol-water partition coefficients ($LogP_{ow}$, **Table 8**) describing the hydrophobicity of the compounds were found to be quite similar and remarkably high for all examined retinoids. According to literature data, the shape and size of the molecules can also have impact on their membrane partitioning serving an explanation for the observed differences. Since the intracellular concentration of drugs is dependent on their membrane permeability, we estimated the fraction of retinoids accumulated by the cells measuring the absorbance of retinoids in the supernatant before and after incubation with Pgp-negative NIH 3T3 cells (**Fig. 14**). We observed a significant correlation between the $LogP_{ow}$ value and the cellular accumulation of retinoids and Pgp/ABCG2 modulators (**Fig. 14b** and **Table 8**). We did not measure significant differences in the cellular accumulation of 9-*cis*-retinoic acid, ATRA and 13-*cis*-retinoic acid in accordance with their identical $LogP_{ow}$ values (**Fig. 14a**).

Table 8: Octanol-water partition coefficients ($LogP_{ow}$ values) of the studied retinoid derivatives.

Drug	$LogP_{ow}$	Reference
Quercetin	1.8	(302)
Cyclosporine A	2.9	(303)
Ko143	3.5	CID 10322450
Retinol	5.7	CID 445354
All-*trans*-retinoic acid	6.3	CID 444795
9-*cis*-retinoic acid	6.3	CID 449171
13-*cis*-retinoic acid	6.3	CID 5282379
All-*trans*-4-oxo-retinoic acid	4.8	CID 6437063
Retinyl-acetate	6.3	CID 638034
Retinyl-propionate	6.9	CID 73818855
Retinyl-palmitate	13.6	CID 5280531

The values were collected from the National Center for Biotechnology Information. PubChem Compound Database Identification (CID) values are listed in the table.

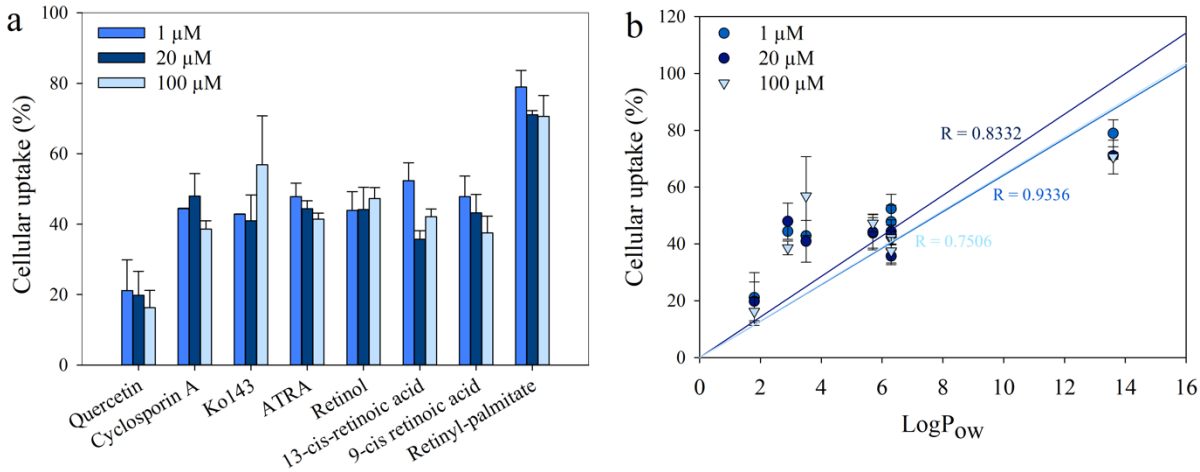

Figure 14: Cellular uptake of retinoids and transporter modulators. Samples containing retinoids or transporter inhibitors were incubated with NIH 3T3 cells (1×10^6/ml) for 30 min at 37°C. Subsequently, cells were pelleted by centrifugation at 400 × g for 5 min and supernatants were collected. The cellular uptake was determined by calculating the ratio of the absorbances measured in the supernatants at the absorption maximum of the examined compound before and after the incubation with cells (n = 3, mean ± SD) (**a**). Correlation plot of $LogP_{ow}$ values and measured cellular uptakes at different retinoid concentrations with calculated Pearson's correlation values (R) (**b**).

6.1.3. Inhibitory retinoids decrease membrane fluidity in the acyl-chain region of the membrane

In view of the hydrophobic character of the studied retinoids (**Table 8** and **Fig. 14**), as well as the intimate association of Pgp and ABCG2 with the lipid bilayer in which they are embedded and from which they can harvest their substrates (see **Fig. 7** and *Section 3.4.5*), we examined the effects of retinoids on the fluidity and packing order of the membrane

(230,231). In order to study the effects of retinoids on the membrane fluidity we carried out fluorescence anisotropy measurements using the membrane specific probes, DPH and TMA-DPH. DPH is an apolar molecule that accumulates in the inner acyl-chain region of the membrane, while TMA-DPH is a positively charged derivative of DPH (304) that is anchored at the lipid/water interface of the membrane. Therefore, using TMA-DPH and DPH the fluidity is estimated in a slightly different depths of the membrane, since the average fluorophore of TMA-DPH is about 3–4 Å closer to the membrane surface as compared to DPH (305,306). Membrane fluidity and fluorescence anisotropy values of DPH and TMA-DPH show an inverse correlation: higher membrane fluidity results in decreased fluorescence anisotropy values due to the increased rotational and vibrational freedom of the dye in the plane of the membrane, while increased anisotropy is indicative of decreased membrane fluidity (305).

Pgp and ABCG2 expressing and non-expressing NIH 3T3 and MDCK cells were treated with DPH and TMA-DPH as described in *Section 5.10*. The fluorescence anisotropy value of DPH was in the range of 0.14 and 0.18 under steady-state conditions (**Fig. 15a, b**) in both cell line pairs indicative of high structural order within the membrane, while the fluorescence anisotropy of TMA-DPH varied between 0.28 and 0.30 (**Fig. 15c, d**), suggesting lower order in the superficial regions of the membrane. The measured anisotropy values were found to be similar in drug sensitive and resistant cell lines in agreement with previous data (307).

Interestingly, retinol, 13-*cis*-retinoic acid and retinyl-acetate, the retinoids that were proved to be capable of transporter inhibition in ATPase and drug transport assays, increased the DPH fluorescence anisotropy values significantly in both NIH 3T3 and MDCK cells, while other examined retinoids did not alter the DPH anisotropy values significantly (**Fig. 15a, b**). Retinol and 13-*cis*-retinoic acid modified the DPH anisotropy similarly in the transporter expressing and non-expressing cell lines suggesting that Pgp and ABCG2 do not alter their membrane distribution. In contrast, retinyl-acetate had significantly lower effect on the DPH fluorescence anisotropy of Pgp-positive cells as compared to the Pgp-negative NIH 3T3 cells (**Fig. 15a**) apparently because of its Pgp-mediated transport (**Fig. 15a**).

Membrane fluidity in the hydrophilic head-group region was unaffected by retinoids, as it was indicated by the similar TMA-DPH fluorescence anisotropy values with the exception of retinyl-palmitate that decreased the TMA-DPH fluorescence anisotropy significantly in the NIH 3T3 cell pair. In control experiments, CsA, a competitive Pgp-specific modulator had no effect on DPH and TMA-DPH anisotropies (**Fig. 15**), supporting

that it does not affect the membrane structure, rather it can act directly through binding to the drug-binding pocket of the transporter.

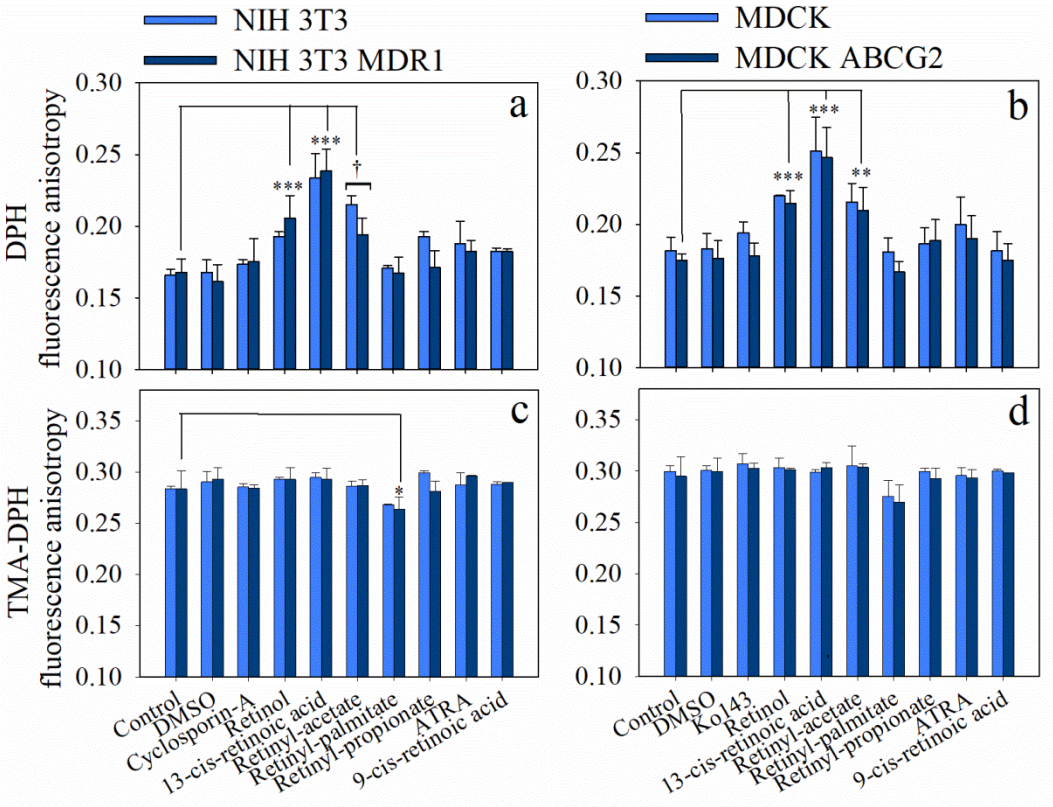

Figure 15: Effects of retinoids on the DPH (a, b) and TMA-DPH (c, d) fluorescence anisotropies measured in Pgp-positive and negative NIH 3T3 cells (a, c) and ABCG2-positive and negative MDCK cells (b, d). Cells were pre-treated with retinoids applied at 100 µM concentration or transporter inhibitors (10 µM CsA or 2 µM Ko143) for 10 min at 37 ºC and then further incubated with 2 µM DPH or TMA-DPH for another 20 min at room temperature in dark. Fluorescence anisotropy values were measured at 37 ºC. Significant differences as compared to control are shown by ***: P<0.001, **: P<0.01, *: P<0.05. Significant difference between transporter expressing and non-expressing cells is shown by †: P<0.05 (n = 3, mean ± SD, ANOVA, Holm-Sidak *post-hoc* analysis).

6.1.4. Retinoids hamper substrate stimulation of Pgp and ABCG2 ATPase activity through mixed-type inhibition

The inhibitory effect of retinoids observed in the previous experiments may be attributed to a competitive mechanism due to the direct interaction of retinoids with the substrate-binding site(s) of the transporters or to an allosteric effect probably related to structural changes of the plasma membrane brought about by certain retinoids. To gain insight into the action mechanism of retinoids, we analyzed how the kinetic parameters (K_M *and* v_{max}) of the substrate-stimulated ATPase activity were influenced by retinol and 13-*cis*-retinoic acid, the retinoid derivatives that were found to be effective Pgp and ABCG2 inhibitors in both ATPase and drug transport measurements. The ATPase activity of Pgp and ABCG2 was

stimulated by increasing concentrations of verapamil and quercetin in the presence of different concentrations of retinol and 13-*cis*-retinoic acid. Dose-response curves obtained by fitting the data points with a modified Michaelis-Menten equation showed that retinol increased the K_M and decreased the v_{max} values of both transporters (**Fig. 16a and c, Fig. 17a, b, e and f**) suggesting a mixed-type inhibition.

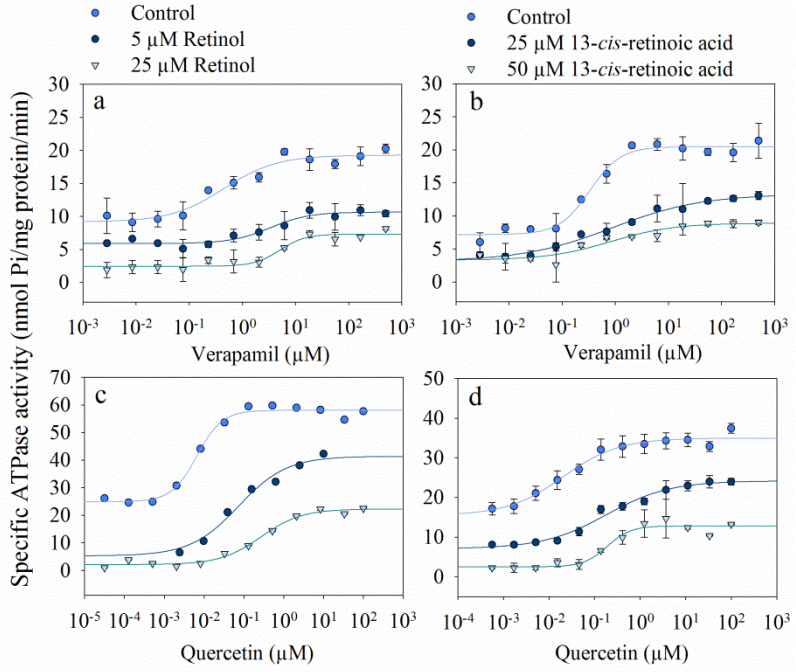

Figure 16: Inhibition of the substrate-stimulated ATPase activity of Pgp and ABCG2 by retinol (a, c) and 13-*cis*-retinoic acid (b, d) applied at different concentrations. The ATPase activity of Pgp was stimulated by increasing concentrations of verapamil, while ABCG2 was activated by quercetin. A representative data set is shown out of three independent experiments performed in triplicate (mean ± SD). The curves were obtained by fitting the data points to a modified form of the Michaelis-Menten equation (see *Section 5.8*, ($R^2 \geq 0.95$)).

13-*cis*-retinoic acid treatment also resulted in a mixed-type inhibition of ABCG2 (**Fig. 16d, Fig. 17g and h**), however, in case of Pgp, it did not induce a statistically significant increase of K_M, while decreased the v_{max} (**Fig. 16b, Fig. 17c and d**) suggesting a non-competitive inhibition of Pgp.

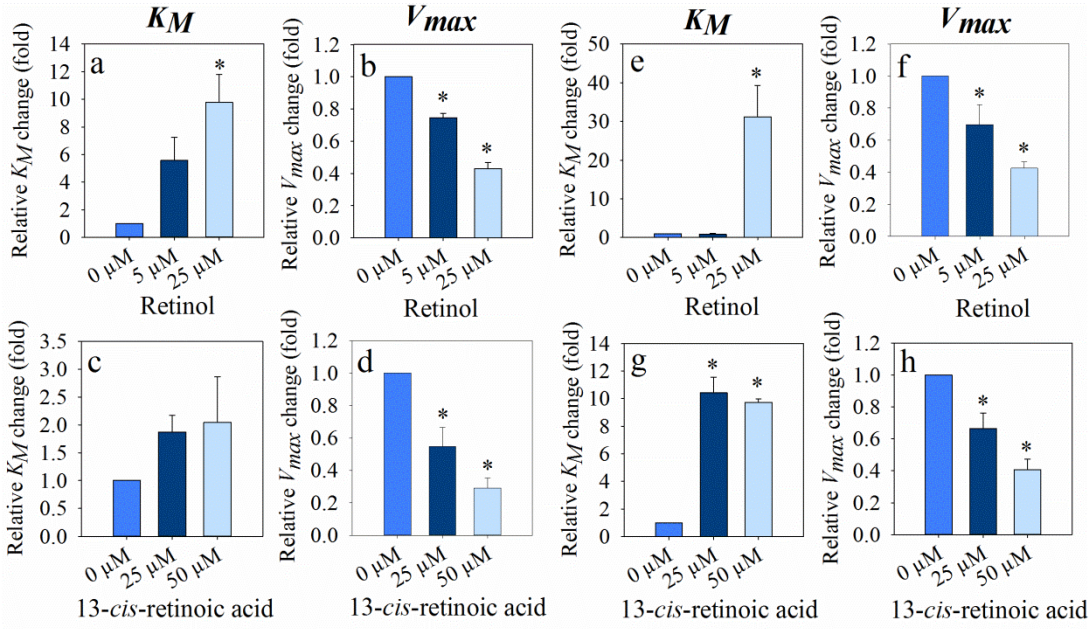

Figure 17: Changes of apparent K_M and v_{max} values of Pgp (a, b, c, d) and ABCG2 ATPase activity (e, f, g, h) in response to retinol (a, b, e, f) and 13-*cis*-retinoic acid (c, d, g, h) treatment. The apparent K_M and v_{max} values were obtained by fitting the data points using a modified form of the Michaelis-Menten equation. The ATPase activity of Pgp and ABCG2 was stimulated by increasing concentrations of verapamil and quercetin, respectively. (* = Significant difference compared to control (n = 3, mean ± SEM, ANOVA, Holm-Sidak *post-hoc* analysis, $P < 0.05$)).

6.2. Studying the catalytic cycle of Pgp using ATP-binding site mutants

6.2.1. Quadruple mutant Pgps with a non-canonical NBS1 escape conformational lock

As it was discussed in *Section 3.4.2*, several ABC exporters carry a degenerate NBS that is unable to hydrolyze ATP at a rate sufficient for maintaining transport activity. A hallmark of a degenerate NBS is the lack of the "catalytic glutamate" in the Walker B motif. Pgp has two canonical NBSs, and mutation of the "catalytic glutamate" (E556) in NBS1 makes it transport-incompetent. In contrast, the closely related bile salt export pump ABCB11 (BSEP), which shares 49% sequence identity with human Pgp, naturally contains a methionine in the place of "catalytic glutamate". The NBD-NBD interfaces of Pgp and ABCB11 differ only in four amino acid residues, all within NBS1 (see **Fig. 5**). To study the role of the four non-canonical amino acids in the degenerate NBS1 of ABCB11, we have introduced the corresponding mutations into the NBS1 of human Pgp. First, we engineered a Pgp variant containing the E556M mutation of the "catalytic glutamate". To fully mimic NBS1 of ABCB11 in the context of Pgp, we have generated a "quadruple mutant" that also contains the three additional diverging amino acid residues (S474E, G1178R and Q1180E).

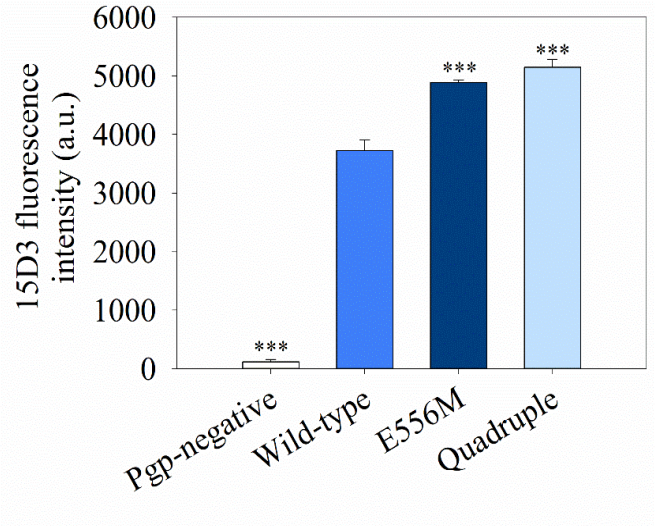

Figure 18: Cell surface expression of Pgp variants in NIH 3T3 cells. Cells were labeled for 30 min at 37 °C with 15D3-A647 anti-Pgp antibody (Mean ± SD, out of n=5 independent measurements) Significant differences as compared to wild-type Pgp expressing NIH 3T3 cells are shown by ***: P<0.001, ANOVA, Holm-Sidak *post hoc* analysis).

All Pgp variants showed comparable cell surface expression in NIH 3T3 cells, as measured in direct immunofluorescence labeling experiments using the conformation insensitive 15D3 antibody. The E556M and the quadruple mutant expressing cells showed app. 20% higher Pgp expression level as compared to wild-type Pgp expressing cells (**Fig. 18**)

indicating that the mutations do not have any effect on the stability and intracellular trafficking of the transporters.

To evaluate the conformational flexibility of single and quadruple mutant Pgps, we performed UIC2 staining experiments in the presence of a Pgp inhibitor CsA (10 μM) or following ATP depletion of cells (**Fig. 19**). Wild-type Pgps showed low UIC2-reactivity in untreated cells as only a minor fraction (app. 20%) of cell surface Pgps were labeled with the conformation-sensitive UIC2 antibody (**Fig. 19**). On the other hand, depletion of ATP resulted in UIC2 labeling of all cell surface Pgp molecules in accordance with previous data showing that UIC2 mAb has high affinity for the nucleotide-free conformation of Pgp (112,177,308). CsA treatment also stabilized the UIC2-reactive conformation of wild-type Pgps.

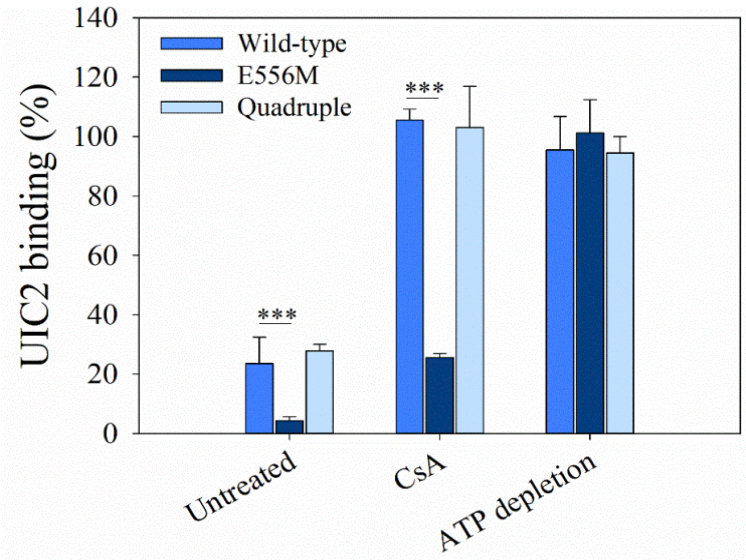

Figure 19: Conformational response of wild-type and mutant Pgp molecules to CsA treatment and ATP depletion as visualized by UIC2-reactivity. NIH 3T3 cells expressing the Pgp variants were labeled with Alexa 647 conjugated UIC2 or 15D3 mAbs (with comparable dye to antibody ratio (F/P)). The percentage of UIC2-bound Pgp conformers was calculated relative to the total cell surface Pgp expression levels determined by 15D3 labeling (mean ± SD of n = 3-5 independent experiments). Significant differences compared to wild-type Pgp are shown by *** ($p<0.001$, ANOVA, Holm-Sidak *post hoc* analysis).

Single E556M mutant Pgps showed a remarkably different behavior as compared to wild-type Pgps. In untreated cells, only app. 5% of cell surface Pgps were in a UIC2-reactive conformation and CsA treatment could only moderately increase their UIC2-reactivity (up to 20%, **Fig. 19**). Since the reactivity of nucleotide-bound Pgps to UIC2 is generally low, these data can be explained by tight ATP binding, that results in the arrest of transporter molecules in a UIC2-dim conformation. Interestingly, quadruple mutant Pgps showed very similar UIC2-reactivity pattern to wild-type (**Fig. 19**). In untreated cells, app. 20% of cell surface

Pgps were in the UIC2-reactive inward-facing conformation and practically the whole cell surface Pgp pool switched to the inward-facing UIC2-reactive conformation in response to CsA treatment (**Fig. 19**). These results strongly suggest that quadruple mutants can avoid the conformational lock that is observed in single E556M mutant Pgps. Notably, each Pgp variant showed high UIC2-reactivity in response to ATP depletion, suggesting that they adopt a similar conformation in the absence of ATP (**Fig. 19**).

Nucleotide binding to the NBDs triggers conformational changes in the TMD regions of the transporter due to allosteric coupling. Therefore, analysis of UIC2-reactivity can be used for the detection of NBD conformational changes. Using SLO-permeabilized cells, we could systematically change the intracellular ATP concentration while maintaining the natural membrane environment of Pgp molecules. In the presence of increasing concentrations of MgATP or MgATP/vanadate, we determined dose-response curves for the different Pgp variants (**Fig. 20**). In accordance with an ATP-regulated switch in the TMD conformation, increasing MgATP concentrations decreased UIC2 staining. The apparent affinity of MgATP for wild-type Pgp **(Fig. 20a, d)** (K_A=1.56 ± 0.46 mM) was found to be 3-4-fold lower than the reported K_M values for ATP hydrolysis (K_M = 0.3 - 0.5 mM) (309). Phosphate analogues such as vanadate (Vi) are known to trap ABC transporters in a post-hydrolytic state by forming a ternary complex (Pgp-ADP-Vi) replacing the cleaved gamma phosphate after ATP hydrolysis. Vi treatment increased the apparent nucleotide affinity of wild-type Pgp by 2-3 orders of magnitude (K_A = 0.081 ± 0.014 mM) (181).

As opposed to wild-type Pgp, the E556M variant exhibited similarly high apparent affinities for ATP in the absence (K_A = 0.077 ± 0.02 mM) or presence (K_A = 0.027 ± 0.001 mM) of vanadate (**Fig. 20b, d**), indicating that the lack of the "catalytic glutamate" results in a state with a tightly bound nucleotide. However, ATP binding was less tight in the quadruple mutant as compared to the single mutant Pgp as it was indicated by the elevated K_A value (K_A = 1.12 ± 0.6 mM; **Fig. 20d**). In contrast to the single mutant, quadruple mutant Pgps showed increased apparent ATP-binding affinity in the presence of Vi (K_A = 0.38 ± 0.001 mM) similarly to wild-type Pgps, consistent with the ATP hydrolysis activity of the quadruple mutant at least at its intact NBS (**Fig. 20c, d**).

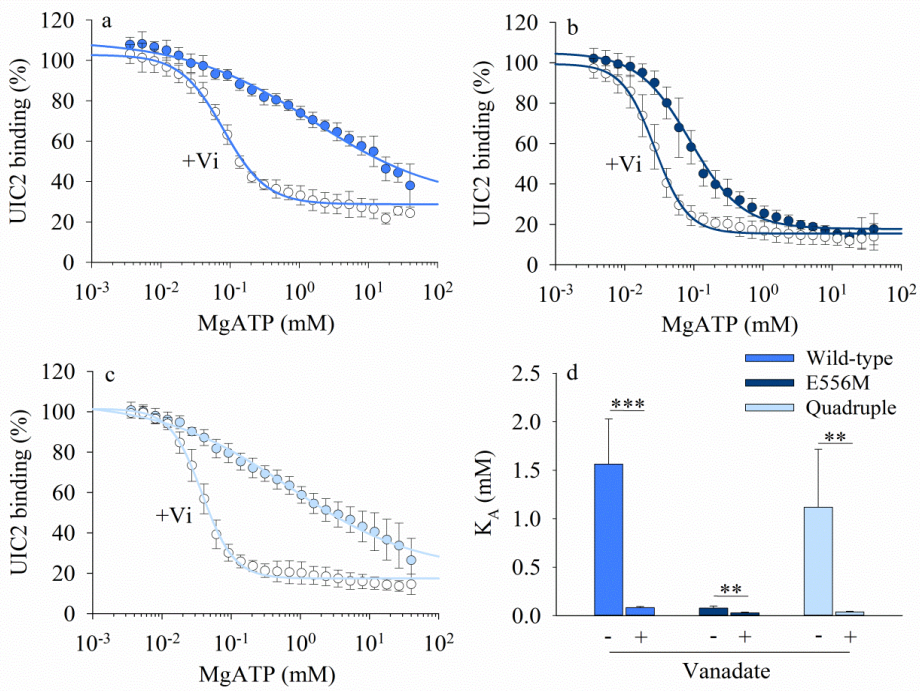

Figure 20: MgATP dependence of UIC2 binding. NIH 3T3 cells expressing wild-type, E556M and quadruple mutant Pgps were permeabilized with SLO toxin to allow for changing intracellular nucleotide concentrations. Different concentrations of MgATP were added to the cells for 30 min at 37°C with or without 0.5 mM vanadate (Vi). After incubation with nucleotides 10 µg/ml UIC2-A647 was added to the samples for 30 min at 37°C. Dose-response curves of UIC2 binding, with increasing concentrations of MgATP in the absence or presence of Vi, were obtained for wild-type (**a**), E556M- (**b**) and quadruple mutant (**c**) variants by fitting the data points to a four-parameter Hill-function (see *Section 5.13*). Mean apparent nucleotide affinity (K_A) values are summarized in panel (**d**) (n = 5-6, mean ± SD, unpaired t-test (two-tailed); ***p<0.001, **p<0.01).

6.2.2. Quadruple mutant Pgps regain their transport and ATPase activity

In the following experiments, we aimed to examine the functional activity of mutant Pgps applying ATPase activity and drug accumulation measurements.

Membranes isolated from NIH 3T3 cells expressing wild-type and mutant Pgps showed similarly high expression levels as it was demonstrated in our western blot experiments **(Fig. 21a)**. Wild-type Pgps showed the expected basal ATPase activity, which was stimulated about 4-fold by the addition of verapamil. Strikingly, the quadruple mutant showed a low steady state ATPase activity (**Fig. 21b**) that could be stimulated by verapamil. Although the basal ATPase activity was significantly reduced, the degree of stimulation by verapamil was almost identical to wild-type, showing that substrate-stimulation of the ATPase activity was restored in the quadruple mutant (**Fig. 21b, c**). In contrast, the "catalytic glutamate" mutant (E556M) showed no significant basal or verapamil-stimulated ATPase activity (**Fig. 21b**).

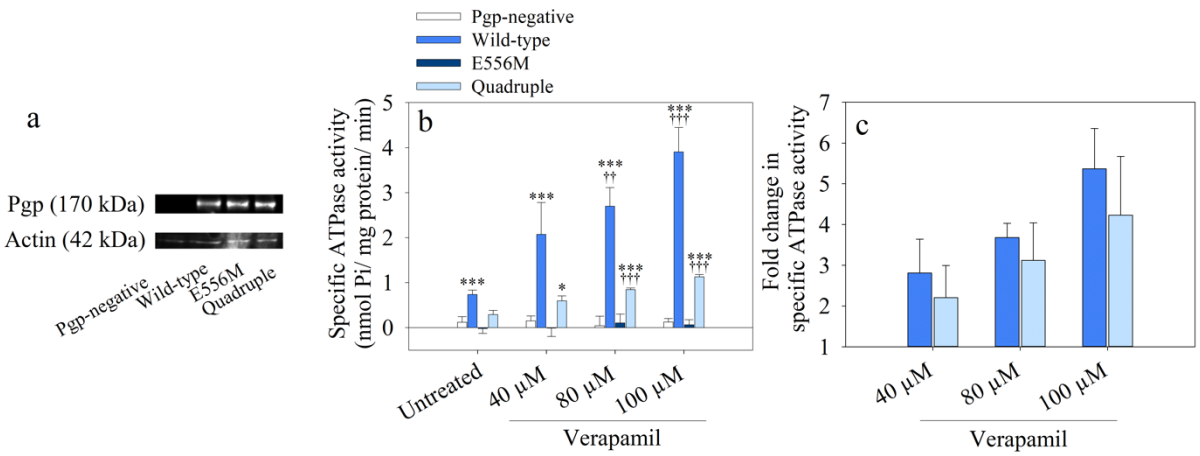

Figure 21: Effects of E556M and E556M/S474E/G1178R/1180E mutations on the basal and verapamil-stimulated ATPase activity of Pgp. Pgp expression level of the membrane samples (5 µg membrane protein/slot) was checked by immunoblot using the G-1 anti-Pgp mAb and C-2 anti-actin mAb (**a**).Wild-type-, single- and quadruple mutant Pgp expressing and Pgp negative NIH 3T3 cell membrane preparations (15 µg/sample) were incubated in the presence of 3 mM MgATP for 25 min. The substrate-dependent ATPase activity of Pgp was measured in the presence of increasing concentrations of verapamil (**b**) (n = 5, mean ± SD, ANOVA, Dunnett T3 *post hoc* test, significant differences compared to untreated NIH 3T3 control membrane are shown by ***: P<0.001, **: P<0.01, *: P<0.05; significant differences between verapamil treated and untreated samples are presented as †††: P<0.001, ††: P<0.01, †: P<0.05). Wild-type and quadruple mutant Pgps show similar relative changes in their ATPase activity in the presence of different verapamil concentrations (**c**).

To answer the question whether quadruple mutant Pgps are able to couple their ATPase activity to uphill drug transport, we performed calcein and Hoechst 33342 accumulation experiments using intact cells (see *Section 5.5*). To quantify the transport activity of the different Pgp variants, we calculated TAF values corresponding to the normalized tariquidar dependent increase of Hoechst 33342 or calcein fluorescence intensities (see *Section 5.5*). As expected, the TAF value was close to 0 in cells devoid of Pgp, while expression of wild-type Pgp effectively prevented the intracellular accumulation of Hoechst 33342 and calcein **(Fig. 22)** resulting in elevated TAF values. The E556M mutant did not show any transport activity in agreement with the loss of steady state ATPase activity and the reduced conformational flexibility. In sharp contrast, the quadruple mutant was able to limit Hoechst 33342 and calcein accumulation, though not as efficiently as wild-type Pgp. These data clearly demonstrate that despite the absence of the "catalytic glutamate", the quadruple mutant regained the ability to efflux Hoechst 33342 and calcein. At higher concentrations of Hoechst 33342 (> 1 µM) and calcein-AM (> 0.1 µM), TAF values decreased in a substrate concentration dependent manner in accordance with the gradual saturation of the transport capacity of Pgps (**Fig. 22**) (310). The ratios of the TAF values between wild-type and quadruple mutant are comparable for both Hoechst 33342 and calcein-AM and are

concentration independent, suggesting that transport specificity is unchanged for these two substrates.

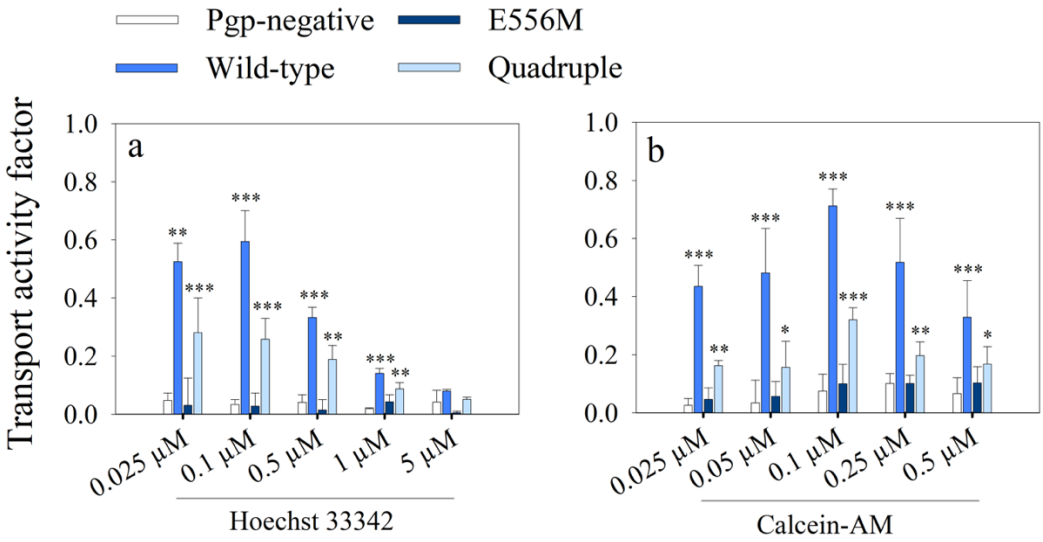

Figure 22: Transport activity of Pgp variants. Pgp dependent (**a**) Hoechst 33342 and (**b**) calcein-AM transport were quantified by the transport activity factor (TAF) as it was described in *Section 5.5*. NIH 3T3 cells expressing Pgp variants were stained with Hoechst 33342 or calcein-AM, in the absence or presence of a Pgp inhibitor tariquidar, for 30 min at 37 °C. Mean ± SD values of three independent experiments are shown. Significant differences as compared to Pgp-negative cells: ***: P<0.001, **: P<0.01 (ANOVA, Holm-Sidak *post hoc* analysis).

6.2.3. Vanadate increases the apparent ATP-binding affinity of single A-loop and Walker B mutants

Previous studies, performed on purified proteins or heterologous expression systems, demonstrated that point mutations introduced into key residues of the A-loop (Y401A and/or Y1044A) or Walker B sequences (D555N and/or D1200N) inactivate Pgp either present in one or both NBSs (see *Section 3.3.4*) (153,157). To study the conformational activity of these Pgp variants, we carried out UIC2-labeling experiments using intact mammalian cells.

As a first step, using 15D3 antibody, we have determined the cell surface expression of the mutant Pgp variants in NIH 3T3 cells (**Fig. 23**). All Pgp variants showed comparable cell surface expression in NIH 3T3 cells and only D1200N Walker B mutant expressing cells showed app. 25% higher Pgp expression level as compared to wild-type Pgp expressing cells (**Fig. 23**) indicating that, similarly to E556M and the "quadruple" mutations (see **Fig. 18**), A-loop and Walker B mutations did not have any effect on the stability and intracellular trafficking of the transporters.

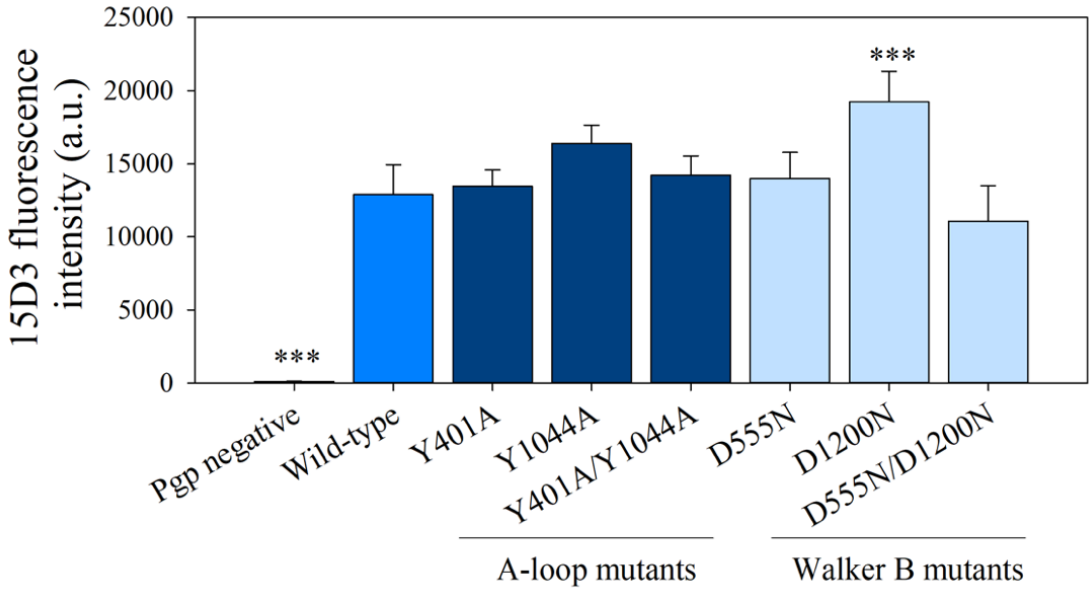

Figure 23: Cell surface expression of A-loop and Walker B mutant Pgp variants in NIH 3T3 cells. Cells were labeled with 15D3-A647 anti-Pgp antibody for 30 min at 37 ºC and subsequently were stained with PI to exclude dead cells from the analysis. Bars represent means ± SD of n=3 independent experiments. Significant differences as compared to wild-type Pgp expressing NIH 3T3 cells are shown by ***: P<0.001 (ANOVA, Holm-Sidak *post hoc* analysis).

In good accordance with literature data, wild-type Pgps preferred the UIC2-nonreactive conformation(s) and switched to the UIC2-reactive inward-facing conformation in the presence of CsA or in response to ATP depletion (**Fig. 24**). In contrast to it the A-loop tyrosine and Walker B aspartate mutants exhibited high UIC2-reactivity, which was not increased further by ATP depletion or CsA treatment (**Fig. 24**). These results support the idea that the above mutations favor the ATP-free UIC2-reactive conformation of Pgp in live cells.

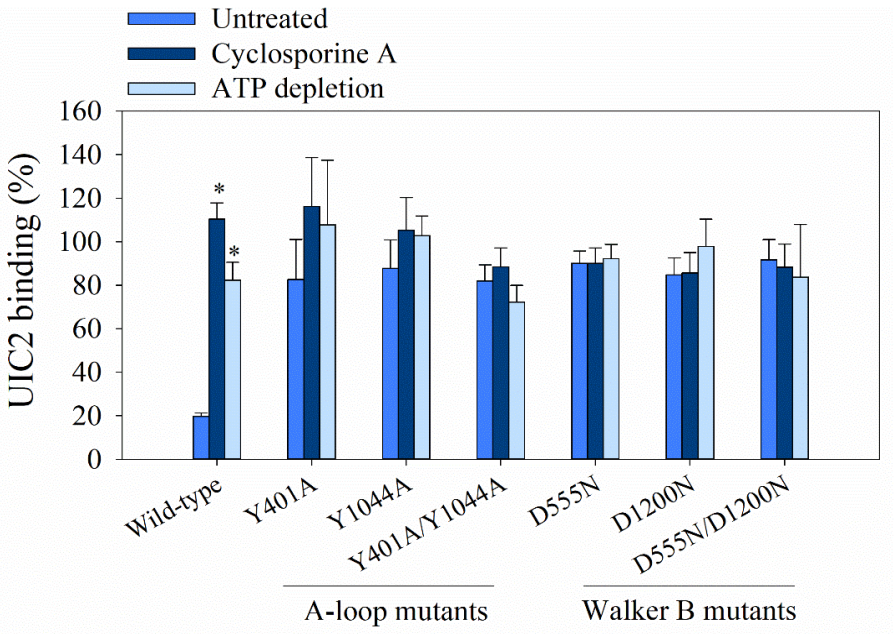

Figure 24: UIC2-reactivity of Walker B and A-loop mutants expressed in NIH 3T3 cells. Cells were pre-treated with 10 µM CsA for 10 min or with 10 mM Na-azide and 8 mM 2-deoxy-D-glucose for 30 min at 37 ºC and were labeled with 10 µg/ml UIC2-A647 or 30 µg/ml 15D3-A647. The percentage of UIC2-bound conformers was calculated relative to the total cell surface Pgp expression levels determined by 15D3 labeling. Bars represent mean ± SD values of n= 3 independent experiments. Significant differences as compared to untreated cells are shown by *: P<0.05 (ANOVA, Holm-Sidak *post hoc* analysis).

Table 9: Apparent ATP-binding affinities (K_A) of single A-loop (Y401A, Y1044A), single Walker B (D555N, D1200N) and Y401A/Y1044A, D555N/D1200N double mutant Pgps.

Pgp variant	Apparent ATP-binding affinity (K_A; mM)	Apparent ATP-binding affinity in the presence of Vi (K_A; mM)
Wild-type	1.62±0.36	0.08±0.01*
Y401A	≥10	1.80±0.19*
Y1044A	≥10	6.49±1.75*
Y401A/Y1044A	≥40	≥40
D555N	≥40	3.48±1.41*
D1200N	≥40	9.62±0.48*
D555N/D1200	≥40	≥40

Dose-response curves of UIC2 binding, with increasing concentrations of MgATP in the absence or presence of vanadate (Vi), were fitted with a four-parameter Hill function to obtain K_A values. (K_A ± SD; n = 3, unpaired t-test (two-tailed), significant differences between Vi treated and untreated samples are shown by *: p<0.05).

To further study the effects of A-loop and Walker B mutations on ATP binding to Pgp, we determined the apparent ATP affinity (K_A) of the mutant Pgp variants measuring the ATP-dependence of UIC2-reactivity in the presence or absence of Vi (**Table 9**). We proved that single A-loop (Y401A or Y1044A) and single Walker B mutant (D555N or D1200N) Pgps exhibited significantly higher K_A values as compared to wild-type (K_A app. 10 mM for single A-loop, ≥40 mM for single Walker B mutants), in accordance with literature data (157,311). Interestingly, Vi treatment decreased the K_A values of single A-loop and Walker B mutants suggesting that they were capable of ATP hydrolysis at least at their intact NBS (**Table 9**). On the other hand, we did not observe any change in response to Vi treatment in case of double mutants (Y401A/Y1044A and D555N/D1200N, respectively) suggesting that they were unable to hydrolyze ATP (**Table 9**).

6.2.4. Single A-loop mutant Pgps can hydrolyze ATP and transport substrates

To further study the effect of the mutations on the functional activity of Pgp, we carried out ATPase activity measurements using membrane preparations derived from NIH 3T3 cells expressing wild-type and the mutant Pgp variants at similarly high level (**Fig. 23**). Wild-type Pgp expressing NIH 3T3 cell membrane samples (**Fig. 25**) exhibited weak basal ATPase activity (app. 2 mmol Pi/mg protein/min) that was increased about 3-fold by verapamil treatment (**Fig. 25**). Single A-loop and single Walker B mutant Pgps showed even weaker basal ATPase activity (app. 0.5-1 mmol Pi/mg protein/min). Interestingly, addition of 40 μM verapamil brought about a two-fold stimulation in the ATPase activity of the Y401A mutant (**Fig. 25**), in accordance with the results of Vi trapping experiments (**Table 9**). Although, the C-terminal A-loop mutant (Y1044A) also showed some specific ATPase activity, we could not detect its significant stimulation by verapamil (**Fig. 25**). Membrane samples expressing double mutant Pgp variants (Y401A/Y1044A or D555N/D1200N) did not show any detectable ATPase activity in agreement with the extremely weak ATP-binding affinity of these Pgp variants (compare **Fig. 25** and **Table 9**).

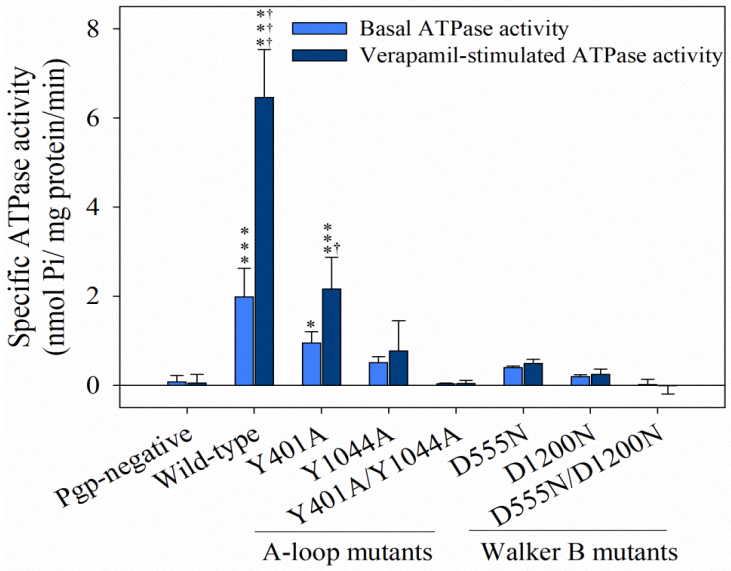

Figure 25: Effects of single- and double A-loop and Walker B mutations on the basal- and verapamil-stimulated ATPase activity of Pgp. Membrane samples were incubated in the absence or presence of verapamil and 3mM MgATP for 25 min at 37 ºC (n = 3, mean ± SD, ANOVA, Dunnett T3 *post hoc* analysis, significant differences as compared to Pgp-negative NIH 3T3 membrane samples are shown by ***: P<0.001, *: P<0.05, significant differences between verapamil treated and untreated samples are indicated by †††: P<0.001, †: P<0.05).

In further experiments, we have studied how the different mutations of these key residues affect the transport activity of Pgp. By measuring the intracellular accumulation of calcein, we observed about 60% and 40% residual transport activity as compared to wild-type Pgp in case of Y401A and Y1044A single A-loop mutants, respectively (**Fig. 26**).

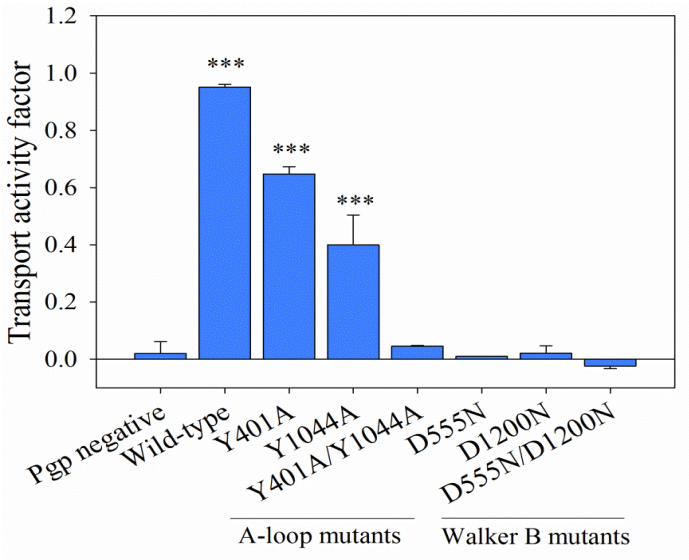

Figure 26: Transport activity of mutant Pgp variants. Pgp dependent calcein-AM transport was described by the transport activity factor (*Section 5.5*) (n = 3, mean ± SD, ANOVA, Holm-Sidak *post hoc* analysis, significant differences as compared to wild-type expressing NIH 3T3 cells are shown by ***: P<0.001).

Walker B aspartate mutant variants and the Y401A/Y1044A double A-loop mutant did not show any detectable calcein-AM transport in accordance with their weak ATP-binding affinity and low ATP hydrolysis rate at physiological MgATP concentrations (compare **Fig. 25, 26** and **Table 9**). Similarly, in cytotoxicity assays using a Pgp substrate vinblastine, we demonstrated that single A-loop mutants showed significantly increased IC_{50} values as compared to Pgp negative cells in accordance with their pronounced transport activity (**Fig. 27a**) On the other hand, Walker B mutants were unable to protect cells from the cytotoxic effect of vinblastine (**Fig. 27b**).

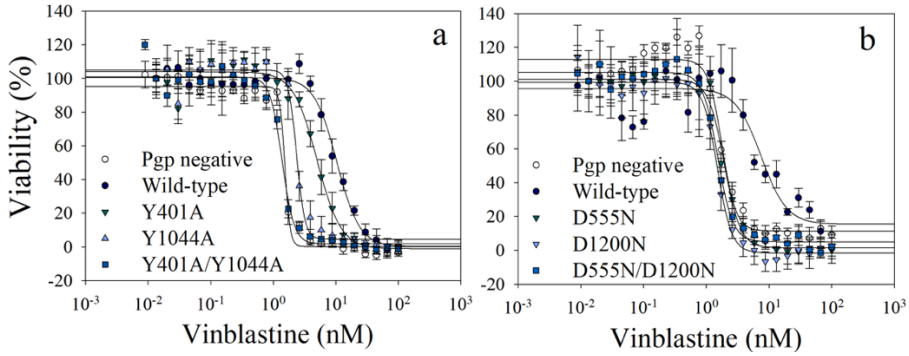

	Pgp negative	Wild-type	Y401A	Y1044A	Y401A/ Y1044A	D555N	D1200N	D555N/ D1200N
IC_{50} (nM)	1.68±0.18	13.76±2.83***	5.25±0.2***	2.7±0.42**	1.55±0.21	1.76±0.09	1.53±0.37	1.65±0.2

Figure 27: Cytotoxic effect of vinblastine in Pgp-negative, wild-type and A-loop (a) or Walker B (b) mutant Pgp expressing NIH 3T3 cells. Alamar Blue based *in vitro* cytotoxicity assays were performed as previously described (see *Section 5.11 and 6.2*). The Alamar Blue fluorescence intensity of the samples was normalized to the fluorescence of the vinblastine untreated sample and plotted as a function of vinblastine concentration. Data points are means of eight parallel samples (± SD). IC_{50} values were calculated by fitting the dose-response curves from three independent experiments. Significant differences compared to Pgp-negative NIH 3T3 cells are shown by ***: P<0.001, **: P<0.01, ANOVA, Dunnett T3 *post hoc* analysis).

6.2.5. Single A-loop and Walker B mutant Pgps are able to pass on several conformational cycles

According to our previous results, UIC2 binding to Pgp is reversible and the dissociation of the antibody can be stimulated by MgATP and Pgp substrates (177). In the following experiments, we analyzed the kinetics of UIC2 dissociation using UIC2-Fab fragments and SLO toxin permeabilized NIH 3T3 cells expressing wild-type and mutant Pgp variants (**Fig. 28**). In the absence of MgATP, we did not observe significant UIC2 dissociation (**Fig. 28**). However, in response to MgATP treatment, we measured significant

UIC2-Fab dissociation in case of single A-loop (**Fig. 28c, d**) and Walker B mutants (**Fig. 28f, g**), similarly to wild-type Pgps. In accordance with the substrate stimulation of Pgp activity, verapamil treatment significantly increased the rate of UIC2-Fab dissociation in case of the wild-type (**Fig. 28a)** and the transport competent mutant Pgp variants (for Y401A see **Fig. 28c,** for Y1044A see **Fig. 28d**). In case of the quadruple mutant, characterized in *Sections 7.1* and *7.2,* we also observed elevated UIC2-Fab dissociation, in the presence of verapamil (**Fig. 28b**). Of note, the ATPase- and transport-function deficient double Walker B and A-loop mutants did not show significant UIC2-Fab dissociation (**Fig. 28e, h**). Although, Pgp can bind ATP even in the absence of Mg^{2+} ions and can switch into a UIC2-dim state, ATP-hydrolysis is completely inhibited and the catalytic cycle is blocked at this condition (177). Interestingly, in the absence of Mg^{2+}, addition of ATP did not induce significant UIC2-Fab dissociation in wild-type Pgp expressing cells (**Fig. 28a**) suggesting that Pgps should hydrolyze ATP and pass on many conformational cycles to lose the bound UIC2-Fab.

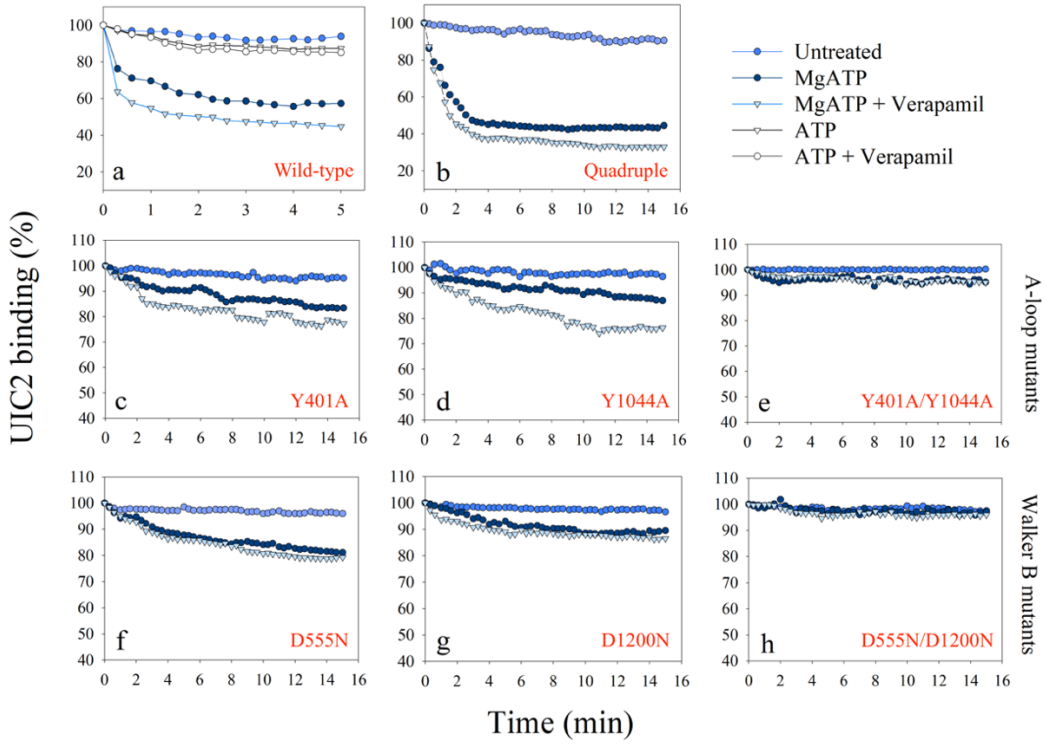

Figure 28: UIC2-Fab dissociation curves of wild-type (a), quadruple (b), single- (c, d, f, g) and double (e, h) Walker B and A-loop mutant Pgps expressed in NIH 3T3 cells. Cells were permeabilized with SLO toxin (as described in *Section 5.12*), washed three times with ice-cold PBS to remove the nucleotides and then labeled with 10 µg/ml UIC2-A647 Fab fragments and PI. Cells were kept on ice until flow cytometry measurements. UIC2-Fab dissociation was followed by measuring the UIC2-A647 fluorescence intensity of cells at 37°C for 15 min, in the absence or presence of 3 mM ATP (**a, b)** or 10 mM ATP (**c-h),** with or without Mg^{2+} and 40 µM verapamil. Mean values of UIC2-A647 fluorescence intensities were averaged for 20 s intervals (see *Section 5.15*). Representative graphs from three independent experiments are shown.

7. Discussion

7.1. Discussion I

We have studied the possible interactions between Pgp or ABCG2 and several physiologically relevant retinoid derivatives including all-*trans*-retinoic acid, 13-*cis*-retinoic acid, retinol and certain retinoid metabolites (**Fig. 8**, **Table 7**).

We have proved that retinol, 13-*cis*-retinoic acid and retinyl-acetate are effective inhibitors of Pgp- and ABCG2-mediated substrate transport **Fig. 9a, b**). The highly lipophilic character of the examined retinoid derivatives (**Table 7**) as well as their possible bioconversion by cellular enzymes renders the assessing of binding and transport of retinoids by membrane transporters difficult in live cells (**Fig. 8**) (209). Therefore, we carried out ATPase activity measurements using Pgp and ABCG2 expressing Sf9 cell membrane preparations. ATPase activity measurements confirmed the inhibitory effect of retinol, 13-*cis*-retinoic acid and retinyl-acetate (**Fig. 12**). Interestingly, these experiments also demonstrated that retinyl-acetate had a weak stimulatory effect on the basal ATPase activity of Pgp at approx. 10 μM concentration (**Fig. 12e**) indicating that retinyl-acetate might be a substrate of Pgp. In line with these observations, our DPH anisotropy measurements also indicated altered membrane distribution of retinyl-acetate in Pgp-positive cells (**Fig. 15a**). Nevertheless, we observed identical cytotoxicity profiles of retinyl-acetate in Pgp-positive and negative cells (**Fig. 13**) suggesting that even if it is really transported by Pgp, its active efflux is negligible as compared to its passive membrane permeation.

Interestingly enough, 13-*cis*-retinoic acid had a pronounced inhibitory effect on the ATPase and transport activity of both Pgp and ABCG2, while its stereoisomers ATRA and 9-*cis*-retinoic acid did not modify the functional activity of the transporters (**Fig. 9** and **Table 7**). Considering the wide substrate specificity of Pgp and ABCG2, this stereospecific interaction is striking and might provide previously unknown details of drug recognition and binding by Pgp and ABCG2 and probably by other multidrug transporters. In fact, it has been shown in several publications that stereo-selective differences can be observed in the interaction of certain modulators with Pgp. High-resolution X-ray crystal structures of mouse Pgp demonstrated that stereoisomers of a cyclic oligopeptide, QZ59-RRR and QZ59-SSS, interact with Pgp differently: QZ59-RRR binds to Pgp at only one site located at the center of the drug-binding pocket, while QZ59-SSS binds at two distinct sites (96). Similarly, *cis*- and

trans-stereoisomers of flupentixol have been shown to display stereochemical differences in their Pgp modulatory effects. Although both flupentixol stereoisomers inhibit Pgp-mediated drug transport and reverse drug resistance, they have opposite effects on the rate of ATP hydrolysis and photo-affinity labeling of Pgp with the substrate analogue, [125I]IAAP (312). Additionally, stereospecific differences have been found between the two epimers of ginsenoside Rh2 and their de-glycosylation metabolites. 20(S)-ginsenoside Rh2 reverses Pgp-mediated drug resistance in Caco-2 cells in a concentration dependent manner, while 20(R)-ginsenoside Rh2-dependent MDR-reversal is only observed at lower concentrations (313). Taken together, previous studies observed stereospecific differences between ligands in their mode of interaction with Pgp. In contrast, we observed that the recognition of certain retinoids by Pgp and ABCG2 is stereo-selective.

Stereo-selective recognition of the ligands may occur at the level of the drug-binding site(s) or allosteric site(s) of the transporter or alternatively, at the level of the plasma membrane from where substrates and modulators can reach the drug binding pocket. We observed high cellular accumulation of the tested retinoids in NIH 3T3 cells (**Fig. 14**) that exhibited strong correlation with their $LogP_{ow}$ values (**Table 8**). Since the retinoid stereoisomers showed similar cellular accumulation and $LogP_{ow}$ values suggesting similar extent of membrane partitioning, it seems likely that distinct intramembrane localization of the stereoisomers can explain their different behavior. In agreement with this hypothesis, *cis* and *tran*s isomers of zeaxanthin have been observed to display different orientations in dimyristoyl phosphatidylcholine bilayer membranes. Interestingly, these stereoisomers modified the biophysical properties of the membrane including hydrophobicity, membrane order and membrane fluidity at different depths of the membrane (314). In agreement with this finding, we observed that retinol, 13-*cis*-retinoic acid and retinyl-acetate, the retinoid derivatives acting as potent inhibitors of Pgp and ABCG2, selectively decreased the membrane fluidity and increased the packing density of the inner hydrophobic region of the membrane, as it was indicated by DPH anisotropy measurements. On the other hand, non-inhibitory retinoids e.g., ATRA or 9-*cis*-retinoic acid did not alter DPH anisotropy (**Fig. 15**). These results imply that the trans-membrane orientation of the retinoic acid stereoisomers is different. Differences in the net length of their isoprene tail depending on the presence and position of the kink introduced by the *cis* double bond might explain their different orientation. This observation is in good agreement with publications emphasizing the role of membrane-mediated substrate and modulator interactions in the determination of the substrate spectrum of Pgp and ABCG2 (315).

To analyze the interactions of retinol and 13-*cis*-retinoic acid with the transporters in more detail, we studied their effects of on the kinetic parameters (K_M and v_{max}) of the substrate-stimulated ATPase activity of Pgp and ABCG2 (**Fig. 16 and 17**). For stimulation of ATPase activity, we applied verapamil (316,317) and quercetin (318) that are well-known transported substrates of Pgp and ABCG2, respectively. Therefore, changes in the kinetic parameters of ATPase stimulation in response to retinoids truly represent alterations in substrate binding/transport by the transporters. The apparent increase of the K_M values of verapamil and quercetin in the presence of increasing concentrations of retinol seems to indicate direct interactions of retinol with both transporters (**Fig. 16 and 17**). 13-*cis*-retinoic acid increased the K_M of quercetin stimulation in ABCG2 while leaving the K_M of verapamil stimulation unaltered in Pgp (**Fig. 17c**). In addition, retinol and 13-*cis*-retinoic acid decreased the v_{max} value of both transporters (**Fig. 16 and 17**), that can be attributed to a non-competitive inhibition of the transporters or alternatively to a decreased effective concentration of the substrates (verapamil/quercetin) in the plasma membrane. In previous studies it has been proposed that changes in membrane fluidity, lipid composition or membrane packing density can significantly alter the conformational flexibility, and consequently, functional activity of Pgp (319,320). Additionally, local concentration of Pgp and ABCG2 substrates within the membrane and their accessibility to the drug binding site(s) might also be altered by changes in the membrane structure (209,227). However, further studies are required to fully understand these details.

As it was highlighted previously, retinol and its natural derivatives reach nano-molar concentrations under physiological circumstances in human tissues (*Section 3.6*), however, in our study half-inhibitory concentrations of retinoids were found to be between 20-70 μM (**Table 7**). This remarkable difference makes it unlikely that retinoids inhibit Pgp and ABCG2 *in vivo* under physiological conditions (321). However, retinoid therapy or retinol supplementation can significantly increase the concentration of retinoids in the blood or in case of oral administration in the intestinal epithelium that may inhibit Pgp or ABCG2 expressed in physiological barriers (255-257,322). Inhibition of Pgp and ABCG2 caused by retinoid therapy may also affect the pharmacokinetics of other co-administered chemotherapeutic drugs. The above effects should be considered upon therapeutic application of retinoids to avoid the possibility of drug-drug interactions occurring at the level of Pgp or ABCG2.

In conclusion, the different intramembrane orientation of certain retinoid stereoisomers might be important in their selective recognition by Pgp and ABCG2.

7.2. Discussion II

Biochemical and biophysical experiments, as well as X-ray crystallography structures and recent cryo-EM data, demonstrated that Pgp undergoes a series of conformation changes in an ATP binding and hydrolysis dependent manner to transport its substrates. ATP hydrolysis by the NBDs converts the chemical energy stored in the phosphate bonds of ATP into NBD motions that are propagated to the TMDs through a conformational cross-talk. Evidence for the inter-domain cross-talk come from i) crystal structures showing correlated conformational changes in TMDs and NBDs (96,108,112,113); ii) substrate-stimulated ATPase activity, revealing that substrate-induced conformational changes in the TMDs are propagated to the NBDs (297,323); iii) biochemical experiments showing that substrate binding to the TMDs results in conformational changes of the NBDs (109,324,325). Our observations support that nucleotides are the main determinants of the Pgp conformation, as nucleotide binding (ATP, ADP or ADP + Vi) shapes the transporter conformation in a mutation dependent manner, while all Pgp variants were equally well recognized by the UIC2 antibody in the absence of nucleotides. ATP is the primary nucleotide controlling Pgp conformation in well-energized cells, because its intracellular concentration is an order of magnitude higher than the ADP concentration and typically 10-fold above the K_D of ATP for Pgp (175). In agreement with our data, luminescence resonance energy transfer (LRET) (109), Förster resonance energy transfer (FRET) (326) and EPR (192) experiments showed that the NBDs assume larger inter-domain distances and flexibility in the absence of ATP.

Pgp has two canonical ATP-binding sites each being capable to bind and hydrolyze ATP to fuel the transport cycle (see *Section 3.4.2*). Opposed to Pgp, several ABC proteins including CFTR, SUR1 and ABCB11 possess only one canonical ATP-binding site, while in their NBS1 the "catalytic glutamate" necessary for efficient ATP hydrolysis is missing. The exact role of the "catalytic glutamate" in ATP hydrolysis is still not completely understood. A direct contact between the negatively charged "catalytic glutamate" and the negatively charged phosphate moieties of ATP seems unlikely, suggesting the indirect role of "catalytic glutamate" in ATP hydrolysis. A nucleophilic attack on the phosphate atoms leading to bond breakage between the β and γ-phosphate of ATP may be mediated by an activated OH^- nucleophile generated with the contribution from residue E556 (327,328). When we have replaced the "catalytic glutamate" in the NBS1 of human Pgp with methionine (E556M), similarly to ABCB11, we have found that Pgp became conformationally trapped, transport

incompetent and ATP hydrolysis deficient (**Figs 19-22**), confirming earlier findings (325,329).

The NBD-NBD interface of ABC transporters exhibits a remarkable level of amino acid sequence conservation demonstrating the critical role of the conserved NBD sequences in ATP binding and hydrolysis (see *Section 3.3.4*). Sequence alignment of ABCB11 and Pgp revealed that besides the "catalytic glutamate" three other amino acid residues of the NBD-NBD interfaces differ between Pgp and ABCB11 and all of them belong to NBS1 (**Fig. 5**). Generating a quadruple mutant Pgp, we have mimicked the complete non-canonical NBS1 of ABCB11 and studied it in the context of Pgp. Strikingly, in case of the "quadruple mutant" Pgp, we have observed restored conformational dynamics (**Figs 19, 20**), substrate-stimulated ATPase activity (**Fig. 21**) and transport function (**Fig. 22**). The above data suggest that quadruple mutant Pgps can avoid the high-affinity ATP binding and trapping which is observed in the E556M "catalytic glutamate" mutant Pgp variant (**Fig. 19 and 20**). Binding of ATP to the "quadruple mutant" was weaker (**Fig. 20**), as hydration of the phosphate atoms increased, and the NBD separation was more pronounced as it was demonstrated in molecular dynamic simulations (data not shown). Importantly, the alignment of the Walker A and signature sequence α-helices and therefore their dipoles deviate in the quadruple mutant from the optimal alignment of wild-type Pgp, while the increased NBD separation reduces the extent of ATP interaction with both NBDs. We can infer from these data that the ABCB11-like NBS1 of the "quadruple mutant" allows for ATP binding, but it prevents occlusion through altered interactions, thereby avoiding strong binding of ATP.

The quadruple mutant Pgp is reminiscent of ABC transporters possessing a degenerate NBS. Although the degenerate NBS of such ABC transporters is inactive, it has been shown to be important in the formation of the NBD dimer and play a regulatory role in the catalytic cycle (330,331). This notion has been validated for the ABCB11-like NBS1 in our molecular dynamic simulations (data not shown). Further studies may clarify whether ATP remains loosely bound to the degenerate NBS1 throughout the whole catalytic cycle keeping the two NBDs in close contact, or alternatively whether ATP dissociates without hydrolysis from the degenerate site in every cycle, as it was proposed for the yeast Pdr5 transporter (332,333).

In our further experiments, we studied single and double Walker B aspartate and A-loop tyrosine mutant Pgp variants and portrayed their conformational dynamics, transport and ATPase activity.

It has been proposed in several studies that mutations of the Walker B aspartate or the A-loop tyrosine lead to the inactivation of the transporter either the mutation is present in one

or in both NBSs (151,153,157,158,329). Our results proved that double mutant Pgps (Y401A/Y1044A or D555N/D1200N) did not show any transport and ATPase activity (**Fig. 25-27**) and they were locked in a UIC2-reactive conformation either in the presence or absence of MgATP and substrates (**Fig. 24** and **Table 9**).

Interestingly, single A-loop tyrosine mutant Pgp variants showed significant verapamil stimulated ATPase activity and transport function, while single Walker B aspartate mutants did not show any measurable transport and ATPase activity (**Fig. 25-27**), probably because of their very weak ATP-binding affinity (**Table 9**). Further studying the conformational activity of single Walker B aspartate mutants, we have found that they are not conformationally locked, they can switch into a UIC2-dim outward-facing conformation in an MgATP concentration dependent manner, although at much higher ATP concentrations as compared to wild-type (**Table 9**). In addition, Vi treatment increased their apparent ATP-binding affinity about 5 to 10-fold supporting that they can hydrolyze ATP at least at their intact NBD. Similar to wild-type Pgp and the transport competent mutant variants, single Walker B aspartate mutants also showed ATP hydrolysis dependent UIC2 dissociation in permeabilized NIH 3T3 cells (**Fig. 28**), further supporting that they can pass on several conformational cycles, albeit at a low turnover rate, not sufficient for measurable drug transport (**Fig. 26 and 27**).

It was described earlier that ABC transporters are enormously sensitive to their membrane microenvironment and changes in membrane properties can affect their functional activity (*Section 3.4.5*). In previous studies reporting the inactivating effect of single Walker B and A-loop mutations, heterologous expression systems (e.g., Sf9 or *Saccharomyces cerevisiae* cells) or purified and reconstituted proteins were used for the functional characterization (296). In contrast, we have targeted the different Pgp variants in their natural plasma membrane environment in mammalian cells. Plasma membrane of insect cells (e.g., Sf9) or lower eukaryotic organisms (e.g., *Saccharomyces cerevisiae*) contains significantly lower amounts of cholesterol as compared to mammalian cells (296,334), probably explaining the different results.

Our results regarding the functional activity of Pgp variants with one intact catalytic center including A-loop (Y401A or Y1044A), Walker A (K433M or K1076M) (177) and quadruple mutant Pgp challenge models assuming strictly alternating catalysis (174,175), proposing the continuous switching of ATP hydrolysis between the two NBSs (335). Assuming strict alternation between NBS1 and NBS2, in Pgp molecules with a single intact NBS, every second ATP-hydrolysis event would occur at the inactive NBS leading to

inhibition of the catalytic cycle. Our data also argue against a model which predicts that a second ATP hydrolysis event in the second NBS is needed to reset Pgp to start a new transport cycle. Taken together, the functional activity of mutant Pgp variants with one intact catalytic center supports random recruitment of the two catalytic centers for ATP hydrolysis in Pgp (177).

8. Summary

8.1. Summary of results

In the first part of our work, we studied the effects of various retinoids on the transport- and ATPase activity of Pgp and ABCG2. We have found the followings:

1. Certain retinoids including retinol, 13-*cis*-retinoic acid and retinyl-acetate inhibit the ATPase and the transport activity of Pgp and ABCG2 in a concentration-dependent manner.
2. Other investigated retinoids (all-*trans*-retinoic acid, 9-*cis*-retinoic acid, 9-*cis*-4-oxo-retinoic acid, retinyl-propionate and retinyl-palmitate) did not have any effect on the functional activity of Pgp and ABCG2.
3. Retinoids that inhibit Pgp preferentially accumulate within the hydrophobic core of the membrane and decrease the membrane fluidity based on our DPH and TMA-DPH fluorescence anisotropy measurements.
4. Intramembrane distribution might be an important factor in the recognition of retinoids by ABC transporters.
5. Retinoid therapy may result in Pgp and ABCG2 inhibition that may change the pharmacokinetics of other co-administered drugs.

In the second part of our work, we investigated the functional cooperation between the nucleotide binding sites of Pgp by studying the functional and conformational activity of Pgp variants carrying mutations in one or both catalytic sites. We came to the following conclusions:

1. Exchange of the “catalytic glutamate” to methionine (E556M) in the NBS1 of human Pgp results in a catalytically inactive transporter variant.
2. Simultaneous introduction of three other amino acid changes resulting in an ABCB11-like NBS1 leads to rescue of conformational response and ATPase and transport function of Pgp.
3. Simultaneous mutation of the A-loop tyrosine in both NBSs of Pgp leads to a catalytically dead protein showing no conformational and functional activity, while single A-loop mutants are functionally active.
4. Simultaneous mutation of the Walker B aspartate in both NBSs of Pgp results in a completely dead protein, while single mutants can possess ATP binding and

hydrolysis dependent conformational cycles at low turnover rate, not sufficient for measurable drug transport.

5. Catalytic activity of single A-loop mutant Pgps and Pgp molecules harboring an ABCB11-like degenerate NBS1 suggests that a single intact ATP-binding site might be sufficient for maintaining steady state ATPase activity and uphill substrate transport in Pgp.

6. Our results support the random recruitment of the two catalytic centers for ATP hydrolysis in Pgp.

8.2. Eredmények összefoglalása

Munkánk első részében különböző retinoid származékok a Pgp és ABCG2 transzport és ATPáz aktivitására kifejtett hatását vizsgáltuk, melynek során az alábbi következtetésekre jutottunk:

1. Egyes retinoid származékok (retinol, 13-*cisz*-retinsav, retinil-acetát) koncentráció-függő módon gátolják a Pgp és az ABCG2 transzport és ATPáz aktivitását.

2. A többi vizsgált retinoid (all-*transz*-retinsav, 9-*cisz*-retinsav, 9-*cisz*-4-oxo-retinsav, retinil-propionát és retinil-palmitát) nem befolyásolta a Pgp és az ABCG2 funkcionális aktivitását.

3. DPH és TMA-DPH fluoreszcencia anizotrópia méréseink alapján a Pgp-t és ABCG2-t gátló retinoid származékok elsősorban a membrán belső, hidrofób rétegében halmozódnak fel és ott lokálisan csökkentik a membrán fluiditását.

4. A retinoidok ABC transzporterek általi felismerését és megkötését befolyásolja membránon belüli elhelyezkedésük.

5. A retinoid terápia gátolhatja a szöveti barrierekben kifejeződő Pgp és ABCG2 molekulákat, ami megváltoztathatja az együttesen alkalmazott egyéb gyógyszerek farmakokinetikáját.

Munkánk második felében a Pgp két nukleotid-kötőhelye közötti funkcionális együttműködést tanulmányoztuk egyik vagy mindkét oldali kötőhelyben mutációt hordozó Pgp variánsok konformáció változásait és katalitikus aktivitását vizsgálva. Kísérleteink alapján az alábbi következtetéseket vontuk le:

1. A „katalitikus glutamát" metioninra történő cseréje (E556M) a Pgp N-terminális ATP-kötőhelyében mérhető transzport és ATPáz aktivitással nem rendelkező fehérjét eredményez.
2. Az E556M mutáció mellett, az ABCB11-re jellemző másik 3 aminosav szimultán cseréje a Pgp N-terminális ATP-kötőhelyében konformáció változásokra képes és mérhető transzport és ATPáz aktivitással rendelkező fehérje változatot eredményez.
3. Az A-hurok tirozin szimultán mutációja mindkét nukleotid kötőhelyben katalitikusan inaktív és konformáció változásra is képtelen Pgp variánsokat eredményez, míg a féloldali mutánsok funkcióképesek.
4. A Walker B aszparaginsav szimultán mutációja mindkét nukleotid kötőhelyben katalitikusan inaktív és konformáció változásra is képtelen Pgp variánsokat eredményez, míg a féloldali mutánsok képesek ATP kötés és hidrolízis függő konformáció változásokra, azonban mérhető transzport aktivitással nem rendelkeznek.
5. A féloldali A-hurok mutáns és az ABCB11-szerű degenerált N-terminális ATP-kötőhellyel rendelkező Pgp-k működőképessége arra utal, hogy egy intakt ATP-kötőhely elégséges a Pgp katalitikus aktivitásához.
6. Eredményeink támogatják azokat a katalitikus ciklus modelleket, amelyek a két katalitikus centrum random elköteleződését feltételezik az ATP hidrolízis irányában.

9. References

1. Bray, F., Ferlay, J., Soerjomataram, I., Siegel, R. L., Torre, L. A., and Jemal, A. (2018) Global cancer statistics 2018: GLOBOCAN estimates of incidence and mortality worldwide for 36 cancers in 185 countries. *CA: a cancer journal for clinicians* **68**, 394-424
2. Falzone, L., Salomone, S., and Libra, M. (2018) Evolution of Cancer Pharmacological Treatments at the Turn of the Third Millennium. *Frontiers in pharmacology* **9**, 1300
3. Redmond, K. M., Wilson, T. R., Johnston, P. G., and Longley, D. B. (2008) Resistance mechanisms to cancer chemotherapy. *Frontiers in bioscience : a journal and virtual library* **13**, 5138-5154
4. Minchinton, A. I., and Tannock, I. F. (2006) Drug penetration in solid tumours. *Nature reviews. Cancer* **6**, 583-592
5. Kissel, C. K., Schadendorf, D., and Rockmann, H. (2006) The altered apoptotic pathways in cisplatin and etoposide-resistant melanoma cells are drug specific. *Melanoma Res* **16**, 527-535
6. Rahman, M., and Hasan, M. R. (2015) Cancer Metabolism and Drug Resistance. *Metabolites* **5**, 571-600
7. Danhier, P., Banski, P., Payen, V. L., Grasso, D., Ippolito, L., Sonveaux, P., and Porporato, P. E. (2017) Cancer metabolism in space and time: Beyond the Warburg effect. *Biochimica et biophysica acta* **1858**, 556-572
8. Torgovnick, A., and Schumacher, B. (2015) DNA repair mechanisms in cancer development and therapy. *Front Genet* **6**, 157
9. O'Loughlin, C., Heenan, M., Coyle, S., and Clynes, M. (2000) Altered cell cycle response of drug-resistant lung carcinoma cells to doxorubicin. *European journal of cancer* **36**, 1149-1160
10. Choi, C. H. (2005) ABC transporters as multidrug resistance mechanisms and the development of chemosensitizers for their reversal. *Cancer cell international* **5**, 30
11. Sheps, J. A., and Ling, V. (2007) Preface: the concept and consequences of multidrug resistance. *Pflugers Archiv : European journal of physiology* **453**, 545-553
12. Longley, D. B., and Johnston, P. G. (2005) Molecular mechanisms of drug resistance. *The Journal of pathology* **205**, 275-292
13. Biedler, J. L., and Riehm, H. (1970) Cellular resistance to actinomycin D in Chinese hamster cells in vitro: cross-resistance, radioautographic, and cytogenetic studies. *Cancer research* **30**, 1174-1184
14. Dano, K. (1971) Development of resistance to daunomycin (NSC-82151) in Ehrlich ascites tumor. *Cancer chemotherapy reports* **55**, 133-141
15. Dano, K. (1973) Active outward transport of daunomycin in resistant Ehrlich ascites tumor cells. *Biochimica et biophysica acta* **323**, 466-483
16. Skovsgaard, T. (1978) Mechanism of cross-resistance between vincristine and daunorubicin in Ehrlich ascites tumor cells. *Cancer research* **38**, 4722-4727
17. Debenham, P. G., Kartner, N., Siminovitch, L., Riordan, J. R., and Ling, V. (1982) DNA-mediated transfer of multiple drug resistance and plasma membrane glycoprotein expression. *Molecular and cellular biology* **2**, 881-889
18. Juliano, R. L., and Ling, V. (1976) A surface glycoprotein modulating drug permeability in Chinese hamster ovary cell mutants. *Biochimica et biophysica acta* **455**, 152-162
19. Juliano, R. (1976) Drug-resistant mutants of Chinese hamster ovary cells possess an altered cell surface carbohydrate component. *Journal of supramolecular structure* **4**, 521-526
20. Kartner, N., Riordan, J. R., and Ling, V. (1983) Cell surface P-glycoprotein associated with multidrug resistance in mammalian cell lines. *Science* **221**, 1285-1288
21. Kartner, N., Evernden-Porelle, D., Bradley, G., and Ling, V. (1985) Detection of P-glycoprotein in multidrug-resistant cell lines by monoclonal antibodies. *Nature* **316**, 820-823
22. Bell, D. R., Gerlach, J. H., Kartner, N., Buick, R. N., and Ling, V. (1985) Detection of P-glycoprotein in ovarian cancer: a molecular marker associated with multidrug resistance. *Journal of clinical oncology : official journal of the American Society of Clinical Oncology* **3**, 311-315
23. Akiyama, S., Fojo, A., Hanover, J. A., Pastan, I., and Gottesman, M. M. (1985) Isolation and genetic characterization of human KB cell lines resistant to multiple drugs. *Somat Cell Mol Genet* **11**, 117-126
24. Ueda, K., Cardarelli, C., Gottesman, M. M., and Pastan, I. (1987) Expression of a full-length cDNA for the human "MDR1" gene confers resistance to colchicine, doxorubicin, and vinblastine. *Proceedings of the National Academy of Sciences of the United States of America* **84**, 3004-3008
25. Riordan, J. R., and Ling, V. (1979) Purification of P-glycoprotein from plasma membrane vesicles of Chinese hamster ovary cell mutants with reduced colchicine permeability. *The Journal of biological chemistry* **254**, 12701-12705
26. Robey, R. W., Honjo, Y., van de Laar, A., Miyake, K., Regis, J. T., Litman, T., and Bates, S. E. (2001) A functional assay for detection of the mitoxantrone resistance protein, MXR (ABCG2). *Biochimica et biophysica acta* **1512**, 171-182
27. Pedersen, P. L. (2002) Transport ATPases in biological systems and relationship to human disease: a brief overview. *Journal of bioenergetics and biomembranes* **34**, 327-332
28. Allenby, N. E., O'Connor, N., Pragai, Z., Carter, N. M., Miethke, M., Engelmann, S., Hecker, M., Wipat, A., Ward, A. C., and Harwood, C. R. (2004) Post-transcriptional regulation of the Bacillus subtilis pst operon encoding a phosphate-specific ABC transporter. *Microbiology* **150**, 2619-2628
29. Dong, J., Lai, R., Jennings, J. L., Link, A. J., and Hinnebusch, A. G. (2005) The novel ATP-binding cassette protein ARB1 is a shuttling factor that stimulates 40S and 60S ribosome biogenesis. *Molecular and cellular biology* **25**, 9859-9873

30. Williams, G. J., Williams, R. S., Williams, J. S., Moncalian, G., Arvai, A. S., Limbo, O., Guenther, G., SilDas, S., Hammel, M., Russell, P., and Tainer, J. A. (2011) ABC ATPase signature helices in Rad50 link nucleotide state to Mre11 interface for DNA repair. *Nature structural & molecular biology* **18**, 423-431
31. Holland, I. B., and Blight, M. A. (1999) ABC-ATPases, adaptable energy generators fuelling transmembrane movement of a variety of molecules in organisms from bacteria to humans. *Journal of molecular biology* **293**, 381-399
32. Cui, J., and Davidson, A. L. (2011) ABC solute importers in bacteria. *Essays in biochemistry* **50**, 85-99
33. Maqbool, A., Horler, R. S., Muller, A., Wilkinson, A. J., Wilson, K. S., and Thomas, G. H. (2015) The substrate-binding protein in bacterial ABC transporters: dissecting roles in the evolution of substrate specificity. *Biochemical Society transactions* **43**, 1011-1017
34. Oldham, M. L., and Chen, J. (2011) Snapshots of the maltose transporter during ATP hydrolysis. *Proceedings of the National Academy of Sciences of the United States of America* **108**, 15152-15156
35. Doerrler, W. T., Reedy, M. C., and Raetz, C. R. (2001) An Escherichia coli mutant defective in lipid export. *The Journal of biological chemistry* **276**, 11461-11464
36. Doerrler, W. T., Gibbons, H. S., and Raetz, C. R. (2004) MsbA-dependent translocation of lipids across the inner membrane of Escherichia coli. *The Journal of biological chemistry* **279**, 45102-45109
37. van Veen, H. W., Callaghan, R., Soceneantu, L., Sardini, A., Konings, W. N., and Higgins, C. F. (1998) A bacterial antibiotic-resistance gene that complements the human multidrug-resistance P-glycoprotein gene. *Nature* **391**, 291-295
38. Jones, P. M., and George, A. M. (2015) The Nucleotide-Free State of the Multidrug Resistance ABC Transporter LmrA: Sulfhydryl Cross-Linking Supports a Constant Contact, Head-to-Tail Configuration of the Nucleotide-Binding Domains. *PloS one* **10**, e0131505
39. VanVeen, H. W., Venema, K., Bolhuis, H., Oussenko, I., Kok, J., Poolman, B., Driessen, A. J. M., and Konings, W. N. (1996) Multidrug resistance mediated by a bacterial homolog of the human multidrug transporter MDR1. *Proceedings of the National Academy of Sciences of the United States of America* **93**, 10668-10672
40. Higgins, C. F., and Linton, K. J. (2001) Structural biology. The xyz of ABC transporters. *Science* **293**, 1782-1784
41. Kerr, I. D., Reynolds, E. D., and Cove, J. H. (2005) ABC proteins and antibiotic drug resistance: is it all about transport? *Biochemical Society transactions* **33**, 1000-1002
42. Garmory, H. S., and Titball, R. W. (2004) ATP-binding cassette transporters are targets for the development of antibacterial vaccines and therapies. *Infection and immunity* **72**, 6757-6763
43. Liu, X. (2019) ABC Family Transporters. *Advances in experimental medicine and biology* **1141**, 13-100
44. Kang, J., Park, J., Choi, H., Burla, B., Kretzschmar, T., Lee, Y., and Martinoia, E. (2011) Plant ABC Transporters. *Arabidopsis Book* **9**, e0153
45. Kovalchuk, A., and Driessen, A. J. (2010) Phylogenetic analysis of fungal ABC transporters. *BMC Genomics* **11**, 177
46. Velamakanni, S., Wei, S. L., Janvilisri, T., and van Veen, H. W. (2007) ABCG transporters: structure, substrate specificities and physiological roles : a brief overview. *Journal of bioenergetics and biomembranes* **39**, 465-471
47. Dean, M., Rzhetsky, A., and Allikmets, R. (2001) The human ATP-binding cassette (ABC) transporter superfamily. *Genome research* **11**, 1156-1166
48. Oswald, C., Holland, I. B., and Schmitt, L. (2006) The motor domains of ABC-transporters. What can structures tell us? *Naunyn-Schmiedeberg's archives of pharmacology* **372**, 385-399
49. Siarheyeva, A., and Sharom, F. J. (2009) The ABC transporter MsbA interacts with lipid A and amphipathic drugs at different sites. *The Biochemical journal* **419**, 317-328
50. Dean, M., and Annilo, T. (2005) Evolution of the ATP-binding cassette (ABC) transporter superfamily in vertebrates. *Annual review of genomics and human genetics* **6**, 123-142
51. Moitra, K., and Dean, M. (2011) Evolution of ABC transporters by gene duplication and their role in human disease. *Biol Chem* **392**, 29-37
52. Biswas-Fiss, E. E., Affet, S., Ha, M., and Biswas, S. B. (2012) Retinoid binding properties of nucleotide binding domain 1 of the Stargardt disease-associated ATP binding cassette (ABC) transporter, ABCA4. *The Journal of biological chemistry* **287**, 44097-44107
53. Rosenberg, M. F., Oleschuk, C. J., Wu, P., Mao, Q., Deeley, R. G., Cole, S. P., and Ford, R. C. (2010) Structure of a human multidrug transporter in an inward-facing conformation. *Journal of structural biology* **170**, 540-547
54. Hunt, J. F., Wang, C., and Ford, R. C. (2013) Cystic fibrosis transmembrane conductance regulator (ABCC7) structure. *Cold Spring Harbor perspectives in medicine* **3**, a009514
55. Vasiliou, V., Vasiliou, K., and Nebert, D. W. (2009) Human ATP-binding cassette (ABC) transporter family. *Human genomics* **3**, 281-290
56. Theodoulou, F. L., and Kerr, I. D. (2015) ABC transporter research: going strong 40 years on. *Biochemical Society transactions* **43**, 1033-1040
57. Dean, M., Hamon, Y., and Chimini, G. (2001) The human ATP-binding cassette (ABC) transporter superfamily. *J Lipid Res* **42**, 1007-1017
58. Gottesman, M. M., and Ambudkar, S. V. (2001) Overview: ABC transporters and human disease. *J Bioenerg Biomembr* **33**, 453-458
59. Tall, A. R., and Wang, N. (2000) Tangier disease as a test of the reverse cholesterol transport hypothesis. *J Clin Invest* **106**, 1205-1207
60. Serfaty-Lacrosniere, C., Civeira, F., Lanzberg, A., Isaia, P., Berg, J., Janus, E. D., Smith, M. P., Jr., Pritchard, P. H., Frohlich, J., Lees, R. S., and et al. (1994) Homozygous Tangier disease and cardiovascular disease. *Atherosclerosis* **107**, 85-98

61. Brooks-Wilson, A., Marcil, M., Clee, S. M., Zhang, L. H., Roomp, K., van Dam, M., Yu, L., Brewer, C., Collins, J. A., Molhuizen, H. O., Loubser, O., Ouelette, B. F., Fichter, K., Ashbourne-Excoffon, K. J., Sensen, C. W., Scherer, S., Mott, S., Denis, M., Martindale, D., Frohlich, J., Morgan, K., Koop, B., Pimstone, S., Kastelein, J. J., Genest, J., Jr., and Hayden, M. R. (1999) Mutations in ABC1 in Tangier disease and familial high-density lipoprotein deficiency. *Nature genetics* **22**, 336-345
62. Puntoni, M., Sbrana, F., Bigazzi, F., and Sampietro, T. (2012) Tangier disease: epidemiology, pathophysiology, and management. *Am J Cardiovasc Drugs* **12**, 303-311
63. McGuinness, M. C., Lu, J. F., Zhang, H. P., Dong, G. X., Heinzer, A. K., Watkins, P. A., Powers, J., and Smith, K. D. (2003) Role of ALDP (ABCD1) and mitochondria in X-linked adrenoleukodystrophy. *Molecular and cellular biology* **23**, 744-753
64. Wagner, M., Zollner, G., and Trauner, M. (2009) New molecular insights into the mechanisms of cholestasis. *Journal of hepatology* **51**, 565-580
65. Stieger, B., and Geier, A. (2011) Genetic variations of bile salt transporters as predisposing factors for drug-induced cholestasis, intrahepatic cholestasis of pregnancy and therapeutic response of viral hepatitis. *Expert Opin Drug Metab Toxicol* **7**, 411-425
66. Jacquemin, E. (2012) Progressive familial intrahepatic cholestasis. *Clin Res Hepatol Gastroenterol* **36 Suppl 1**, S26-35
67. Le Saux, O., Urban, Z., Tschuch, C., Csiszar, K., Bacchelli, B., Quaglino, D., Pasquali-Ronchetti, I., Pope, F. M., Richards, A., Terry, S., Bercovitch, L., de Paepe, A., and Boyd, C. D. (2000) Mutations in a gene encoding an ABC transporter cause pseudoxanthoma elasticum. *Nature genetics* **25**, 223-227
68. Borst, P., Varadi, A., and van de Wetering, K. (2019) PXE, a Mysterious Inborn Error Clarified. *Trends in biochemical sciences* **44**, 125-140
69. Jansen, R. S., Duijst, S., Mahakena, S., Sommer, D., Szeri, F., Varadi, A., Plomp, A., Bergen, A. A., Oude Elferink, R. P., Borst, P., and van de Wetering, K. (2014) ABCC6-mediated ATP secretion by the liver is the main source of the mineralization inhibitor inorganic pyrophosphate in the systemic circulation-brief report. *Arteriosclerosis, thrombosis, and vascular biology* **34**, 1985-1989
70. Pomozi, V., Brampton, C., Szeri, F., Dedinszki, D., Kozak, E., van de Wetering, K., Hopkins, H., Martin, L., Varadi, A., and Le Saux, O. (2017) Functional Rescue of ABCC6 Deficiency by 4-Phenylbutyrate Therapy Reduces Dystrophic Calcification in Abcc6(-/-) Mice. *The Journal of investigative dermatology* **137**, 595-602
71. Dedinszki, D., Szeri, F., Kozak, E., Pomozi, V., Tokesi, N., Mezei, T. R., Merczel, K., Letavernier, E., Tang, E., Le Saux, O., Aranyi, T., van de Wetering, K., and Varadi, A. (2017) Oral administration of pyrophosphate inhibits connective tissue calcification. *EMBO molecular medicine* **9**, 1463-1470
72. Pomozi, V., Brampton, C., van de Wetering, K., Zoll, J., Calio, B., Pham, K., Owens, J. B., Marh, J., Moisyadi, S., Varadi, A., Martin, L., Bauer, C., Erdmann, J., Aherrahrou, Z., and Le Saux, O. (2017) Pyrophosphate Supplementation Prevents Chronic and Acute Calcification in ABCC6-Deficient Mice. *The American journal of pathology* **187**, 1258-1272
73. Davies, J. C., Alton, E. W., and Bush, A. (2007) Cystic fibrosis. *BMJ* **335**, 1255-1259
74. Riordan, J. R., Rommens, J. M., Kerem, B., Alon, N., Rozmahel, R., Grzelczak, Z., Zielenski, J., Lok, S., Plavsic, N., Chou, J. L., and et al. (1989) Identification of the cystic fibrosis gene: cloning and characterization of complementary DNA. *Science* **245**, 1066-1073
75. Takada, T., Ichida, K., Matsuo, H., Nakayama, A., Murakami, K., Yamanashi, Y., Kasuga, H., Shinomiya, N., and Suzuki, H. (2014) ABCG2 dysfunction increases serum uric acid by decreased intestinal urate excretion. *Nucleosides Nucleotides Nucleic Acids* **33**, 275-281
76. Kondo, C., Suzuki, H., Itoda, M., Ozawa, S., Sawada, J., Kobayashi, D., Ieiri, I., Mine, K., Ohtsubo, K., and Sugiyama, Y. (2004) Functional analysis of SNPs variants of BCRP/ABCG2. *Pharm Res* **21**, 1895-1903
77. Cleophas, M. C., Joosten, L. A., Stamp, L. K., Dalbeth, N., Woodward, O. M., and Merriman, T. R. (2017) ABCG2 polymorphisms in gout: insights into disease susceptibility and treatment approaches. *Pharmgenomics Pers Med* **10**, 129-142
78. Rudashevskaya, E. L., Stockner, T., Trauner, M., Freissmuth, M., and Chiba, P. (2014) Pharmacological correction of misfolding of ABC proteins. *Drug Discov Today Technol* **12**, e87-94
79. Vauthier, V., Housset, C., and Falguieres, T. (2017) Targeted pharmacotherapies for defective ABC transporters. *Biochem Pharmacol* **136**, 1-11
80. Mozner, O., Bartos, Z., Zambo, B., Homolya, L., Hegedus, T., and Sarkadi, B. (2019) Cellular Processing of the ABCG2 Transporter-Potential Effects on Gout and Drug Metabolism. *Cells* **8**
81. Staud, F., Ceckova, M., Micuda, S., and Pavek, P. (2010) Expression and function of p-glycoprotein in normal tissues: effect on pharmacokinetics. *Methods in molecular biology* **596**, 199-222
82. Maliepaard, M., Scheffer, G. L., Faneyte, I. F., van Gastelen, M. A., Pijnenborg, A. C., Schinkel, A. H., van De Vijver, M. J., Scheper, R. J., and Schellens, J. H. (2001) Subcellular localization and distribution of the breast cancer resistance protein transporter in normal human tissues. *Cancer research* **61**, 3458-3464
83. Schinkel, A. H., Mol, C. A., Wagenaar, E., van Deemter, L., Smit, J. J., and Borst, P. (1995) Multidrug resistance and the role of P-glycoprotein knockout mice. *European journal of cancer* **31A**, 1295-1298
84. Schinkel, A. H., Smit, J. J., van Tellingen, O., Beijnen, J. H., Wagenaar, E., van Deemter, L., Mol, C. A., van der Valk, M. A., Robanus-Maandag, E. C., te Riele, H. P., and et al. (1994) Disruption of the mouse mdr1a P-glycoprotein gene leads to a deficiency in the blood-brain barrier and to increased sensitivity to drugs. *Cell* **77**, 491-502
85. Schinkel, A. H. (1999) P-Glycoprotein, a gatekeeper in the blood-brain barrier. *Advanced drug delivery reviews* **36**, 179-194

86. Sharom, F. J. (2011) The P-glycoprotein multidrug transporter. *Essays in biochemistry* **50**, 161-178
87. Thiebaut, F., Tsuruo, T., Hamada, H., Gottesman, M. M., Pastan, I., and Willingham, M. C. (1987) Cellular localization of the multidrug-resistance gene product P-glycoprotein in normal human tissues. *Proceedings of the National Academy of Sciences of the United States of America* **84**, 7735-7738
88. Robey, R. W., To, K. K., Polgar, O., Dohse, M., Fetsch, P., Dean, M., and Bates, S. E. (2009) ABCG2: a perspective. *Advanced drug delivery reviews* **61**, 3-13
89. Chaudhary, P. M., and Roninson, I. B. (1991) Expression and activity of P-glycoprotein, a multidrug efflux pump, in human hematopoietic stem cells. *Cell* **66**, 85-94
90. Zhou, J., and Zhang, Y. (2008) Cancer stem cells: Models, mechanisms and implications for improved treatment. *Cell Cycle* **7**, 1360-1370
91. Wee, B., Pietras, A., Ozawa, T., Bazzoli, E., Podlaha, O., Antczak, C., Westermark, B., Nelander, S., Uhrbom, L., Forsberg-Nilsson, K., Djaballah, H., Michor, F., and Holland, E. C. (2016) ABCG2 regulates self-renewal and stem cell marker expression but not tumorigenicity or radiation resistance of glioma cells. *Scientific reports* **6**, 25956
92. Ding, X. W., Wu, J. H., and Jiang, C. P. (2010) ABCG2: a potential marker of stem cells and novel target in stem cell and cancer therapy. *Life sciences* **86**, 631-637
93. Szakacs, G., Varadi, A., Ozvegy-Laczka, C., and Sarkadi, B. (2008) The role of ABC transporters in drug absorption, distribution, metabolism, excretion and toxicity (ADME-Tox). *Drug Discov Today* **13**, 379-393
94. Mechetner, E. B., Schott, B., Morse, B. S., Stein, W. D., Druley, T., Davis, K. A., Tsuruo, T., and Roninson, I. B. (1997) P-glycoprotein function involves conformational transitions detectable by differential immunoreactivity. *Proc Natl Acad Sci U S A* **94**, 12908-12913
95. Sonveaux, N., Vigano, C., Shapiro, A. B., Ling, V., and Ruysschaert, J. M. (1999) Ligand-mediated tertiary structure changes of reconstituted P-glycoprotein. A tryptophan fluorescence quenching analysis. *J Biol Chem* **274**, 17649-17654
96. Aller, S. G., Yu, J., Ward, A., Weng, Y., Chittaboina, S., Zhuo, R., Harrell, P. M., Trinh, Y. T., Zhang, Q., Urbatsch, I. L., and Chang, G. (2009) Structure of P-glycoprotein reveals a molecular basis for poly-specific drug binding. *Science* **323**, 1718-1722
97. Lee, J. Y., Kinch, L. N., Borek, D. M., Wang, J., Wang, J., Urbatsch, I. L., Xie, X. S., Grishin, N. V., Cohen, J. C., Otwinowski, Z., Hobbs, H. H., and Rosenbaum, D. M. (2016) Crystal structure of the human sterol transporter ABCG5/ABCG8. *Nature* **533**, 561-564
98. ter Beek, J., Guskov, A., and Slotboom, D. J. (2014) Structural diversity of ABC transporters. *J Gen Physiol* **143**, 419-435
99. Rosenberg, M. F., Callaghan, R., Modok, S., Higgins, C. F., and Ford, R. C. (2005) Three-dimensional structure of P-glycoprotein: the transmembrane regions adopt an asymmetric configuration in the nucleotide-bound state. *The Journal of biological chemistry* **280**, 2857-2862
100. Ward, A. B., Szewczyk, P., Grimard, V., Lee, C. W., Martinez, L., Doshi, R., Caya, A., Villaluz, M., Pardon, E., Cregger, C., Swartz, D. J., Falson, P. G., Urbatsch, I. L., Govaerts, C., Steyaert, J., and Chang, G. (2013) Structures of P-glycoprotein reveal its conformational flexibility and an epitope on the nucleotide-binding domain. *Proceedings of the National Academy of Sciences of the United States of America* **110**, 13386-13391
101. Alam, A., Kowal, J., Broude, E., Roninson, I., and Locher, K. P. (2019) Structural insight into substrate and inhibitor discrimination by human P-glycoprotein. *Science* **363**, 753-756
102. Manolaridis, I., Jackson, S. M., Taylor, N. M. I., Kowal, J., Stahlberg, H., and Locher, K. P. (2018) Cryo-EM structures of a human ABCG2 mutant trapped in ATP-bound and substrate-bound states. *Nature* **563**, 426-430
103. McDevitt, C. A., Collins, R. F., Conway, M., Modok, S., Storm, J., Kerr, I. D., Ford, R. C., and Callaghan, R. (2006) Purification and 3D structural analysis of oligomeric human multidrug transporter ABCG2. *Structure* **14**, 1623-1632
104. Rosenberg, M. F., Bikadi, Z., Chan, J., Liu, X., Ni, Z., Cai, X., Ford, R. C., and Mao, Q. (2010) The human breast cancer resistance protein (BCRP/ABCG2) shows conformational changes with mitoxantrone. *Structure* **18**, 482-493
105. Hazai, E., and Bikadi, Z. (2008) Homology modeling of breast cancer resistance protein (ABCG2). *Journal of structural biology* **162**, 63-74
106. Li, Y. F., Polgar, O., Okada, M., Esser, L., Bates, S. E., and Xia, D. (2007) Towards understanding the mechanism of action of the multidrug resistance-linked half-ABC transporter ABCG2: a molecular modeling study. *Journal of molecular graphics & modelling* **25**, 837-851
107. Khunweeraphong, N., Stockner, T., and Kuchler, K. (2017) The structure of the human ABC transporter ABCG2 reveals a novel mechanism for drug extrusion. *Sci Rep* **7**, 13767
108. Kodan, A., Yamaguchi, T., Nakatsu, T., Matsuoka, K., Kimura, Y., Ueda, K., and Kato, H. (2019) Inward- and outward-facing X-ray crystal structures of homodimeric P-glycoprotein CmABCB1. *Nat Commun* **10**, 88
109. Zoghbi, M. E., Mok, L., Swartz, D. J., Singh, A., Fendley, G. A., Urbatsch, I. L., and Altenberg, G. A. (2017) Substrate-induced conformational changes in the nucleotide-binding domains of lipid bilayer-associated P-glycoprotein during ATP hydrolysis. *J Biol Chem* **292**, 20412-20424
110. Moeller, A., Lee, S. C., Tao, H., Speir, J. A., Chang, G., Urbatsch, I. L., Potter, C. S., Carragher, B., and Zhang, Q. (2015) Distinct conformational spectrum of homologous multidrug ABC transporters. *Structure* **23**, 450-460
111. Lusvarghi, S., Robey, R. W., Gottesman, M. M., and Ambudkar, S. V. (2020) Multidrug transporters: recent insights from cryo-electron microscopy-derived atomic structures and animal models. *F1000Research* **9**
112. Alam, A., Kung, R., Kowal, J., McLeod, R. A., Tremp, N., Broude, E. V., Roninson, I. B., Stahlberg, H., and Locher, K. P. (2018) Structure of a zosuquidar and UIC2-bound human-mouse chimeric ABCB1. *Proc Natl Acad Sci U S A* **115**, E1973-E1982

113. Kim, Y., and Chen, J. (2018) Molecular structure of human P-glycoprotein in the ATP-bound, outward-facing conformation. *Science* **359**, 915-919
114. Taylor, N. M. I., Manolaridis, I., Jackson, S. M., Kowal, J., Stahlberg, H., and Locher, K. P. (2017) Structure of the human multidrug transporter ABCG2. *Nature* **546**, 504-509
115. Jackson, S. M., Manolaridis, I., Kowal, J., Zechner, M., Taylor, N. M. I., Bause, M., Bauer, S., Bartholomaeus, R., Bernhardt, G., Koenig, B., Buschauer, A., Stahlberg, H., Altmann, K. H., and Locher, K. P. (2018) Structural basis of small-molecule inhibition of human multidrug transporter ABCG2. *Nature structural & molecular biology* **25**, 333-340
116. Mi, W., Li, Y., Yoon, S. H., Ernst, R. K., Walz, T., and Liao, M. (2017) Structural basis of MsbA-mediated lipopolysaccharide transport. *Nature* **549**, 233-237
117. Hofmann, S., Januliene, D., Mehdipour, A. R., Thomas, C., Stefan, E., Bruchert, S., Kuhn, B. T., Geertsma, E. R., Hummer, G., Tampe, R., and Moeller, A. (2019) Conformation space of a heterodimeric ABC exporter under turnover conditions. *Nature* **571**, 580-583
118. Gottesman, M. M., and Pastan, I. (1993) Biochemistry of multidrug resistance mediated by the multidrug transporter. *Annu Rev Biochem* **62**, 385-427
119. Pan, L., and Aller, S. G. (2015) Equilibrated atomic models of outward-facing P-glycoprotein and effect of ATP binding on structural dynamics. *Sci Rep* **5**, 7880
120. Gottesman, M. M., Fojo, T., and Bates, S. E. (2002) Multidrug resistance in cancer: role of ATP-dependent transporters. *Nature reviews. Cancer* **2**, 48-58
121. Khunweeraphong, N., Szollosi, D., Stockner, T., and Kuchler, K. (2019) The ABCG2 multidrug transporter is a pump gated by a valve and an extracellular lid. *Nat Commun* **10**, 5433
122. Dey, S., Ramachandra, M., Pastan, I., Gottesman, M. M., and Ambudkar, S. V. (1997) Evidence for two nonidentical drug-interaction sites in the human P-glycoprotein. *Proceedings of the National Academy of Sciences of the United States of America* **94**, 10594-10599
123. Russell, P. L., and Sharom, F. J. (2006) Conformational and functional characterization of trapped complexes of the P-glycoprotein multidrug transporter. *The Biochemical journal* **399**, 315-323
124. Alqawi, O., Bates, S., and Georges, E. (2004) Arginine482 to threonine mutation in the breast cancer resistance protein ABCG2 inhibits rhodamine 123 transport while increasing binding. *The Biochemical journal* **382**, 711-716
125. Safa, A. R. (1999) Photoaffinity analogs for multidrug resistance-related transporters and their use in identifying chemosensitizers. *Drug resistance updates : reviews and commentaries in antimicrobial and anticancer chemotherapy* **2**, 371-381
126. Storm, J., O'Mara, M. L., Crowley, E. H., Peall, J., Tieleman, D. P., Kerr, I. D., and Callaghan, R. (2007) Residue G346 in transmembrane segment six is involved in inter-domain communication in P-glycoprotein. *Biochemistry* **46**, 9899-9910
127. Shapiro, A. B., Fox, K., Lam, P., and Ling, V. (1999) Stimulation of P-glycoprotein-mediated drug transport by prazosin and progesterone. Evidence for a third drug-binding site. *European journal of biochemistry* **259**, 841-850
128. Shapiro, A. B., and Ling, V. (1997) Positively cooperative sites for drug transport by P-glycoprotein with distinct drug specificities. *European journal of biochemistry / FEBS* **250**, 130-137
129. Martin, C., Berridge, G., Mistry, P., Higgins, C., Charlton, P., and Callaghan, R. (1999) The molecular interaction of the high affinity reversal agent XR9576 with P-glycoprotein. *British journal of pharmacology* **128**, 403-411
130. Clark, R., Kerr, I. D., and Callaghan, R. (2006) Multiple drugbinding sites on the R482G isoform of the ABCG2 transporter. *British journal of pharmacology* **149**, 506-515
131. Wong, K., Ma, J., Rothnie, A., Biggin, P. C., and Kerr, I. D. (2014) Towards understanding promiscuity in multidrug efflux pumps. *Trends in biochemical sciences* **39**, 8-16
132. Li, J., Jaimes, K. F., and Aller, S. G. (2014) Refined structures of mouse P-glycoprotein. *Protein science : a publication of the Protein Society* **23**, 34-46
133. Taylor, A. M., Storm, J., Soceneantu, L., Linton, K. J., Gabriel, M., Martin, C., Woodhouse, J., Blott, E., Higgins, C. F., and Callaghan, R. (2001) Detailed characterization of cysteine-less P-glycoprotein reveals subtle pharmacological differences in function from wild-type protein. *British journal of pharmacology* **134**, 1609-1618
134. Loo, T. W., and Clarke, D. M. (1999) Determining the structure and mechanism of the human multidrug resistance P-glycoprotein using cysteine-scanning mutagenesis and thiol-modification techniques. *Biochimica et biophysica acta* **1461**, 315-325
135. Chufan, E. E., Kapoor, K., Sim, H. M., Singh, S., Talele, T. T., Durell, S. R., and Ambudkar, S. V. (2013) Multiple transport-active binding sites are available for a single substrate on human P-glycoprotein (ABCB1). *PloS one* **8**, e82463
136. Pleban, K., Kopp, S., Csaszar, E., Peer, M., Hrebicek, T., Rizzi, A., Ecker, G. F., and Chiba, P. (2005) P-glycoprotein substrate binding domains are located at the transmembrane domain/transmembrane domain interfaces: a combined photoaffinity labeling-protein homology modeling approach. *Molecular pharmacology* **67**, 365-374
137. Donmez Cakil, Y., Khunweeraphong, N., Parveen, Z., Schmid, D., Artaker, M., Ecker, G. F., Sitte, H. H., Pusch, O., Stockner, T., and Chiba, P. (2014) Pore-exposed tyrosine residues of P-glycoprotein are important hydrogen-bonding partners for drugs. *Molecular pharmacology* **85**, 420-428
138. Loo, T. W., Bartlett, M. C., and Clarke, D. M. (2003) Substrate-induced conformational changes in the transmembrane segments of human P-glycoprotein. Direct evidence for the substrate-induced fit mechanism for drug binding. *The Journal of biological chemistry* **278**, 13603-13606
139. Higgins, C. F. (1992) ABC transporters: from microorganisms to man. *Annu Rev Cell Biol* **8**, 67-113

140. Story, R. M., Weber, I. T., and Steitz, T. A. (1992) The structure of the E. coli recA protein monomer and polymer. *Nature* **355**, 318-325
141. Ye, J., Osborne, A. R., Groll, M., and Rapoport, T. A. (2004) RecA-like motor ATPases--lessons from structures. *Biochim Biophys Acta* **1659**, 1-18
142. Newstead, S., Fowler, P. W., Bilton, P., Carpenter, E. P., Sadler, P. J., Campopiano, D. J., Sansom, M. S., and Iwata, S. (2009) Insights into how nucleotide-binding domains power ABC transport. *Structure* **17**, 1213-1222
143. Kapoor, P., Briggs, D. A., Cox, M. H., and Kerr, I. D. (2020) Disruption of the Unique ABCG-Family NBD:NBD Interface Impacts Both Drug Transport and ATP Hydrolysis. *International journal of molecular sciences* **21**
144. Loo, T. W., and Clarke, D. M. (2000) Identification of residues within the drug-binding domain of the human multidrug resistance P-glycoprotein by cysteine-scanning mutagenesis and reaction with dibromobimane. *The Journal of biological chemistry* **275**, 39272-39278
145. Azzaria, M., Schurr, E., and Gros, P. (1989) Discrete mutations introduced in the predicted nucleotide-binding sites of the mdr1 gene abolish its ability to confer multidrug resistance. *Mol Cell Biol* **9**, 5289-5297
146. Muller, M., Bakos, E., Welker, E., Varadi, A., Germann, U. A., Gottesman, M. M., Morse, B. S., Roninson, I. B., and Sarkadi, B. (1996) Altered drug-stimulated ATPase activity in mutants of the human multidrug resistance protein. *The Journal of biological chemistry* **271**, 1877-1883
147. Henriksen, U., Gether, U., and Litman, T. (2005) Effect of Walker A mutation (K86M) on oligomerization and surface targeting of the multidrug resistance transporter ABCG2. *Journal of cell science* **118**, 1417-1426
148. Procko, E., Ferrin-O'Connell, I., Ng, S. L., and Gaudet, R. (2006) Distinct structural and functional properties of the ATPase sites in an asymmetric ABC transporter. *Mol Cell* **24**, 51-62
149. Tombline, G., Bartholomew, L. A., Tyndall, G. A., Gimi, K., Urbatsch, I. L., and Senior, A. E. (2004) Properties of P-glycoprotein with mutations in the "catalytic carboxylate" glutamate residues. *The Journal of biological chemistry* **279**, 46518-46526
150. Qu, Q., Russell, P. L., and Sharom, F. J. (2003) Stoichiometry and affinity of nucleotide binding to P-glycoprotein during the catalytic cycle. *Biochemistry* **42**, 1170-1177
151. Carrier, I., Julien, M., and Gros, P. (2003) Analysis of catalytic carboxylate mutants E552Q and E1197Q suggests asymmetric ATP hydrolysis by the two nucleotide-binding domains of P-glycoprotein. *Biochemistry* **42**, 12875-12885
152. Tombline, G., Bartholomew, L. A., Urbatsch, I. L., and Senior, A. E. (2004) Combined mutation of catalytic glutamate residues in the two nucleotide binding domains of P-glycoprotein generates a conformation that binds ATP and ADP tightly. *J Biol Chem* **279**, 31212-31220
153. Hrycyna, C. A., Ramachandra, M., Germann, U. A., Cheng, P. W., Pastan, I., and Gottesman, M. M. (1999) Both ATP sites of human P-glycoprotein are essential but not symmetric. *Biochemistry* **38**, 13887-13899
154. Hou, Y. X., Li, C. Z., Palaniyandi, K., Magtibay, P. M., Homolya, L., Sarkadi, B., and Chang, X. B. (2009) Effects of putative catalytic base mutation E211Q on ABCG2-mediated methotrexate transport. *Biochemistry* **48**, 9122-9131
155. Bakos, E., Klein, I., Welker, E., Szabo, K., Muller, M., Sarkadi, B., and Varadi, A. (1997) Characterization of the human multidrug resistance protein containing mutations in the ATP-binding cassette signature region. *The Biochemical journal* **323 (Pt 3)**, 777-783
156. Loo, T. W., Bartlett, M. C., and Clarke, D. M. (2002) The "LSGGQ" motif in each nucleotide-binding domain of human P-glycoprotein is adjacent to the opposing walker A sequence. *J Biol Chem* **277**, 41303-41306
157. Kim, I. W., Peng, X. H., Sauna, Z. E., FitzGerald, P. C., Xia, D., Muller, M., Nandigama, K., and Ambudkar, S. V. (2006) The conserved tyrosine residues 401 and 1044 in ATP sites of human P-glycoprotein are critical for ATP binding and hydrolysis: evidence for a conserved subdomain, the A-loop in the ATP-binding cassette. *Biochemistry* **45**, 7605-7616
158. Ambudkar, S. V., Kim, I. W., Xia, D., and Sauna, Z. E. (2006) The A-loop, a novel conserved aromatic acid subdomain upstream of the Walker A motif in ABC transporters, is critical for ATP binding. *FEBS letters* **580**, 1049-1055
159. Carrier, I., Urbatsch, I. L., Senior, A. E., and Gros, P. (2007) Mutational analysis of conserved aromatic residues in the A-loop of the ABC transporter ABCB1A (mouse Mdr3). *FEBS letters* **581**, 301-308
160. Lawson, J., O'Mara, M. L., and Kerr, I. D. (2008) Structure-based interpretation of the mutagenesis database for the nucleotide binding domains of P-glycoprotein. *Biochimica et biophysica acta* **1778**, 376-391
161. Eckenstaler, R., and Benndorf, R. A. (2020) 3D structure of the transporter ABCG2-What's new? *British journal of pharmacology* **177**, 1485-1496
162. Zolnerciks, J. K., Akkaya, B. G., Snippe, M., Chiba, P., Seelig, A., and Linton, K. J. (2014) The Q loops of the human multidrug resistance transporter ABCB1 are necessary to couple drug binding to the ATP catalytic cycle. *FASEB journal : official publication of the Federation of American Societies for Experimental Biology* **28**, 4335-4346
163. Sauna, Z. E., and Ambudkar, S. V. (2007) About a switch: how P-glycoprotein (ABCB1) harnesses the energy of ATP binding and hydrolysis to do mechanical work. *Mol Cancer Ther* **6**, 13-23
164. Seeger, M. A., and van Veen, H. W. (2009) Molecular basis of multidrug transport by ABC transporters. *Biochimica et biophysica acta* **1794**, 725-737
165. Garrigues, A., Escargueil, A. E., and Orlowski, S. (2002) The multidrug transporter, P-glycoprotein, actively mediates cholesterol redistribution in the cell membrane. *Proceedings of the National Academy of Sciences of the United States of America* **99**, 10347-10352

166. van Helvoort, A., Smith, A. J., Sprong, H., Fritzsche, I., Schinkel, A. H., Borst, P., and van Meer, G. (1996) MDR1 P-glycoprotein is a lipid translocase of broad specificity, while MDR3 P-glycoprotein specifically translocates phosphatidylcholine. *Cell* **87**, 507-517
167. Al-Shawi, M. K., and Omote, H. (2005) The remarkable transport mechanism of P-glycoprotein: a multidrug transporter. *J Bioenerg Biomembr* **37**, 489-496
168. Parker, J. L., and Newstead, S. (2016) Membrane Protein Crystallisation: Current Trends and Future Perspectives. *Adv Exp Med Biol* **922**, 61-72
169. Chang, S. Y., Liu, F. F., Dong, X. Y., and Sun, Y. (2013) Molecular insight into conformational transmission of human P-glycoprotein. *The Journal of chemical physics* **139**, 225102
170. Prajapati, R., and Sangamwar, A. T. (2014) Translocation mechanism of P-glycoprotein and conformational changes occurring at drug-binding site: Insights from multi-targeted molecular dynamics. *Biochimica et biophysica acta* **1838**, 2882-2898
171. Stockner, T., Mullen, A., and MacMillan, F. (2015) Investigating the dynamic nature of the ABC transporters: ABCB1 and MsbA as examples for the potential synergies of MD theory and EPR applications. *Biochem Soc Trans* **43**, 1023-1032
172. Higgins, C. F., and Linton, K. J. (2004) The ATP switch model for ABC transporters. *Nat Struct Mol Biol* **11**, 918-926
173. Janas, E., Hofacker, M., Chen, M., Gompf, S., van der Does, C., and Tampe, R. (2003) The ATP hydrolysis cycle of the nucleotide-binding domain of the mitochondrial ATP-binding cassette transporter Mdl1p. *J Biol Chem* **278**, 26862-26869
174. Senior, A. E., al-Shawi, M. K., and Urbatsch, I. L. (1995) The catalytic cycle of P-glycoprotein. *FEBS Lett* **377**, 285-289
175. Siarheyeva, A., Liu, R., and Sharom, F. J. (2010) Characterization of an asymmetric occluded state of P-glycoprotein with two bound nucleotides: implications for catalysis. *J Biol Chem* **285**, 7575-7586
176. Jones, P. M., and George, A. M. (2009) Opening of the ADP-bound active site in the ABC transporter ATPase dimer: evidence for a constant contact, alternating sites model for the catalytic cycle. *Proteins* **75**, 387-396
177. Barsony, O., Szaloki, G., Turk, D., Tarapcsak, S., Gutay-Toth, Z., Bacso, Z., Holb, I. J., Szekvolgyi, L., Szabo, G., Csanady, L., Szakacs, G., and Goda, K. (2016) A single active catalytic site is sufficient to promote transport in P-glycoprotein. *Sci Rep* **6**, 24810
178. Loo, T. W., and Clarke, D. M. (1995) Covalent modification of human P-glycoprotein mutants containing a single cysteine in either nucleotide-binding fold abolishes drug-stimulated ATPase activity. *J Biol Chem* **270**, 22957-22961
179. Szollosi, D., Rose-Sperling, D., Hellmich, U. A., and Stockner, T. (2017) Comparison of mechanistic transport cycle models of ABC exporters. *Biochimica et biophysica acta*
180. Tombline, G., Muharemagic, A., White, L. B., and Senior, A. E. (2005) Involvement of the "occluded nucleotide conformation" of P-glycoprotein in the catalytic pathway. *Biochemistry* **44**, 12879-12886
181. Urbatsch, I. L., Sankaran, B., Weber, J., and Senior, A. E. (1995) P-glycoprotein is stably inhibited by vanadate-induced trapping of nucleotide at a single catalytic site. *J Biol Chem* **270**, 19383-19390
182. Szabo, K., Welker, E., Bakos, Muller, M., Roninson, I., Varadi, A., and Sarkadi, B. (1998) Drug-stimulated nucleotide trapping in the human multidrug transporter MDR1. Cooperation of the nucleotide binding domains. *The Journal of biological chemistry* **273**, 10132-10138
183. Urbatsch, I. L., Beaudet, L., Carrier, I., and Gros, P. (1998) Mutations in either nucleotide-binding site of P-glycoprotein (Mdr3) prevent vanadate trapping of nucleotide at both sites. *Biochemistry* **37**, 4592-4602
184. Zoghbi, M. E., and Altenberg, G. A. (2014) ATP binding to two sites is necessary for dimerization of nucleotide-binding domains of ABC proteins. *Biochemical and biophysical research communications* **443**, 97-102
185. Procko, E., O'Mara, M. L., Bennett, W. F., Tieleman, D. P., and Gaudet, R. (2009) The mechanism of ABC transporters: general lessons from structural and functional studies of an antigenic peptide transporter. *FASEB J* **23**, 1287-1302
186. Payen, L. F., Gao, M., Westlake, C. J., Cole, S. P., and Deeley, R. G. (2003) Role of carboxylate residues adjacent to the conserved core Walker B motifs in the catalytic cycle of multidrug resistance protein 1 (ABCC1). *The Journal of biological chemistry* **278**, 38537-38547
187. Hopfner, K. P., Karcher, A., Shin, D. S., Craig, L., Arthur, L. M., Carney, J. P., and Tainer, J. A. (2000) Structural biology of Rad50 ATPase: ATP-driven conformational control in DNA double-strand break repair and the ABC-ATPase superfamily. *Cell* **101**, 789-800
188. Stratford, F. L., Ramjeesingh, M., Cheung, J. C., Huan, L. J., and Bear, C. E. (2007) The Walker B motif of the second nucleotide-binding domain (NBD2) of CFTR plays a key role in ATPase activity by the NBD1-NBD2 heterodimer. *The Biochemical journal* **401**, 581-586
189. Sohail, M. I., Schmid, D., Wlcek, K., Spork, M., Szakacs, G., Trauner, M., Stockner, T., and Chiba, P. (2017) Molecular Mechanism of Taurocholate Transport by the Bile Salt Export Pump, an ABC Transporter Associated with Intrahepatic Cholestasis. *Molecular pharmacology* **92**, 401-413
190. Gao, M., Cui, H. R., Loe, D. W., Grant, C. E., Almquist, K. C., Cole, S. P., and Deeley, R. G. (2000) Comparison of the functional characteristics of the nucleotide binding domains of multidrug resistance protein 1. *The Journal of biological chemistry* **275**, 13098-13108
191. Basso, C., Vergani, P., Nairn, A. C., and Gadsby, D. C. (2003) Prolonged nonhydrolytic interaction of nucleotide with CFTR's NH2-terminal nucleotide binding domain and its role in channel gating. *J Gen Physiol* **122**, 333-348

192. Verhalen, B., Dastvan, R., Thangapandian, S., Peskova, Y., Koteiche, H. A., Nakamoto, R. K., Tajkhorshid, E., and McHaourab, H. S. (2017) Energy transduction and alternating access of the mammalian ABC transporter P-glycoprotein. *Nature* **543**, 738-741
193. Dastvan, R., Mishra, S., Peskova, Y. B., Nakamoto, R. K., and McHaourab, H. S. (2019) Mechanism of allosteric modulation of P-glycoprotein by transport substrates and inhibitors. *Science* **364**, 689-692
194. Pan, L., and Aller, S. G. (2018) Allosteric Role of Substrate Occupancy Toward the Alignment of P-glycoprotein Nucleotide Binding Domains. *Scientific reports* **8**, 14643
195. Cianfriglia, M., Willingham, M. C., Tombesi, M., Scagliotti, G. V., Frasca, G., and Chersi, A. (1994) P-glycoprotein epitope mapping. I. Identification of a linear human-specific epitope in the fourth loop of the P-glycoprotein extracellular domain by MM4.17 murine monoclonal antibody to human multi-drug-resistant cells. *International journal of cancer. Journal international du cancer* **56**, 153-160
196. Georges, E., Tsuruo, T., and Ling, V. (1993) Topology of P-glycoprotein as determined by epitope mapping of MRK-16 monoclonal antibody. *The Journal of biological chemistry* **268**, 1792-1798
197. Cianfriglia, M., Romagnoli, G., Tombesi, M., Poloni, F., Falasca, G., Di Modugno, F., Castagna, M., and Chersi, A. (1995) P-glycoprotein epitope mapping. II. The murine monoclonal antibody MM6.15 to human multidrug-resistant cells binds with three distinct loops in the MDR1-P-glycoprotein extracellular domain. *International journal of cancer. Journal international du cancer* **61**, 142-147
198. Mechetner, E. B., and Roninson, I. B. (1992) Efficient inhibition of P-glycoprotein-mediated multidrug resistance with a monoclonal antibody. *Proceedings of the National Academy of Sciences of the United States of America* **89**, 5824-5828
199. Watanabe, T., Naito, M., Kokubu, N., and Tsuruo, T. (1997) Regression of established tumors expressing P-glycoprotein by combinations of adriamycin, cyclosporin derivatives, and MRK-16 antibodies. *Journal of the National Cancer Institute* **89**, 512-518
200. Naito, M., Watanabe, T., Tsuge, H., Koyama, T., Oh-hara, T., and Tsuruo, T. (1996) Potentiation of the reversal activity of SDZ PSC833 on multi-drug resistance by an anti-P-glycoprotein monoclonal antibody MRK-16. *International journal of cancer. Journal international du cancer* **67**, 435-440
201. Rittmann-Grauer, L. S., Yong, M. A., Sanders, V., and Mackensen, D. G. (1992) Reversal of Vinca alkaloid resistance by anti-P-glycoprotein monoclonal antibody HYB-241 in a human tumor xenograft. *Cancer research* **52**, 1810-1816
202. Druley, T. E., Stein, W. D., and Roninson, I. B. (2001) Analysis of MDR1 P-glycoprotein conformational changes in permeabilized cells using differential immunoreactivity. *Biochemistry* **40**, 4312-4322
203. Esser, L., Shukla, S., Zhou, F., Ambudkar, S. V., and Xia, D. (2016) Crystal structure of the antigen-binding fragment of a monoclonal antibody specific for the multidrug-resistance-linked ABC transporter human P-glycoprotein. *Acta crystallographica. Section F, Structural biology communications* **72**, 636-641
204. Vasudevan, S., Tsuruo, T., and Rose, D. R. (1998) Mode of binding of anti-P-glycoprotein antibody MRK-16 to its antigen. A crystallographic and molecular modeling study. *The Journal of biological chemistry* **273**, 25413-25419
205. Schinkel, A. H., Arceci, R. J., Smit, J. J., Wagenaar, E., Baas, F., Dolle, M., Tsuruo, T., Mechetner, E. B., Roninson, I. B., and Borst, P. (1993) Binding properties of monoclonal antibodies recognizing external epitopes of the human MDR1 P-glycoprotein. *International journal of cancer. Journal international du cancer* **55**, 478-484
206. Zhou, Y., Gottesman, M. M., and Pastan, I. (1999) The extracellular loop between TM5 and TM6 of P-glycoprotein is required for reactivity with monoclonal antibody UIC2. *Archives of biochemistry and biophysics* **367**, 74-80
207. Vahedi, S., Lusvarghi, S., Pluchino, K., Shafrir, Y., Durell, S. R., Gottesman, M. M., and Ambudkar, S. V. (2018) Mapping discontinuous epitopes for MRK-16, UIC2 and 4E3 antibodies to extracellular loops 1 and 4 of human P-glycoprotein. *Scientific reports* **8**, 12716
208. Sharom, F. J. (1997) The P-glycoprotein efflux pump: how does it transport drugs? *The Journal of membrane biology* **160**, 161-175
209. Sharom, F. J. (2014) Complex Interplay between the P-Glycoprotein Multidrug Efflux Pump and the Membrane: Its Role in Modulating Protein Function. *Front Oncol* **4**, 41
210. Raviv, Y., Pollard, H. B., Bruggemann, E. P., Pastan, I., and Gottesman, M. M. (1990) Photosensitized labeling of a functional multidrug transporter in living drug-resistant tumor cells. *The Journal of biological chemistry* **265**, 3975-3980
211. Homolya, L., Hollo, Z., Germann, U. A., Pastan, I., Gottesman, M. M., and Sarkadi, B. (1993) Fluorescent cellular indicators are extruded by the multidrug resistance protein. *The Journal of biological chemistry* **268**, 21493-21496
212. Homolya, L., Orban, T. I., Csanady, L., and Sarkadi, B. (2011) Mitoxantrone is expelled by the ABCG2 multidrug transporter directly from the plasma membrane. *Biochimica et biophysica acta* **1808**, 154-163
213. Kapoor, P., Horsey, A. J., Cox, M. H., and Kerr, I. D. (2018) ABCG2: does resolving its structure elucidate the mechanism? *Biochemical Society transactions* **46**, 1485-1494
214. Higgins, C. F., and Gottesman, M. M. (1992) Is the multidrug transporter a flippase? *Trends in biochemical sciences* **17**, 18-21
215. Eytan, G. D. (2005) Mechanism of multidrug resistance in relation to passive membrane permeation. *Biomedicine & pharmacotherapy = Biomedecine & pharmacotherapie* **59**, 90-97
216. Siarheyeva, A., Lopez, J. J., and Glaubitz, C. (2006) Localization of multidrug transporter substrates within model membranes. *Biochemistry* **45**, 6203-6211
217. Hegedus, C., Telbisz, A., Hegedus, T., Sarkadi, B., and Ozvegy-Laczka, C. (2015) Lipid regulation of the ABCB1 and ABCG2 multidrug transporters. *Adv Cancer Res* **125**, 97-137

218. Doige, C. A., Yu, X., and Sharom, F. J. (1993) The effects of lipids and detergents on ATPase-active P-glycoprotein. *Biochim Biophys Acta* **1146**, 65-72
219. Loo, T. W., and Clarke, D. M. (2016) P-glycoprotein ATPase activity requires lipids to activate a switch at the first transmission interface. *Biochem Biophys Res Commun* **472**, 379-383
220. Telbisz, A., Ozvegy-Laczka, C., Hegedus, T., Varadi, A., and Sarkadi, B. (2013) Effects of the lipid environment, cholesterol and bile acids on the function of the purified and reconstituted human ABCG2 protein. *Biochem J* **450**, 387-395
221. Radeva, G., Perabo, J., and Sharom, F. J. (2005) P-Glycoprotein is localized in intermediate-density membrane microdomains distinct from classical lipid rafts and caveolar domains. *FEBS J* **272**, 4924-4937
222. Storch, C. H., Ehehalt, R., Haefeli, W. E., and Weiss, J. (2007) Localization of the human breast cancer resistance protein (BCRP/ABCG2) in lipid rafts/caveolae and modulation of its activity by cholesterol in vitro. *J Pharmacol Exp Ther* **323**, 257-264
223. Troost, J., Lindenmaier, H., Haefeli, W. E., and Weiss, J. (2004) Modulation of cellular cholesterol alters P-glycoprotein activity in multidrug-resistant cells. *Molecular pharmacology* **66**, 1332-1339
224. Shukla, S., Abel, B., Chufan, E. E., and Ambudkar, S. V. (2017) Effects of a detergent micelle environment on P-glycoprotein (ABCB1)-ligand interactions. *The Journal of biological chemistry* **292**, 7066-7076
225. Clouser, A. F., Alam, Y. H., and Atkins, W. M. (2021) Cholesterol Asymmetrically Modulates the Conformational Ensemble of the Nucleotide-Binding Domains of P-Glycoprotein in Lipid Nanodiscs. *Biochemistry* **60**, 85-94
226. Aanismaa, P., and Seelig, A. (2007) P-Glycoprotein kinetics measured in plasma membrane vesicles and living cells. *Biochemistry* **46**, 3394-3404
227. Clay, A. T., and Sharom, F. J. (2013) Lipid bilayer properties control membrane partitioning, binding, and transport of p-glycoprotein substrates. *Biochemistry* **52**, 343-354
228. Sharom, F. J. (1997) The P-glycoprotein multidrug transporter: interactions with membrane lipids, and their modulation of activity. *Biochemical Society transactions* **25**, 1088-1096
229. Zhao, W., Alama, T., Kusamori, K., Katsumi, H., Sakane, T., and Yamamoto, A. (2016) Effects of 2 Polyoxyethylene Alkyl Ethers on the Function of Intestinal P-glycoprotein and Their Inhibitory Mechanisms. *Journal of pharmaceutical sciences* **105**, 3668-3679
230. Sinicrope, F. A., Dudeja, P. K., Bissonnette, B. M., Safa, A. R., and Brasitus, T. A. (1992) Modulation of P-glycoprotein-mediated drug transport by alterations in lipid fluidity of rat liver canalicular membrane vesicles. *The Journal of biological chemistry* **267**, 24995-25002
231. Regev, R., Assaraf, Y. G., and Eytan, G. D. (1999) Membrane fluidization by ether, other anesthetics, and certain agents abolishes P-glycoprotein ATPase activity and modulates efflux from multidrug-resistant cells. *European journal of biochemistry* **259**, 18-24
232. Qu, Q., and Sharom, F. J. (2001) FRET analysis indicates that the two ATPase active sites of the P-glycoprotein multidrug transporter are closely associated. *Biochemistry* **40**, 1413-1422
233. Futamata, R., Ogasawara, F., Ichikawa, T., Kodan, A., Kimura, Y., Kioka, N., and Ueda, K. (2020) In vivo FRET analyses reveal a role of ATP hydrolysis-associated conformational changes in human P-glycoprotein. *J Biol Chem* **295**, 5002-5011
234. Sharom, F. J. (2008) ABC multidrug transporters: structure, function and role in chemoresistance. *Pharmacogenomics* **9**, 105-127
235. Kim, R. B. (2002) Drugs as P-glycoprotein substrates, inhibitors, and inducers. *Drug metabolism reviews* **34**, 47-54
236. Szollosi, D., Rose-Sperling, D., Hellmich, U. A., and Stockner, T. (2018) Comparison of mechanistic transport cycle models of ABC exporters. *Biochim Biophys Acta Biomembr* **1860**, 818-832
237. Woodward, O. M., Kottgen, A., Coresh, J., Boerwinkle, E., Guggino, W. B., and Kottgen, M. (2009) Identification of a urate transporter, ABCG2, with a common functional polymorphism causing gout. *Proceedings of the National Academy of Sciences of the United States of America* **106**, 10338-10342
238. Romsicki, Y., and Sharom, F. J. (2001) Phospholipid flippase activity of the reconstituted P-glycoprotein multidrug transporter. *Biochemistry* **40**, 6937-6947
239. Eckford, P. D., and Sharom, F. J. (2005) The reconstituted P-glycoprotein multidrug transporter is a flippase for glucosylceramide and other simple glycosphingolipids. *The Biochemical journal* **389**, 517-526
240. Parker, R. B., Yates, C. R., Laizure, S. C., and Weber, K. T. (2006) P-glycoprotein modulates aldosterone plasma disposition and tissue uptake. *Journal of cardiovascular pharmacology* **47**, 55-59
241. Liu, Y., Huang, L., Hoffman, T., Gosland, M., and Vore, M. (1996) MDR1 substrates/modulators protect against beta-estradiol-17beta-D-glucuronide cholestasis in rat liver. *Cancer research* **56**, 4992-4997
242. Pawlik, A., Baskiewicz-Masiuk, M., Machalinski, B., Safranow, K., and Gawronska-Szklarz, B. (2005) Involvement of P-glycoprotein in the release of cytokines from peripheral blood mononuclear cells treated with methotrexate and dexamethasone. *The Journal of pharmacy and pharmacology* **57**, 1421-1425
243. Abdallah, H. M., Al-Abd, A. M., El-Dine, R. S., and El-Halawany, A. M. (2015) P-glycoprotein inhibitors of natural origin as potential tumor chemo-sensitizers: A review. *J Adv Res* **6**, 45-62
244. Dantzig, A. H., de Alwis, D. P., and Burgess, M. (2003) Considerations in the design and development of transport inhibitors as adjuncts to drug therapy. *Advanced drug delivery reviews* **55**, 133-150
245. Nanayakkara, A. K., Follit, C. A., Chen, G., Williams, N. S., Vogel, P. D., and Wise, J. G. (2018) Targeted inhibitors of P-glycoprotein increase chemotherapeutic-induced mortality of multidrug resistant tumor cells. *Scientific reports* **8**, 967
246. Namanja, H. A., Emmert, D., Pires, M. M., Hrycyna, C. A., and Chmielewski, J. (2009) Inhibition of human P-glycoprotein transport and substrate binding using a galantamine dimer. *Biochemical and biophysical research communications* **388**, 672-676

247. Maki, N., Hafkemeyer, P., and Dey, S. (2003) Allosteric modulation of human P-glycoprotein. Inhibition of transport by preventing substrate translocation and dissociation. *The Journal of biological chemistry* **278**, 18132-18139
248. Nosol, K., Romane, K., Irobalieva, R. N., Alam, A., Kowal, J., Fujita, N., and Locher, K. P. (2020) Cryo-EM structures reveal distinct mechanisms of inhibition of the human multidrug transporter ABCB1. *Proc Natl Acad Sci U S A* **117**, 26245-26253
249. Chen, Y., Derguini, F., and Buck, J. (1997) Vitamin A in serum is a survival factor for fibroblasts. *Proceedings of the National Academy of Sciences of the United States of America* **94**, 10205-10208
250. Zhong, G., Kirkwood, J., Won, K. J., Tjota, N., Jeong, H., and Isoherranen, N. (2019) Characterization of Vitamin A Metabolome in Human Livers With and Without Nonalcoholic Fatty Liver Disease. *The Journal of pharmacology and experimental therapeutics* **370**, 92-103
251. Redfern, C. P., Lovat, P. E., Malcolm, A. J., and Pearson, A. D. (1994) Differential effects of 9-cis and all-trans retinoic acid on the induction of retinoic acid receptor-beta and cellular retinoic acid-binding protein II in human neuroblastoma cells. *The Biochemical journal* **304 (Pt 1)**, 147-154
252. Kurlandsky, S. B., Gamble, M. V., Ramakrishnan, R., and Blaner, W. S. (1995) Plasma delivery of retinoic acid to tissues in the rat. *The Journal of biological chemistry* **270**, 17850-17857
253. Yu, V. C., Delsert, C., Andersen, B., Holloway, J. M., Devary, O. V., Naar, A. M., Kim, S. Y., Boutin, J. M., Glass, C. K., and Rosenfeld, M. G. (1991) RXR beta: a coregulator that enhances binding of retinoic acid, thyroid hormone, and vitamin D receptors to their cognate response elements. *Cell* **67**, 1251-1266
254. Kliewer, S. A., Umesono, K., Noonan, D. J., Heyman, R. A., and Evans, R. M. (1992) Convergence of 9-Cis Retinoic Acid and Peroxisome Proliferator Signaling Pathways through Heterodimer Formation of Their Receptors. *Nature* **358**, 771-774
255. Wise, E. M., and Graber, E. M. (2011) Clinical pearl: comedone extraction for persistent macrocomedones while on isotretinoin therapy. *The Journal of clinical and aesthetic dermatology* **4**, 20-21
256. Skeel, R. T., Huang, J., Manola, J., Wilding, G., Dreicer, R., Walker, P., Muggia, F., Crawford, E. D., Dutcher, J. P., and Loehrer, P. J. (2003) A phase II study of 13-cis retinoic acid plus interferon alpha-2a in advanced stage penile carcinoma: an Eastern Cooperative Oncology Group study (E3893). *Cancer investigation* **21**, 41-46
257. Veal, G. J., Errington, J., Rowbotham, S. E., Illingworth, N. A., Malik, G., Cole, M., Daly, A. K., Pearson, A. D., and Boddy, A. V. (2013) Adaptive dosing approaches to the individualization of 13-cis-retinoic Acid (isotretinoin) treatment for children with high-risk neuroblastoma. *Clinical cancer research : an official journal of the American Association for Cancer Research* **19**, 469-479
258. Ketley, N. J., Allen, P. D., Kelsey, S. M., and Newland, A. C. (1997) Modulation of idarubicin-induced apoptosis in human acute myeloid leukemia blasts by all-trans retinoic acid, 1,25(OH)2 vitamin D3, and granulocyte-macrophage colony-stimulating factor. *Blood* **90**, 4578-4587
259. Duvic, M., Lemak, N. A., Redman, J. R., Eifel, P. J., Tucker, S. L., Cabanillas, F. F., and Kurzrock, R. (1996) Combined modality therapy for cutaneous T-cell lymphoma. *Journal of the American Academy of Dermatology* **34**, 1022-1029
260. Lupo, M. P. (2001) Antioxidants and vitamins in cosmetics. *Clinics in dermatology* **19**, 467-473
261. Perusek, L., and Maeda, T. (2013) Vitamin A derivatives as treatment options for retinal degenerative diseases. *Nutrients* **5**, 2646-2666
262. Jang, Y. K., Park, J. J., Lee, M. C., Yoon, B. H., Yang, Y. S., Yang, S. E., and Kim, S. U. (2004) Retinoic acid-mediated induction of neurons and glial cells from human umbilical cord-derived hematopoietic stem cells. *Journal of neuroscience research* **75**, 573-584
263. Hessel, S., and Lampen, A. (2010) All-trans retinoic acid enhances the transport of phase II metabolites of benzo[a]pyrene by inducing the Breast Cancer Resistance Protein expression in Caco-2 cells. *Toxicology letters* **197**, 151-155
264. Sulova, Z., Macejova, D., Seres, M., Sedlak, J., Brtko, J., and Breier, A. (2008) Combined treatment of P-gp-positive L1210/VCR cells by verapamil and all-trans retinoic acid. induces down-regulation of P-glycoprotein expression and transport activity. *Toxicology in Vitro* **22**, 96-105
265. Klamt, F., Passos, D. T., Castro, M. A. A., Gelain, D. P., Grivicich, I., and Moreira, J. C. F. (2008) Inhibition of MDR1 expression by retinol treatment increases sensitivity to etoposide (VP16) in human neoplasic cell line. *Toxicology in Vitro* **22**, 873-878
266. Chlapek, P., Slavikova, V., Mazanek, P., Sterba, J., and Veselska, R. (2018) Why Differentiation Therapy Sometimes Fails: Molecular Mechanisms of Resistance to Retinoids. *International journal of molecular sciences* **19**
267. Tzimas, G., Collins, M. D., Burgin, H., Hummler, H., and Nau, H. (1996) Embryotoxic doses of vitamin A to rabbits result in low plasma but high embryonic concentrations of all-trans-retinoic acid: risk of vitamin A exposure in humans. *The Journal of nutrition* **126**, 2159-2171
268. Iqbal, M., Audette, M. C., Petropoulos, S., Gibb, W., and Matthews, S. G. (2012) Placental drug transporters and their role in fetal protection. *Placenta* **33**, 137-142
269. Lin, J. H., and Yamazaki, M. (2003) Clinical relevance of P-glycoprotein in drug therapy. *Drug metabolism reviews* **35**, 417-454
270. Leonard, G. D., Fojo, T., and Bates, S. E. (2003) The role of ABC transporters in clinical practice. *Oncologist* **8**, 411-424
271. Borst, P. (1991) Genetic mechanisms of drug resistance. A review. *Acta oncologica* **30**, 87-105

272. Steinbach, D., and Legrand, O. (2007) ABC transporters and drug resistance in leukemia: was P-gp nothing but the first head of the Hydra? *Leukemia : official journal of the Leukemia Society of America, Leukemia Research Fund, U.K* **21**, 1172-1176
273. Baekelandt, M. M., Holm, R., Nesland, J. M., Trope, C. G., and Kristensen, G. B. (2000) P-glycoprotein expression is a marker for chemotherapy resistance and prognosis in advanced ovarian cancer. *Anticancer research* **20**, 1061-1067
274. Triller, N., Korosec, P., Kern, I., Kosnik, M., and Debeljak, A. (2006) Multidrug resistance in small cell lung cancer: expression of P-glycoprotein, multidrug resistance protein 1 and lung resistance protein in chemo-naive patients and in relapsed disease. *Lung Cancer* **54**, 235-240
275. Yeh, J. J., Hsu, W. H., Wang, J. J., Ho, S. T., and Kao, A. (2003) Predicting chemotherapy response to paclitaxel-based therapy in advanced non-small-cell lung cancer with P-glycoprotein expression. *Respiration* **70**, 32-35
276. Szakacs, G., Paterson, J. K., Ludwig, J. A., Booth-Genthe, C., and Gottesman, M. M. (2006) Targeting multidrug resistance in cancer. *Nat Rev Drug Discov* **5**, 219-234
277. Trock, B. J., Leonessa, F., and Clarke, R. (1997) Multidrug resistance in breast cancer: a meta-analysis of MDR1/gp170 expression and its possible functional significance. *J Natl Cancer Inst* **89**, 917-931
278. Omran, O. M. (2012) The prognostic value of breast cancer resistance protein (BCRB/ABCG2) expression in breast carcinomas. *Journal of environmental pathology, toxicology and oncology : official organ of the International Society for Environmental Toxicology and Cancer* **31**, 367-376
279. Zhou, D. C., Zittoun, R., and Marie, J. P. (1995) Expression of multidrug resistance-associated protein (MRP) and multidrug resistance (MDR1) genes in acute myeloid leukemia. *Leukemia* **9**, 1661-1666
280. Grogan, T. M., Spier, C. M., Salmon, S. E., Matzner, M., Rybski, J., Weinstein, R. S., Scheper, R. J., and Dalton, W. S. (1993) P-glycoprotein expression in human plasma cell myeloma: correlation with prior chemotherapy. *Blood* **81**, 490-495
281. Turner, J. G., Gump, J. L., Zhang, C., Cook, J. M., Marchion, D., Hazlehurst, L., Munster, P., Schell, M. J., Dalton, W. S., and Sullivan, D. M. (2006) ABCG2 expression, function, and promoter methylation in human multiple myeloma. *Blood* **108**, 3881-3889
282. Candeil, L., Gourdier, I., Peyron, D., Vezzio, N., Copois, V., Bibeau, F., Orsetti, B., Scheffer, G. L., Ychou, M., Khan, Q. A., Pommier, Y., Pau, B., Martineau, P., and Del Rio, M. (2004) ABCG2 overexpression in colon cancer cells resistant to SN38 and in irinotecan-treated metastases. *International journal of cancer* **109**, 848-854
283. Crowley, E., McDevitt, C. A., and Callaghan, R. (2010) Generating inhibitors of P-glycoprotein: where to, now? *Methods in molecular biology* **596**, 405-432
284. Akhtar, N., Ahad, A., Khar, R. K., Jaggi, M., Aqil, M., Iqbal, Z., Ahmad, F. J., and Talegaonkar, S. (2011) The emerging role of P-glycoprotein inhibitors in drug delivery: a patent review. *Expert Opin Ther Pat* **21**, 561-576
285. Pusztai, L., Wagner, P., Ibrahim, N., Rivera, E., Theriault, R., Booser, D., Symmans, F. W., Wong, F., Blumenschein, G., Fleming, D. R., Rouzier, R., Boniface, G., and Hortobagyi, G. N. (2005) Phase II study of tariquidar, a selective P-glycoprotein inhibitor, in patients with chemotherapy-resistant, advanced breast carcinoma. *Cancer* **104**, 682-691
286. Cripe, L. D., Uno, H., Paietta, E. M., Litzow, M. R., Ketterling, R. P., Bennett, J. M., Rowe, J. M., Lazarus, H. M., Luger, S., and Tallman, M. S. (2010) Zosuquidar, a novel modulator of P-glycoprotein, does not improve the outcome of older patients with newly diagnosed acute myeloid leukemia: a randomized, placebo-controlled trial of the Eastern Cooperative Oncology Group 3999. *Blood* **116**, 4077-4085
287. Greenberg, P. L., Lee, S. J., Advani, R., Tallman, M. S., Sikic, B. I., Letendre, L., Dugan, K., Lum, B., Chin, D. L., Dewald, G., Paietta, E., Bennett, J. M., and Rowe, J. M. (2004) Mitoxantrone, etoposide, and cytarabine with or without valspodar in patients with relapsed or refractory acute myeloid leukemia and high-risk myelodysplastic syndrome: a phase III trial (E2995). *Journal of clinical oncology : official journal of the American Society of Clinical Oncology* **22**, 1078-1086
288. Bartsevich, V. V., and Juliano, R. L. (2000) Regulation of the MDR1 gene by transcriptional repressors selected using peptide combinatorial libraries. *Mol Pharmacol* **58**, 1-10
289. Scotto, K. W. (2003) Transcriptional regulation of ABC drug transporters. *Oncogene* **22**, 7496-7511
290. Szakacs, G., Annereau, J. P., Lababidi, S., Shankavaram, U., Arciello, A., Bussey, K. J., Reinhold, W., Guo, Y., Kruh, G. D., Reimers, M., Weinstein, J. N., and Gottesman, M. M. (2004) Predicting drug sensitivity and resistance: profiling ABC transporter genes in cancer cells. *Cancer Cell* **6**, 129-137
291. Pluchino, K. M., Hall, M. D., Goldsborough, A. S., Callaghan, R., and Gottesman, M. M. (2012) Collateral sensitivity as a strategy against cancer multidrug resistance. *Drug Resist Updat* **15**, 98-105
292. Pape, V. F. S., Gaal, A., Szatmari, I., Kucsma, N., Szoboszlai, N., Streli, C., Fulop, F., Enyedy, E. A., and Szakacs, G. (2021) Relation of Metal-Binding Property and Selective Toxicity of 8-Hydroxyquinoline Derived Mannich Bases Targeting Multidrug Resistant Cancer Cells. *Cancers (Basel)* **13**
293. Ozvegy-Laczka, C., Koblos, G., Sarkadi, B., and Varadi, A. (2005) Single amino acid (482) variants of the ABCG2 multidrug transporter: major differences in transport capacity and substrate recognition. *Biochim Biophys Acta* **1668**, 53-63
294. Lowry, O. H., Rosebrough, N. J., Farr, A. L., and Randall, R. J. (1951) Protein measurement with the Folin phenol reagent. *The Journal of biological chemistry* **193**, 265-275
295. Telbisz, A., Muller, M., Ozvegy-Laczka, C., Homolya, L., Szente, L., Varadi, A., and Sarkadi, B. (2007) Membrane cholesterol selectively modulates the activity of the human ABCG2 multidrug transporter. *Biochim Biophys Acta* **1768**, 2698-2713

296. Pal, A., Mehn, D., Molnar, E., Gedey, S., Meszaros, P., Nagy, T., Glavinas, H., Janaky, T., von Richter, O., Bathori, G., Szente, L., and Krajcsi, P. (2007) Cholesterol potentiates ABCG2 activity in a heterologous expression system: improved in vitro model to study function of human ABCG2. *J Pharmacol Exp Ther* **321**, 1085-1094
297. Sarkadi, B., Price, E. M., Boucher, R. C., Germann, U. A., and Scarborough, G. A. (1992) Expression of the human multidrug resistance cDNA in insect cells generates a high activity drug-stimulated membrane ATPase. *J Biol Chem* **267**, 4854-4858
298. Nelson, S. C., Neeley, S. K., Melonakos, E. D., Bell, J. D., and Busath, D. D. (2012) Fluorescence anisotropy of diphenylhexatriene and its cationic Trimethylamino derivative in liquid dipalmitoylphosphatidylcholine liposomes: opposing responses to isoflurane. *BMC Biophys* **5**, 5
299. Bhakdi, S., Tranum-Jensen, J., and Sziegoleit, A. (1985) Mechanism of membrane damage by streptolysin-O. *Infection and immunity* **47**, 52-60
300. Pares, X., Farres, J., Kedishvili, N., and Duester, G. (2008) Medium- and short-chain dehydrogenase/reductase gene and protein families : Medium-chain and short-chain dehydrogenases/reductases in retinoid metabolism. *Cellular and molecular life sciences : CMLS* **65**, 3936-3949
301. Szaloki, G., Krasznai, Z. T., Toth, A., Vizkeleti, L., Szollosi, A. G., Trencsenyi, G., Lajtos, I., Juhasz, I., Krasznai, Z., Marian, T., Balazs, M., Szabo, G., and Goda, K. (2014) The strong in vivo anti-tumor effect of the UIC2 monoclonal antibody is the combined result of Pgp inhibition and antibody dependent cell-mediated cytotoxicity. *PloS one* **9**, e107875
302. Rothwell, J. A., Day, A. J., and Morgan, M. R. (2005) Experimental determination of octanol-water partition coefficients of quercetin and related flavonoids. *Journal of agricultural and food chemistry* **53**, 4355-4360
303. el Tayar, N., Mark, A. E., Vallat, P., Brunne, R. M., Testa, B., and van Gunsteren, W. F. (1993) Solvent-dependent conformation and hydrogen-bonding capacity of cyclosporin A: evidence from partition coefficients and molecular dynamics simulations. *J Med Chem* **36**, 3757-3764
304. Prendergast, F. G., Haugland, R. P., and Callahan, P. J. (1981) 1-[4-(Trimethylamino)phenyl]-6-phenylhexa-1,3,5-triene: synthesis, fluorescence properties, and use as a fluorescence probe of lipid bilayers. *Biochemistry* **20**, 7333-7338
305. Stott, B. M., Vu, M. P., McLemore, C. O., Lund, M. S., Gibbons, E., Brueseke, T. J., Wilson-Ashworth, H. A., and Bell, J. D. (2008) Use of fluorescence to determine the effects of cholesterol on lipid behavior in sphingomyelin liposomes and erythrocyte membranes. *Journal of lipid research* **49**, 1202-1215
306. do Canto, A., Robalo, J. R., Santos, P. D., Carvalho, A. J. P., Ramalho, J. P. P., and Loura, L. M. S. (2016) Diphenylhexatriene membrane probes DPH and TMA-DPH: A comparative molecular dynamics simulation study. *Biochimica et biophysica acta* **1858**, 2647-2661
307. Kessel, D. (1988) Probing membrane alterations associated with anthracycline resistance using fluorescent dyes. *Biochemical pharmacology* **37**, 4253-4256
308. Goda, K., Nagy, H., Mechetner, E., Cianfriglia, M., and Szabo, G., Jr. (2002) Effects of ATP depletion and phosphate analogues on P-glycoprotein conformation in live cells. *Eur J Biochem* **269**, 2672-2677
309. Kerr, K. M., Sauna, Z. E., and Ambudkar, S. V. (2001) Correlation between steady-state ATP hydrolysis and vanadate-induced ADP trapping in Human P-glycoprotein. Evidence for ADP release as the rate-limiting step in the catalytic cycle and its modulation by substrates. *J Biol Chem* **276**, 8657-8664
310. Essodaigui, M., Broxterman, H. J., and Garnier-Suillerot, A. (1998) Kinetic analysis of calcein and calcein-acetoxymethylester efflux mediated by the multidrug resistance protein and P-glycoprotein. *Biochemistry* **37**, 2243-2250
311. Booth, C. L., Pulaski, L., Gottesman, M. M., and Pastan, I. (2000) Analysis of the properties of the N-terminal nucleotide-binding domain of human P-glycoprotein. *Biochemistry* **39**, 5518-5526
312. Dey, S., Hafkemeyer, P., Pastan, I., and Gottesman, M. M. (1999) A single amino acid residue contributes to distinct mechanisms of inhibition of the human multidrug transporter by stereoisomers of the dopamine receptor antagonist flupentixol. *Biochemistry* **38**, 6630-6639
313. Zhang, J., Zhou, F., Niu, F., Lu, M., Wu, X., Sun, J., and Wang, G. (2012) Stereoselective regulations of P-glycoprotein by ginsenoside Rh2 epimers and the potential mechanisms from the view of pharmacokinetics. *PloS one* **7**, e35768
314. Widomska, J., and Subczynski, W. K. (2008) Transmembrane localization of cis-isomers of zeaxanthin in the host dimyristoylphosphatidylcholine bilayer membrane. *Biochimica et biophysica acta* **1778**, 10-19
315. Xu, Y., Egido, E., Li-Blatter, X., Muller, R., Merino, G., Berneche, S., and Seelig, A. (2015) Allocrite Sensing and Binding by the Breast Cancer Resistance Protein (ABCG2) and P-Glycoprotein (ABCB1). *Biochemistry* **54**, 6195-6206
316. Romermann, K., Wanek, T., Bankstahl, M., Bankstahl, J. P., Fedrowitz, M., Muller, M., Loscher, W., Kuntner, C., and Langer, O. (2013) (R)-[(11)C]verapamil is selectively transported by murine and human P-glycoprotein at the blood-brain barrier, and not by MRP1 and BCRP. *Nuclear medicine and biology* **40**, 873-878
317. Shirasaka, Y., Sakane, T., and Yamashita, S. (2008) Effect of P-glycoprotein expression levels on the concentration-dependent permeability of drugs to the cell membrane. *Journal of pharmaceutical sciences* **97**, 553-565
318. An, G., Gallegos, J., and Morris, M. E. (2011) The bioflavonoid kaempferol is an Abcg2 substrate and inhibits Abcg2-mediated quercetin efflux. *Drug metabolism and disposition: the biological fate of chemicals* **39**, 426-432
319. Wen, P. C., Verhalen, B., Wilkens, S., McHaourab, H. S., and Tajkhorshid, E. (2013) On the origin of large flexibility of P-glycoprotein in the inward-facing state. *The Journal of biological chemistry* **288**, 19211-19220
320. Aanismaa, P., Gatlik-Landwojtowicz, E., and Seelig, A. (2008) P-glycoprotein senses its substrates and the lateral membrane packing density: consequences for the catalytic cycle. *Biochemistry* **47**, 10197-10207

321. Arnold, S. L., Amory, J. K., Walsh, T. J., and Isoherranen, N. (2012) A sensitive and specific method for measurement of multiple retinoids in human serum with UHPLC-MS/MS. *Journal of lipid research* **53**, 587-598
322. Reynolds, C. P., Matthay, K. K., Villablanca, J. G., and Maurer, B. J. (2003) Retinoid therapy of high-risk neuroblastoma. *Cancer letters* **197**, 185-192
323. Ambudkar, S. V., Lelong, I. H., Zhang, J., Cardarelli, C. O., Gottesman, M. M., and Pastan, I. (1992) Partial purification and reconstitution of the human multidrug-resistance pump: characterization of the drug-stimulatable ATP hydrolysis. *Proc Natl Acad Sci U S A* **89**, 8472-8476
324. van Wonderen, J. H., McMahon, R. M., O'Mara, M. L., McDevitt, C. A., Thomson, A. J., Kerr, I. D., MacMillan, F., and Callaghan, R. (2014) The central cavity of ABCB1 undergoes alternating access during ATP hydrolysis. *FEBS J* **281**, 2190-2201
325. Loo, T. W., and Clarke, D. M. (2017) Attachment of a 'molecular spring' restores drug-stimulated ATPase activity to P-glycoprotein lacking both Q loop glutamines. *Biochem Biophys Res Commun* **483**, 366-370
326. Zarrabi, N., Ernst, S., Verhalen, B., Wilkens, S., and Borsch, M. (2014) Analyzing conformational dynamics of single P-glycoprotein transporters by Forster resonance energy transfer using hidden Markov models. *Methods* **66**, 168-179
327. Priess, M., Goddeke, H., Groenhof, G., and Schafer, L. V. (2018) Molecular Mechanism of ATP Hydrolysis in an ABC Transporter. *ACS Cent Sci* **4**, 1334-1343
328. Hsu, W. L., Furuta, T., and Sakurai, M. (2016) ATP Hydrolysis Mechanism in a Maltose Transporter Explored by QM/MM Metadynamics Simulation. *J Phys Chem B* **120**, 11102-11112
329. Sauna, Z. E., Muller, M., Peng, X. H., and Ambudkar, S. V. (2002) Importance of the conserved Walker B glutamate residues, 556 and 1201, for the completion of the catalytic cycle of ATP hydrolysis by human P-glycoprotein (ABCB1). *Biochemistry* **41**, 13989-14000
330. Berger, A. L., Ikuma, M., and Welsh, M. J. (2005) Normal gating of CFTR requires ATP binding to both nucleotide-binding domains and hydrolysis at the second nucleotide-binding domain. *Proc Natl Acad Sci U S A* **102**, 455-460
331. Yang, R., Cui, L., Hou, Y. X., Riordan, J. R., and Chang, X. B. (2003) ATP binding to the first nucleotide binding domain of multidrug resistance-associated protein plays a regulatory role at low nucleotide concentration, whereas ATP hydrolysis at the second plays a dominant role in ATP-dependent leukotriene C4 transport. *J Biol Chem* **278**, 30764-30771
332. Jones, P. M., and George, A. M. (2013) Mechanism of the ABC transporter ATPase domains: catalytic models and the biochemical and biophysical record. *Crit Rev Biochem Mol Biol* **48**, 39-50
333. Furman, C., Mehla, J., Ananthaswamy, N., Arya, N., Kulesh, B., Kovach, I., Ambudkar, S. V., and Golin, J. (2013) The deviant ATP-binding site of the multidrug efflux pump Pdr5 plays an active role in the transport cycle. *J Biol Chem* **288**, 30420-30431
334. Grillitsch, K., Tarazona, P., Klug, L., Wriessnegger, T., Zellnig, G., Leitner, E., Feussner, I., and Daum, G. (2014) Isolation and characterization of the plasma membrane from the yeast Pichia pastoris. *Biochim Biophys Acta* **1838**, 1889-1897
335. Szakacs, G., Ozvegy, C., Bakos, E., Sarkadi, B., and Varadi, A. (2000) Transition-state formation in ATPase-negative mutants of human MDR1 protein. *Biochem Biophys Res Commun* **276**, 1314-1319

10. Acknowledgement

Throughout the writing of this dissertation, I have received a great deal of support and assistance from colleagues, collaborators, friends and family.

I would first like to thank my supervisor, Dr. Katalin Goda, whose expertise and help was invaluable in formulating the scientific questions and methodology of our research. Her guidance, support and patience throughout the years constantly pushed me to bring my work and my scientific understanding to higher levels.

My sincere thanks go to Prof. Dr. Gábor Szabó, the head of our research group for the possibility to work in his group and for all his help throughout the years.

I would like to thank Prof. Dr. János Szöllősi and Prof. Dr. György Panyi, former and present Heads of the Department of Biophysics and Cell Biology for the opportunity to work and complete my dissertation in their Department. Moreover, I would like to thank all my colleagues from the Department of Biophysics and Cell Biology for their help and suggestions and for their personal support.

I am also thankful to my co-authors for their invaluable contributions to the work presented in this thesis.

I would like to acknowledge Prof. László Takács, member of my advisory committee, whose selfless help opened new and exciting opportunities for me. I will always be grateful for his support!

Lastly, I wish to express my deepest gratitude to my Family and Friends for their endless support, patience and understanding.

11. Keywords and appendix

Keywords: Multidrug resistance, ABC transporter, P-glycoprotein, ABCG2, ABCB11, retinoids, catalytic cycle, UIC2 antibody, ATPase activity, cell membrane

Tárgyszavak: Multidrog rezisztencia, ABC transzporter, P-glikoprotein, ABCG2, ABCB11, retinoidok, katalitikus ciklus, UIC2 antitest, ATPáz aktivitás, sejtmembrán

UNIVERSITY AND NATIONAL LIBRARY
UNIVERSITY OF DEBRECEN
H-4002 Egyetem tér 1, Debrecen
Phone: +3652/410-443, email: publikaciok@lib.unideb.hu

Registry number: DEENK/337/2020.PL
Subject: PhD Publication List

Candidate: Szabolcs Tarapcsák
Doctoral School: Doctoral School of Molecular Cellular and Immune Biology

List of publications related to the dissertation

1. Goda, K., Dönmez-Cakil, Y., **Tarapcsák, S.**, Szalóki, G., Szöllősi, D., Parveen, Z., Türk, D., Szakács, G., Chiba, P., Stockner, T.: Human ABCB1 with an ABCB11-like degenerate nucleotide binding site maintains transport activity by avoiding nucleotide occlusion.
PLoS Genet. 16 (10), 1-21, 2020.
DOI: http://dx.doi.org/10.1371/journal.pgen.1009016
IF: 5.174 (2019)

2. **Tarapcsák, S.**, Szalóki, G., Telbisz, Á., Gyöngy, Z., Matúz, K., Csősz, É., Nagy, P., Holb, I., Rühl, R., Nagy, L., Szabó, G., Goda, K.: Interactions of retinoids with the ABC transporters P-glycoprotein and Breast Cancer Resistance Protein.
Sci Rep. 7 (41376), 1-31, 2017.
DOI: http://dx.doi.org/10.1038/srep41376
IF: 4.122

List of other publications

3. Firouzi Niaki, E., Van Acker, T., Imre, L., Nánási, P. P. i., **Tarapcsák, S.**, Bacsó, Z., Vanhaecke, F., Szabó, G.: Interactions of Cisplatin and Daunorubicin at the Chromatin Level.
Sci. Rep. 10 (1), 1-12, 2020.
DOI: http://dx.doi.org/10.1038/s41598-020-57702-7
IF: 3.998 (2019)

4. Ireland, A. S., Micinski, A. M., Kastner, D. W., Guo, B., Wait, S. J., Spainhower, K. B., Conley, C. C., Chen, O. S., Guthrie, M. R., Soltero, D., Qiao, Y., Huang, X., **Tarapcsák, S.**, Devarakonda, S., Chalishazar, M. D., Gertz, J., Moser, J. C., Marth, G., Puri, S., Witt, B. L., Spike, B. T., Oliver, T. G.: MYC Drives Temporal Evolution of Small Cell Lung Cancer Subtypes by Reprogramming Neuroendocrine Fate.
Cancer Cell. 38 (1), 60-78; e1-e12, 2020.
DOI: http://dx.doi.org/10.1016/j.ccell.2020.05.001
IF: 26.602 (2019)

UNIVERSITY AND NATIONAL LIBRARY
UNIVERSITY OF DEBRECEN
H-4002 Egyetem tér 1, Debrecen
Phone: +3652/410-443, email: publikaciok@lib.unideb.hu

5. Kiss, A., Ráduly, A. P., Regdon, Z., Polgár, Z., **Tarapcsák, S.**, Sturniolo, I., El-Hamoly, T., Virág, L., Hegedűs, C.: Targeting nuclear NAD+ synthesis inhibits DNA repair, impairs metabolic adaptation increases chemosensitivity of U-2OS osteosarcoma cells.
Cancers (Basel). 12 (5), 1-27, 2020.
IF: 6.126 (2019)

6. Biró, A., Markovics, A., Homoki, J., Szőllősi, E., Hegedűs, C., **Tarapcsák, S.**, Lukács, J., Stündl, L., Gálné Remenyik, J.: Anthocyanin-Rich Sour Cherry Extract Attenuates the Lipopolysaccharide-Induced Endothelial Inflammatory Response.
Molecules. 24 (19), 3427-3441, 2019.
DOI: http://dx.doi.org/10.3390/molecules24193427
IF: 3.267

7. Bársony, O., Szalóki, G., Türk, D., **Tarapcsák, S.**, Gutay-Tóth, Z., Bacsó, Z., Holb, I., Székvölgyi, L., Szabó, G., Csanády, L., Szakács, G., Goda, K.: A single active catalytic site is sufficient to promote transport in P-glycoprotein.
Sci. Rep. 6 (24810), 1-16, 2016.
DOI: http://dx.doi.org/10.1038/srep24810
IF: 4.259

8. Kerényi, F., **Tarapcsák, S.**, Hrubi, E., Baráthné Szabó, Á., Hegedűs, V., Balogh, S., Bágyi, K., Varga, G., Hegedűs, C.: Fogbél eredetű őssejtek fluoreszcens és mágneses válogatásának összehasonlító vizsgálata.
Fogorv. Szle. 109 (1), 29-33, 2016.

Total IF of journals (all publications): 53,548
Total IF of journals (publications related to the dissertation): 9,296

The Candidate's publication data submitted to the iDEa Tudóstér have been validated by DEENK on the basis of the Journal Citation Report (Impact Factor) database.

12 November, 2020

DEBRECENI EGYETEM Egyetemi és Nemzeti Könyvtár